Naval Command,
Control and Ocean
Surveillance Center RDT&E Division
San Diego, CA
92152-5001

Technical Report 1600
May 1993

Intentionally Short Range Communications (ISRC)

1992 Report

J. Yen
P. Poirier
M. E. O'Brien
L. Gibeson

Technical Report 1600
May 1993

Intentionally Short Range Communications (ISRC)

1992 Report

NAVAL COMMAND, CONTROL AND OCEAN SURVEILLANCE CENTER
RDT&E DIVISION
San Diego, California 92152–5001

J. D. FONTANA, CAPT, USN
Commanding Officer

R. T. SHEARER
Executive Director

ADMINISTRATIVE INFORMATION

The work in this document was performed by the Electro-Optic Devices Branch (Code 843) with support provided by the Satellite System Application Branch (Code 842) of the Naval Command, Control and Ocean Surveillance Center (NCCOSC), Research, Development, Test and Evaluation (RDT&E) Division. The task was sponsored by the Director, Amphibious Warfare Technology Directorate, Marine Corps Systems Command, Quantico, VA.

Released by
D. M. Gookin, Head
Electro-Optic Devices
Branch

Under authority of
C. E. Gibbens, Head
Satellite Communications
Division

PK

OBJECTIVE

1. Perform feasibility study of technologies developed under the Intentionally Short Range Communications (ISRC) project.
2. Further develop test protocols for the ISRC prototype links.

RESULTS

1. Ti:Sapphire laser cavity and efficiency examined.
2. Four Phase I contracts awarded in 1992 were completed and the results evaluated.
3. Ultraviolet (UV) test links tested to begin quantifying the UV link test protocols.
4. Test protocols updated with new technical information.

RECOMMENDATIONS

1. Continue to refine the test protocols for all of the ISRC technologies.
2. Award and monitor the Phase II contracts to develop alternative technologies.
3. Apply the technologies developed for ISRC mission to covert and amphibious missions.

CONTENTS

FIGURES

TABLES

1.0 INTRODUCTION

1.1 OBJECTIVE

The purpose of the USMC ISRC Exploratory Development project is to demonstrate the feasibility of using one or several technologies for short-range data transmissions.

A satisfactory technology may be range-limited based on the physical properties of the atmosphere and the propagation medium. Such a link has an inherent low probability of detection (LPD) capability.

An alternative scheme is the spread spectrum technology, which spreads the signal over a wide-spread bandwidth and, thus, hides the signal in the noise.

1.2 SCOPE

This report encompasses the FY 92 development, fabrication, and testing of several candidate technologies for all three of the ISRC missions: Company Radio, Local Area Network (LAN) Backbone, and Wideband Link.

This report also includes the following:

Appendix A describes the upgraded test protocols, or requirements, that each of these prototype links must satisfy to be considered a viable ISRC system.

Appendix B describes the work performed with respect to the tunable ultraviolet (UV) laserhead development.

Appendices C through F cover the four Phase I contracts awarded in FY 92.

Appendix G studies whether Raman shifting can be applied to UV laser radiation for multichannel capability.

Appendix H studies the best way to build an omnidirectional UV antenna.

Appendix I describes the UV propagation computer model used to simulate the ISRC UV environment.

Appendix J contains the data and analysis for a UV laser link.

Appendix K describes the electronics used in the NRaD link testing.

Appendix L summarizes the proposals submitted for Phase I.

2.0 BACKGROUND

2.1 INTRODUCTION

The USMC expressed interest in developing communications links with ranges intentionally limited to very short distances. These links are described below and their architecture shown in figure 1. This exploratory development report contains the progress-to-date of the feasibility study for all three ISRC missions.

2.1.1 Company Radio

The Company Radio is a very short-range (≤0.5 km), omnidirectional, low-data-rate (≥2400 bps), vehicle-mounted, mobile voice link that can be used by the squad leaders of a company. Two possible applications of the Company Radio are in an urban warfare scenario (figure 2) and as a landing zone communicator (figure 3).

2.1.2 LAN Backbone

The LAN Backbone (figure 4) is a short-range (≤1.0 km), semidirectional, low (≥2400 bps) to high (2 Mbps) data rates, transportable data link for connecting several LANs. The LANs range from the low data rate LAN bridges to high data rate full LANs and wide area networks (WANs). Until further direction, these LANs will be compatible with the Banyan VINES LAN software.

2.1.3 Wideband Link

The Wideband Link is a medium-range (3–5 km), directional, vehicle-mounted or fixed, high data rate and traffic (2 Mbps) link for connecting command posts (CPs) with the antenna farm.

2.1.4 Signal Detection

Most current communication systems (such as radio) have the $1/r^2$ signal attenuation typical of electromagnetic radiations. This means that while our encrypted transmissions cannot be understood, the enemy can still detect their presence, direction find (DF), and take counter-measures. This is a tactical threat to our forces.

2.2 ISRC TERMINOLOGY

2.2.1 Link Definitions

Link type definitions are as follows:

Omnidirectional:	signal sent in all directions azimuthally
Semidirectional:	signal sent into an azimuthal quadrant (±45 deg)
Directional:	direction within ±5 deg
Line-of-sight (LOS)	within ±1 deg
Strictly LOS (SLOS)	within ±0.01 deg
Non-LOS (NLOS)	no LOS between transmitter and receiver

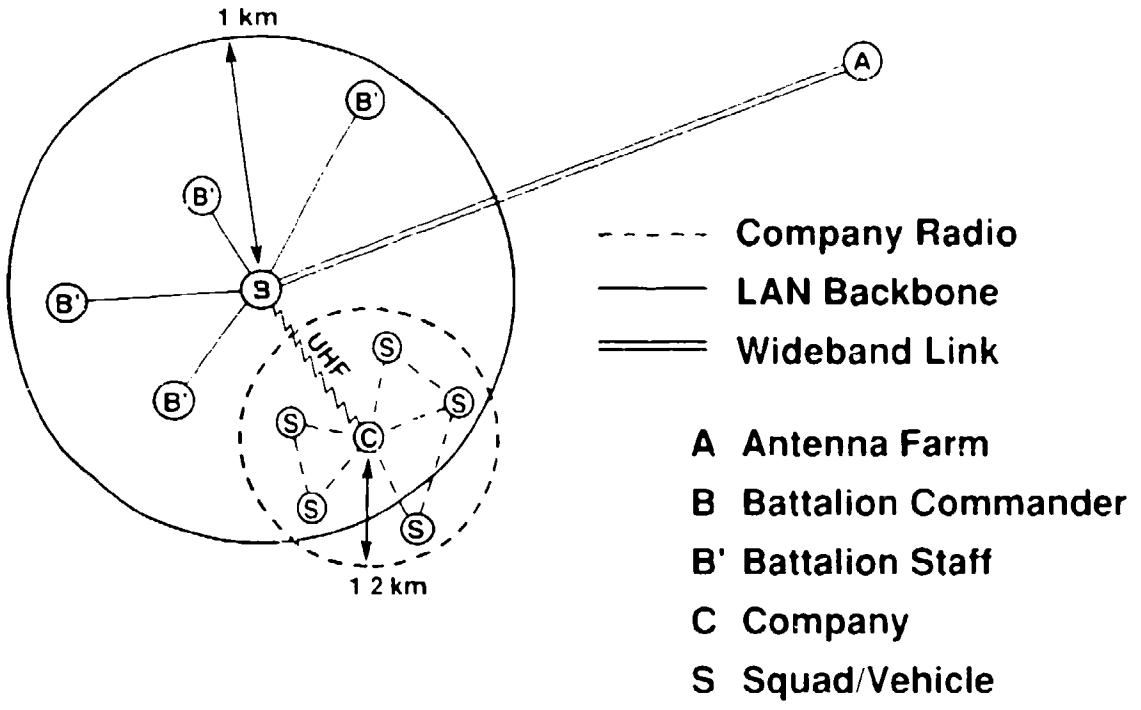

Figure 1. ISRC architecture

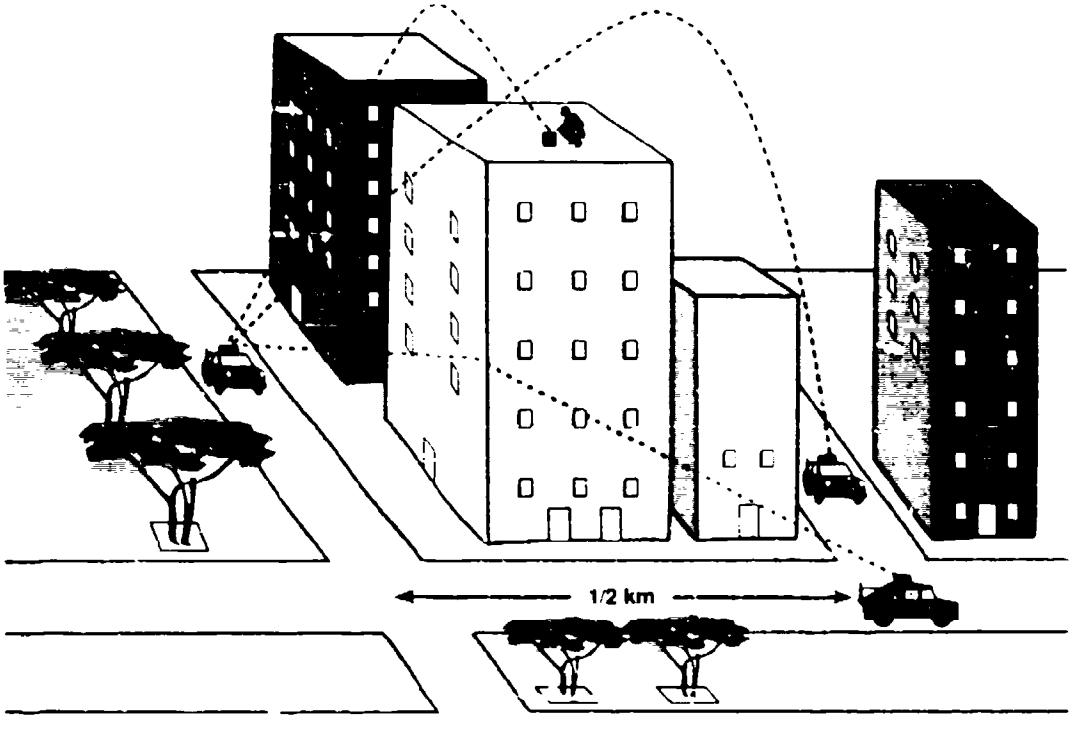

Figure 2. ISRC Company Radio: urban warfare.

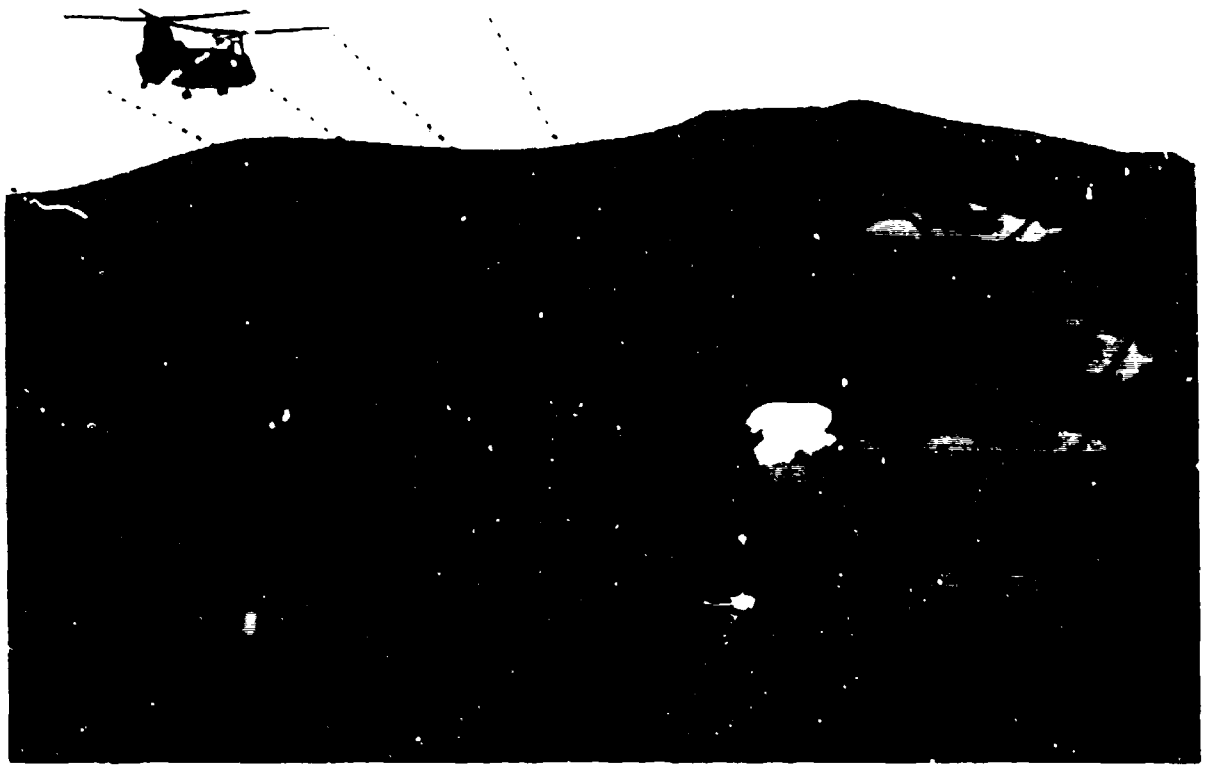

Figure 3. ISRC landing zone communicator.

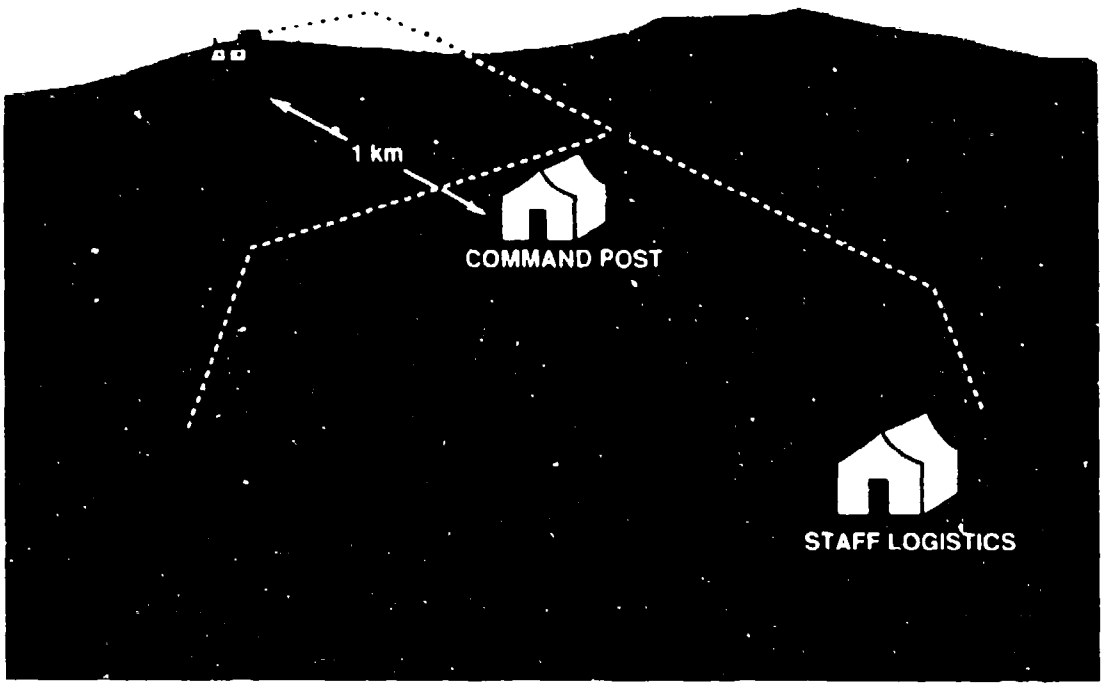

Figure 4. ISRC LAN Backbone.

2.2.2 LPI and LPD

Low probability of intercept (LPI) means that the enemy has a low likelihood of intercepting and understanding our transmissions. An encrypted link is LPI but still detectable by enemies.

Low probability of detection (LPD) means that the enemy has a low likelihood of detecting and direction finding our transmissions. An LPD system is inherently LPI.

2.2.3 Broadband and Wideband

Broadband is defined as a broad spectrum of wavelengths, as distinguished from wideband, which is a wide range of data rates. For example, a broadband lamp emits radiation at wavelengths ranging from infrared to ultraviolet; a wideband communicator can handle data rates ranging from a few kilohertz to many megahertz.

2.2.4 Spread Spectrum

Two techniques are commonly called "spread spectrum": direct sequence and frequency hopping. In direct-sequence spread spectrum (DSSS), the carrier is modulated by a wideband pseudorandom sequence that spreads the signal over a large instantaneous bandwidth. The resultant bandwidth equals the bandwidth of the pseudorandom sequence, which is many times greater than the data bandwidth; thus, individual components are below the noise. In frequency hopping, the instantaneous bandwidth of the signal equals the data bandwidth, but the carrier frequency is hopped over a pseudorandom sequential set of frequencies whose aggregate bandwidth is many times greater than the data bandwidth.

2.3 HISTORY

The history of communications is replete with attempts to increase the operational range. The ISRC program and its predecessor are the first systematic efforts to develop a deliberately limited short-range communications system. This program encompasses several technologies, such as solar-blind UV light, infrared (IR) light, and millimeter waves (MMW).

2.3.1 UV

Communications that use UV light in the solar-blind region were first proposed by Sunstein (1968), Reilly (1976), Kolosov et al. (1976), and Junge (1977).

2.3.1.1 Early Efforts. In the late 1970s, the Army (Ross, 1978) and the Navy (Fishburne et al., 1976; Neer and Schlupf, 1978) did early development work with broadband UV lamps for short-range voice communication links. These efforts indicated the requirement for an efficient UV emitter.

2.3.1.2 NOSC Efforts. In the 1980s, NOSC developed a short-range, 2400-bps, computer-to-computer link for the USMC (Geiler et al., 1986; Johnson, 1986; Yen, 1987). This link used efficient (20% conversion to UV at 254 nm) single-wavelength germicidal lamps for the UV source.

Concurrently, NOSC developed a short-range, 2400-bps, data link to transfer Carrier Aircraft Inertial Navigation System (CAINS) data from the carrier to its aircraft (Nuyda, 1986; Yen, 1987). This link also used single-wavelength germicidal lamps for the UV transmitters.

The feasibility of UV radiation for longer range links was studied next (Yen & Moberg, 1988). This study indicated that several disadvantages must be resolved to make such a UV link practical. The NOSC UV communications (UV Comm) link was subject to interference by fires, flares, explosions, welding, and lightning, so procedures to handle these problems must be implemented. Heavy fog, smog, rain, and smoke can also limit the link distance.

2.3.1.3 Recent Efforts. Currently, NRaD is performing a feasibility study of the ISRC LAN Backbone and Company Radio based upon a UV laser. The pulsed laser approach was adopted, in part, to achieve tunability and noise suppression. With certain types of lasers, the wavelength can be varied (or tuned). The short, but sharp, pulses of a laser may resolve the above mentioned noise problem.

The Marine Corps Systems Command (MCSC) in Quantico, VA, through NRaD, also funded Sparta, Inc., and Mission Research Corp. to develop prototype UV links (appendices E and D, respectively).

2.3.2 IR

Several efforts based on IR lasers were short range by happenstance. The only previous effort known to the author to deliberately limit IR range was a proposal in the mid-1980s. This attempt to develop an IR laser system, with the wavelength in an absorption band, was to support CAINS.

Currently, NRaD/MCSC has funded Titan Systems to develop an IR laser diode prototype link that takes advantage of the 1.39-μm water-absorption band (appendix F).

2.3.3 Millimeter Wave (MMW)

Efforts based on MMW, or extremely high frequency (EHF) radiation or microwaves, were also short range by happenstance. Two previous efforts to deliberately limit range with MMW were known to the author. The first effort to develop a portable short-range communicator was in the early-1980s (Hislop, 1982). The other was a proposal in the mid-1980s to develop a MMW system at the 60-GHz oxygen absorption band in order to support CAINS.

Currently, the United States Army Communications Electronics Command (CECOM) has funded several efforts to develop tactical communications links where the range is limited by absorption of MMW in the atmosphere.

3.0 APPROACHES

A tactical communications link whose range is limited physically by its atmospheric propagation characteristics will not be detectable outside of a limited range. Such a self-limiting link will then be a LPD system. In addition, such approaches as spread spectrum techniques and long-cavity lasers can result in links of limited ranges. Data encryption is still useful as added security within the operational envelope of the system.

There are at least three media in which the link range is limited by the propagation physics: UV light, IR light, and MMWs.

3.1 UV LIGHT

UV light in the solar-blind spectral region (200–300 nm) is strongly attenuated by ozone molecules in the atmosphere (figure 5) (Yen, 1987). The ozone layer in the upper atmosphere essentially absorbs all of the solar UV radiation in the solar-blind region, so almost no solar background appears in this spectral region (figure 6) (Yen, 1987). This low background allows the use of a very small number of received scattered photons for a viable signal, resulting in a NLOS link.

Attenuation by the residual ozone at sea level (5–25 dB/km, depending on the ozone concentration) limits the range of an UV link to several (≤5) kilometers. The ozone attenuation of UV radiation also limits the detection of UV transmissions to short distances, which results in a LPD link. Figure 7 shows a graphical representation of the NLOS UV communications concept.

Given a receiver filter that passes radiation only in the solar-blind region and blocks all other radiations, a UV link can operate with very small received signals due to the lack of solar background.

3.1.1 UV Sensor

To take advantage of the solar-blind region, the receiver filter must be able to block non-solar-blind radiation very effectively. The Honeywell filter that was used for UV Comm was too expensive (≈$10K per unit) for mass use as in the voice and data links. Less expensive, but less effective, filters are available commercially. These commercial filters would require stronger signals to overcome greater background leakages.

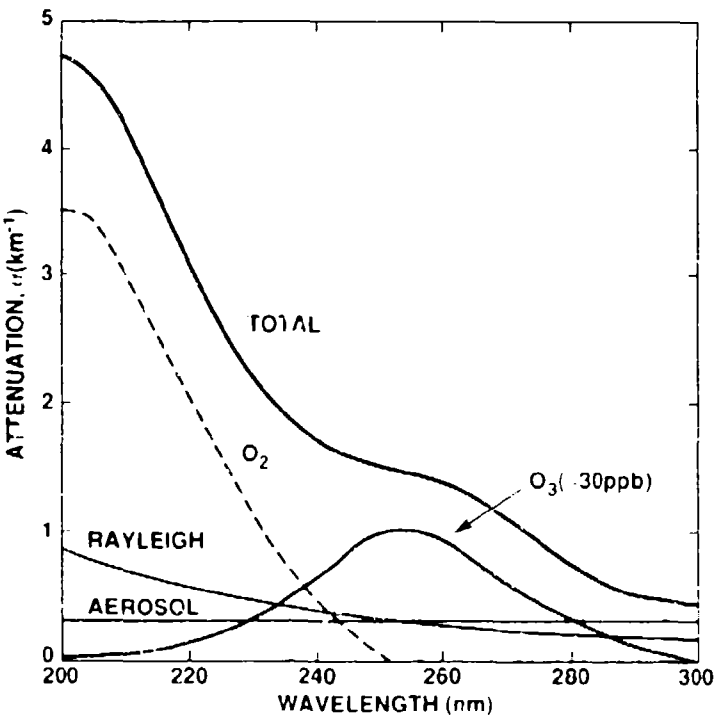

Figure 5. Sea-level extinction coefficients.

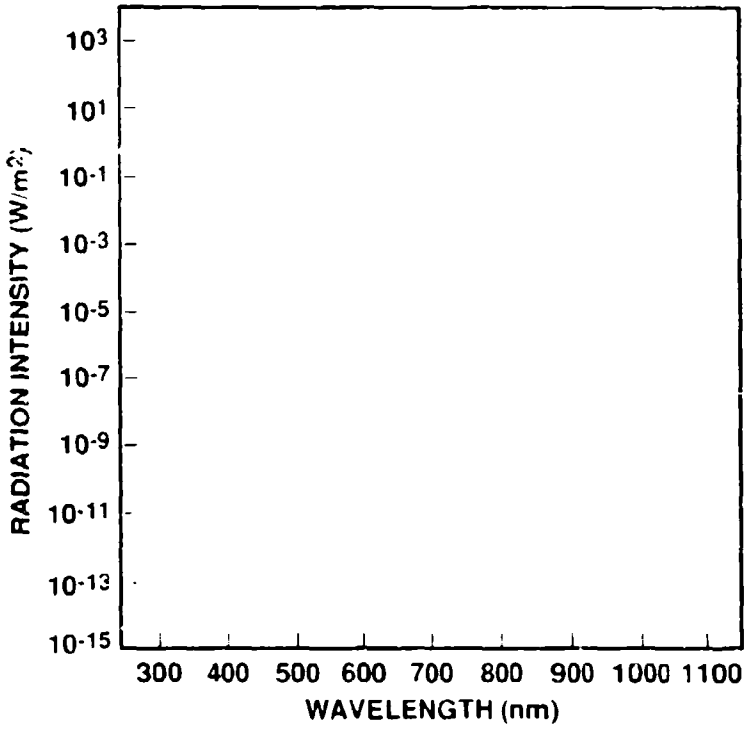

Figure 6. Solar radiation at sea level.

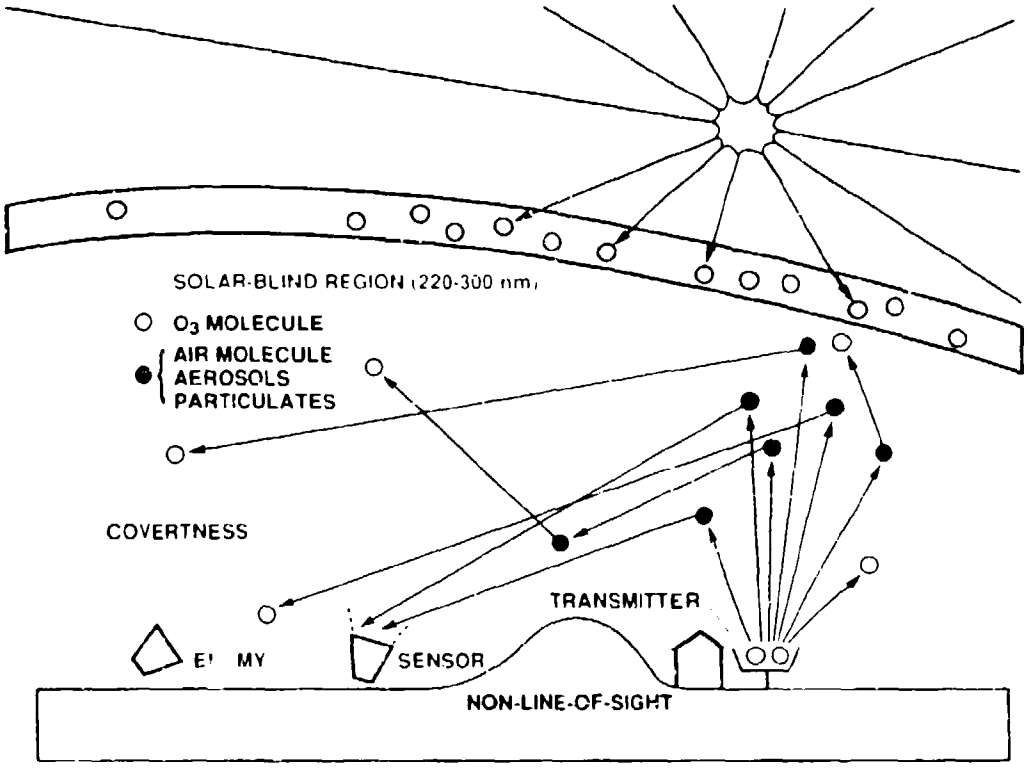

Figure 7. NLOS UV communications.

The photomultiplier tube (PMT) used in the UV Comm sensor is highly sensitive, but also expensive. If the received signal can be boosted significantly, it may be possible to use lesser quality, less sensitive PMTs, which are cheaper and smaller. The currently used PMTs have a dead time of the same magnitude as the laser pulse spread width, which may be problematical for laser links in the near field (where the UV photons will not have been scattered enough to achieve a sufficiently wide time spreading).

The cheaper and smaller solid-state UV detectors have sensitivities with orders of magnitude less than PMTs. To effectively use solid-state detectors, the signal strength must be increased accordingly, which is not practical with current technology. Strong signals of such magnitude would also be counterproductive with respect to LPD.

3.1.2 UV Lamp Transmitter

The UV source (germicidal lamps) used by the UV Comm system was highly efficient in outputting UV light at a single wavelength (254 nm). However, they are bulky, fragile, and restricted in data rates ($\leq$20 kHz at very short ranges). Therefore, germicidal lamps are not recommended for use in the ISRC links with higher data rates.

Arc lamps are compact and easier to ruggedize. However, because they are broadband optical emitters, they are difficult to use for multichannel applications. The output power of arc lamps is also not sufficient for some of the ISRC links. Finally, their IR and visible emissions can prove a detection signature unless filtered out.

UV lamps would be the easiest and least expensive to adapt for use in the low data rate links. This avenue would be desirable for building a feasibility demonstration prototype quickly.

3.1.3 UV Laser Transmitter

The UV laser can increase the signal per pulse detected by eliminating much of the wasted vertical emissions (appendix H) and decreasing the effective detection bin size (due to the very short laser pulses, appendix J). Currently, the size and expense of lasers emitting in the UV make them ineffective for field equipment. However, industry is in the process of miniaturizing the laser components and reducing the power requirements, so UV lasers of practical sizes will be available in the near future.

This will be useful for the Company Radio and the low-data-rate LAN backbone applications because the short effective bin size should suppress UV noise sources. With much smaller bin sizes (5 µs versus 416 µs), the UV noise sources are expected to have time characteristics of longer duration and be spread out over these 83 bins, and to resemble a DC source. The laser "pulse" in one (or two) ON bin would then overwhelm the semiconstant noise.

However, the use of UV lasers may not be as effective for the high-data-rate LAN Backbone and Wideband Link. A data rate of 2 Mbps limits the bin size to 0.5 µs, which is equivalent to 150 m of path difference. This path difference is too small for practical NLOS mode operations. Thus, while some scattered (near receiver) photons are usable, these high-data-rate links will require LOS mode operation.

Since LOS is required for the high-data-rate links to work, the time spreading due to the multipath flux may be negligible relative to the LOS photon flux. However, a likely 10-µs path difference will limit the data rate to 100 kbps.

3.1.3.1 Nd:YAG Laser. A frequency-quadrupled. Nd:YAG laser produces UV light with a wavelength of 266 nm in the solar-blind region. A quadrupled Nd:YAG laser requires only two crystals in addition to the basic Nd:YAG laser, which emits at 1064 nm. This is the simplest solution to obtaining solar-blind UV radiation; but tunability is difficult.

The UV output wavelength can be Raman shifted to various discrete wavelengths with gas cells or optical fibers. However, the threshold laser energy density (at the needed repetition rate) required to initiate the Raman effect is not practical at the present time (appendix G).

A quadrupled Nd:YAG laser can now be made small enough for inclusion in a portable field brassboard (appendix D).

3.1.3.2 Ti:Sapphire Laser. A tunable, frequency-tripled Ti:sapphire ($Ti:Al_2O_3$) laserhead produces UV light with discrete wavelengths ranging from 265 to 280 nm. The laser output can be tuned by rotating a set of birefringent tuning plates (BTPs) inside the laser cavity.

The Ti:sapphire laser can be tuned electro-optically (and mechanically) to various wavelengths for multichannel use. A tunable laser capable of emitting at several distinct wavelengths means that only one transmitter would be necessary to produce the multiple links in a multichannel net.

The Ti:sapphire laserhead will require a pumping laser emitting in the green-yellow spectral region. An obvious candidate is the doubled Nd:YAG green laser. Blue-green laser diodes, which should be commercially available in the near future, are another possibility.

3.1.3.3 Laser Safety. The advantages of using UV laser sources balanced by safety limitations are detailed in Yen et al. (1987) and updated in appendix C of Yen (1992).

3.1.3.4 UV Laser Diodes. Diode-pumped UV lasers of requisite power, rate, and size are expected to be available within the next few years. The USAF Wright Laboratory has shown interest in developing such diodes, although the wavelengths of the newest diodes (300–350 μm) have not reached the solar-blind.

3.1.4 Beam Optics

By channelling the laser output through some optics (appendix H), omnidirectional operations with one laser can be achieved for the Company Radio. By some kind of mechanical beam channel, multiple directions (one at a time) can be achieved for the LAN Backbone.

The Wideband Link presupposes LOS operations, with the terminals fixed after acquisition. Therefore, except for modulation, the beam does not need to be modified.

3.2 INFRARED (IR) LIGHT

IR radiation is strongly absorbed by water vapor between wavelengths of 1 and 8 μm (10 to ≥100 dB/km, figure 8). Existing IR lasers can be tuned to one of the water vapor absorption regions, resulting in a very short operations range.

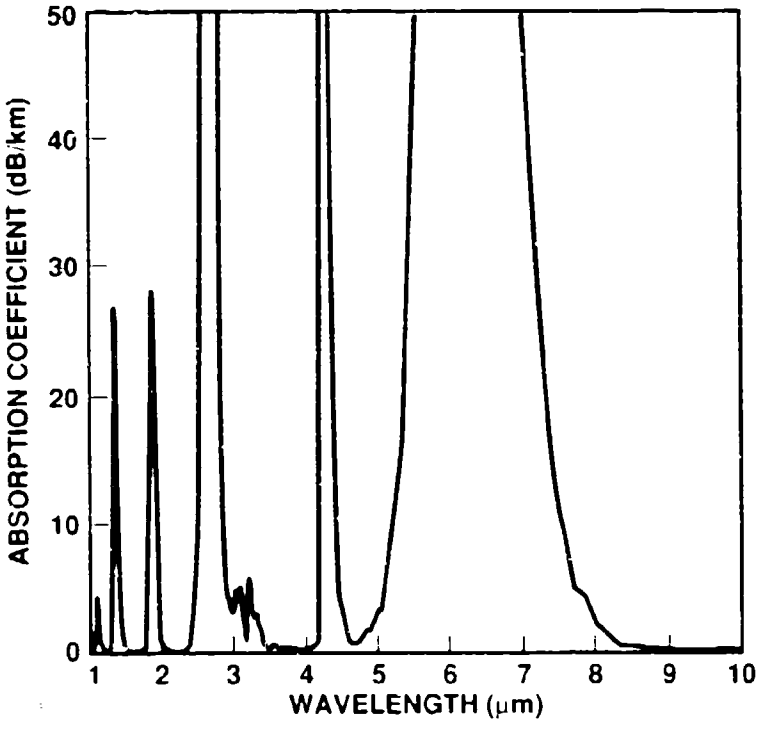

Figure 8. IR absorption in the standard atmosphere.

3.2.1 IR Laser

The absorption coefficient required to reduce the operational range to 0.5 to 1 km is on the orders 5 to 20 dB/km, which means that a possible wavelength region required is, for example, from 1.3 to 1.4 μm. Solid state IR laser diodes that operate in this region, such as InGaAsP (1.39 μm), are now available (appendix F).

3.2.2 Variable Range

Tuning the wavelength along an edge of the absorption band causes the atmospheric absorption coefficient encountered by the signal to vary so the operational and detection ranges can be controlled.

3.2.3 Attenuation

A possible problem that needs to be addressed is the absorption coefficient, which depends on the relative humidity. The humidity is not a constant like oxygen content. In a desert, the daytime humidity can be so low that the IR link range can become large enough to no longer be LPD. In a tropical climate, the humidity may so limit the range as to make it impractical. Therefore, it will probably be necessary to tune, in power or wavelength, the laser to fit the varying local humidity conditions. Similarly, rain attenuation of IR radiation may pose a problem in rainy tropical regions.

3.2.4 Operational Mode

The IR option also requires that the signal be strong enough to overcome solar and other types of interference, even though the water vapor present should considerably reduce the solar

noise at the operations region. The noise and weak atmospheric scattering will require LOS operations.

3.2.5 Data Rate

IR laser diodes can be modulated at rates of the order of Mbps (appendix F), thus satisfying the ISRC missions' data rate requirements.

3.3 MILLIMETER WAVE (MMW)

MMW, a form of microwave, or extremely high-frequency (EHF) radiation, is very strongly absorbed (≈15 dB/km) by the molecular oxygen in the atmosphere at 60 GHz (figure 9 [Ippolito, 1981]). The MMW range is similar to that of the UV links.

3.3.1 Variable Range

Similar to the IR, the frequency can be tuned along the edge of the absorption band, thus varying the atmospheric absorption encountered and the range.

3.3.2 Omnidirectional Antenna

Through the use of a bicone antenna (two cones with their tips touching), MMW can be transmitted and received in all azimuthal directions, thereby satisfying omnidirectionality.

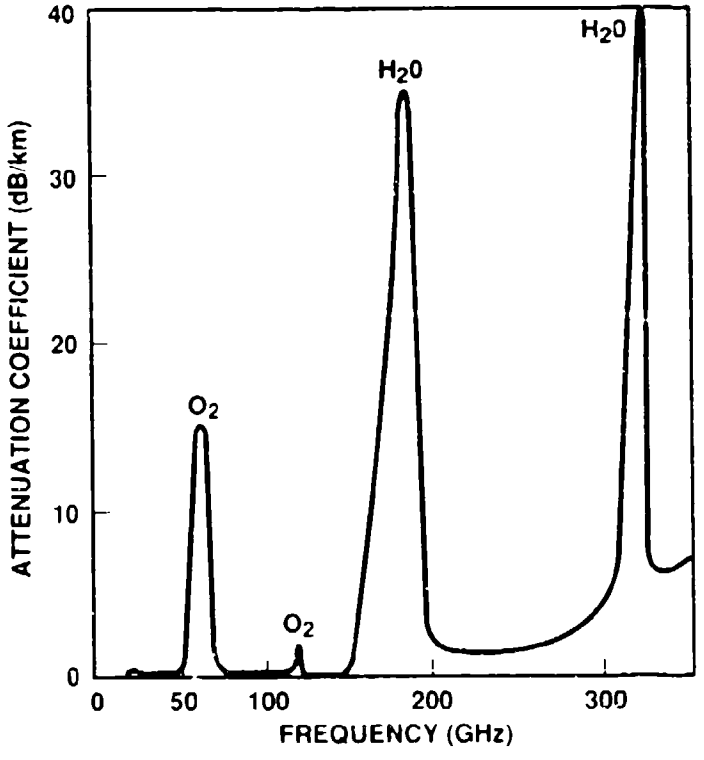

Figure 9. Microwave gaseous attentuation.

3.3.3 Non-Line-of-Sight (NLOS)

The MMW link is primarily a LOS link with no obstructions between antennas. An MMW link with omnidirectional antennas may be able to exploit multipath propagation modes when obstructions to LOS exist between terminals.

3.3.4 Noise

The MMW option also requires that the signal be strong enough to overcome the noise from the solar and background sources, although the molecular oxygen and water vapor present should reduce the solar noise considerably.

3.3.5 Attenuation

The MMW beam will suffer some loss due to water vapor (humidity). MMW will suffer considerable loss due to passage through rain (about 12 dB/km at moderate rain of 1 in hr), although the beam path length is small (figure 10, [Jursa, 1985]).

3.4 OTHER TECHNOLOGIES

In the course of the ISRC development effort, technologies other than the self-limiting media were encountered that showed potential for short-range communications. Two such technologies are spread spectrum RF and long-cavity lasers.

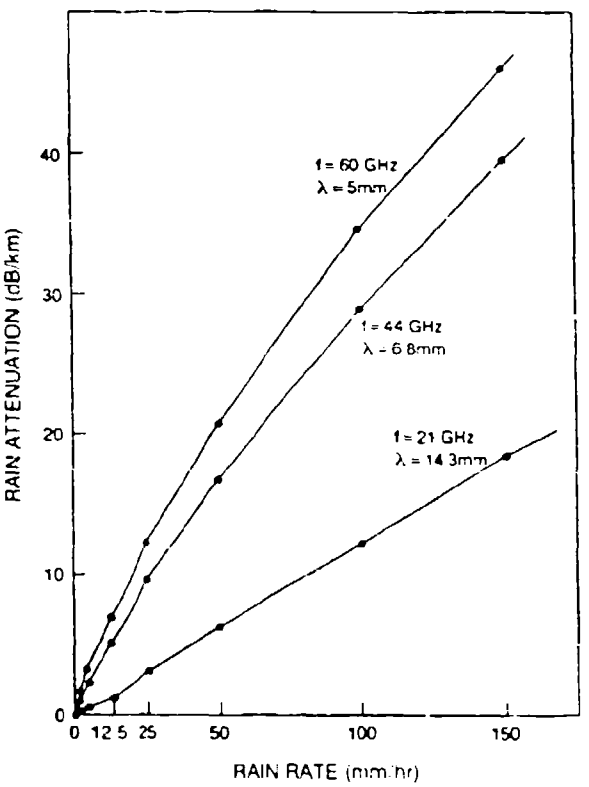

Figure 10. MMW rain attenuation.

3.4.1 Spread Spectrum

The direct-sequence spread spectrum (DSSS) technique uses a pseudorandom sequence to spread the radio frequency (RF) signal over a wide bandwidth, thus reducing the RF power spectral density and hiding the signal in the noise. The receiver, which has the same pseudorandom sequence, knows where in the spectrum to look in order to reconstruct the signal. NRaD and MCSC have funded GTE to develop a spread spectrum prototype link (appendix C).

3.4.1.1 LPD. Since the signal is broken into millions of pieces and spread out over a wide-spread band, the power density at any particular frequency within the spread band will be so small as to be below the noise level. Unless the enemy is physically close to the transmitter, it would be difficult to discern the transmitter's signature from the noise.

Unlike absorption-dependent systems, the detection range of a spread spectrum link is shorter than the operational range. Thus, the operational range can be increased for some applications and still remain LPD.

3.4.1.2 Carrier Frequency. The spread-spectrum technique differs from the frequency-hopping technique, which has been occasionally called spread spectrum. With frequency-hopping technique, the signal is sent out completely at the carrier frequency, which is changed constantly through a pseudorandom sequence.

The spread spectrum technique differs from the frequency-hopping technique in that the carrier frequency remains unchanged, but the entire spread band centered at the carrier frequency is used to transmit data. The spread-spectrum technique can be applied to any carrier frequency, provided that frequency is high enough to support the specified spread bandwidth. In general, for high-throughput rates on the order of Mbps, the spread bandwidth should be tens of MHz. Such a high bandwidth, in turn, requires that the carrier frequency should be at least 1 GHz, that is, super high frequency (SHF) or EHF bands.

3.4.1.3 Range Extension. A spread spectrum link normally operates in a LOS mode, which limits the range to the horizon (generally 30 to 40 km). Through the use of atmospheric evaporation ducts, the range can be extended to over-the-horizon ranges (70 to 90 km) by the use of 8-GHz SHF radiation (Patterson, 1988; Rogers & Anderson, 1992). Such range extension, while preserving LPD, may allow a DSSS link to connect Marine Air–Ground Task Force (MAGTF) ships to onshore forces.

3.4.2 Long-Cavity Lasers

A practical long-cavity laser will be a LPD link by its very definition. Generally, a laser cavity consists of a laser material placed between two mirrors. Light sent into the laser material is amplified, which results in the light being amplified greatly as it reflects between the mirrors. One of the mirrors has some transmittance so that the laser beam will be emitted from the cavity.

By moving one mirror very far from the laser material and the other mirror (on the order of kilometers), the laser cavity thus formed will have no out-cavity emissions. Lasing will occur only within the cavity when the alignment is correct and not lasing otherwise. Such a cavity is detectable only when an observer moves between the mirrors, and the lasing stops once the observer blocks the beam path.

3.4.2.1 Early Experiments. In the mid-1970s, experiments performed at the Hughes Aircraft Company demonstrated the feasibility of long-cavity lasers (Linford & Hill, 1974; Linford et al., 1974). The cavity lengths demonstrated were up to 6 km, and up to 30 km with relays.

3.4.2.2 Applications. A Mission Research Corporation white paper proposed the development of a long-cavity laser for an LPD link (Thomson, 1992). Such a link could fulfill some of the ISRC missions, but questions remain as to the practicality of the idea.

The most immediate reservation is whether the cavity can be aligned in a practical amount of time. If the link requires hours to acquire, then it is obviously impractical. The need also exists for a laser material with sufficient gain.

4.0 MISSION ANALYSIS

4.1 COMPANY RADIO

The best options for the Company Radio voice link seem to be omnidirectional UV or DSSS that permeates a small area. This would remove the need to aim the communications unit.

4.1.1 UV Lasers

A pulsed UV laser would provide a noise suppression advantage. The development of such a laser, with its associated electronics and optics, is needed to satisfy the requirements of the Company Radio.

4.1.2 UV Lamps

Omnidirectional arc lamps should be applied to the voice link. The use of broadband lamps will be problematical when multichannel aspects are to be considered. However, the most significant problem is omnidirectionality, and suggestions of rotating or multiple transceivers are probably impractical. Because a rotating transmitter will spread the signal over all azimuthal angles, the lamp output must be greatly increased. Multiple transceivers will increase the hardware cost correspondingly.

4.1.3 MMW

The Army Communications and Electronics Command's (CECOM) EHF applique should be available for testing during FY 93.

4.1.4 IR

An omnidirectional IR laser link is not likely based on the available information, so it should not be pursued.

4.1.5 Spread Spectrum

An omnidirectional DSSS link (to take advantage of its LPD and potential multipath integration characteristics) should be developed to satisfy the Company Radio requirements.

4.2 LAN BACKBONE, LOW DATA RATE

The best options for the low-data-rate LAN Backbone link seem to be directional UV or DSSS that will cover a small arc and relieve the need to precisely aim the transceiver.

4.2.1 UV Lasers

A pulsed UV laser would provide a noise suppression advange. The development of such a laser, together with its associated electronics and optics, is needed to satisfy the requirements of the low-data-rate LAN Backbone.

4.2.2 UV Lamps

Directional arc lamps may be usable for the low-data-rate links. The use of broadband lamps will be a problem when multichannel aspects are to be considered. Rotating transceivers may be viable if the acquisition and tracking problems are resolved.

4.2.3 MMW

The USA CECOM's EHF Wireless LAN prototype should be available for testing during FY 93.

4.2.4 IR

A directional IR laser diode link should be seriously considered for the low-data-rate LAN Backbone.

4.2.5 Spread Spectrum

A directional DSSS data link should be developed to take advantage of its LPD and high-data-rate characteristics.

4.3 LAN BACKBONE, HIGH DATA RATE

The best options for the high-data-rate LAN Backbone link seem to be the LOS DSSS, IR, or MMW that will cover a small arc. The system should be aimed with some precision.

4.3.1 UV Lasers

An UV laser will not likely satisfy the high-data-rate requirement and should not be pursued at this time.

4.3.2 UV Lamps

UV lamps cannot achieve the necessary data rates at the required ranges and should not be considered.

4.3.3 MMW

The USA CECOM's EHF Wireless LAN prototype should be available for testing during FY 1993.

4.3.4 IR

A directional IR laser diode link is a viable alternative for the high-data-rate LAN Backbone and should be developed.

4.3.5 Spread Spectrum

A directional DSSS LAN Backbone prototype should be developed to take advantage of its LPD and high-data-rate characteristics.

4.4 WIDEBAND LINK

The best options for the Wideband Link seem to be LOS DSSS, IR, or MMW, all of which will cover a small arc. The system can be aimed with precision.

4.4.1 UV Lasers

An UV laser will not likely satisfy the high-data-rate requirement and should not be pursued at this time.

4.4.2 UV Lamps

UV lamps cannot achieve the necessary data rates at the required ranges and should not be considered.

4.4.3 MMW

Adapting the USA CECOM's EHF Wireless LAN prototype to satisfy the requirements of the Wideband Link may be possible. The prototype should be available for testing during FY 93.

4.4.4 IR

A directional IR laser diode link is a viable alternative for the Wideband Link and should be considered.

4.4.5 Spread Spectrum

A directional DSSS Wideband Link prototype should be developed to take advantage of its LPD and high-data-rate characteristics.

5.0 PROGRESS

During FY 92, the ISRC efforts were concentrated in three areas: development of a tunable UV laser source, development of test protocols for the ISRC prototype links, and development of alternative technologies in private industry that satisfy ISRC missions.

5.1 TUNABLE UV LASER

Because of the need to have more than one channel in the solar-blind region for a practical communications system, NRaD is attempting to develop a multiwavelength UV laser. Cost analysis indicates it is better to use just one laser with output of several wavelengths than several different lasers of different wavelengths.

The inhouse effort to develop a tunable UV laser in the solar-blind took two routes. The more ambitious route attempted to fabricate a laser cavity based on the Ti:sapphire laser. The

other route attempted to shift the wavelength of the UV light produced by a quadrupled Nd:YAG laser.

5.1.1 Ti:Sapphire

Titanium-doped sapphire (Ti:S or Ti:Al_2O_3) crystal generates a band of wavelengths in the IR when pumped with green light. The Ti:S emission center can be moved with birefringent tuning plates (BTP); that is, the primary output of the Ti:S cavity can be tuned. By tripling this band of tunable IR light into the UV, a band of tunable UV light is obtained.

To transform IR light into UV light, two conversion processes will have to be performed. The first conversion is the frequency-doubling of the IR light ($\lambda \approx 800$ nm) into blue (or violet, $\lambda \approx 400$ nm) light. The second conversion is the sum-frequency mixing (SFM) of IR and blue light into UV light ($\lambda \approx 266$ nm).

A development effort was initiated in 1992 to make a tunable Ti:S laser cavity (appendix B). To increase the total efficiency of the system, the doubling and mixing conversions are performed in the same laser cavity as the Ti:S. With all three conversions done in the same cavity, it is hoped that the surface and transmission losses will be minimized. However, this also leads to an interdependent cavity configuration, where changing one item in the cavity leads to changes in all the others.

Three of the four required processes, the green-to-IR conversion, the IR tuning, and the IR-to-blue conversion, were achieved. However, the pump laser suffered a hardware breakdown that resulted in less green pump power than specified. Lower pump power resulted in a level of blue light generation that was not sufficient to initiate mixing. Therefore, the final conversion process could not be accomplished, but should be resumed when the pump laser has been repaired.

5.1.2 Raman Shifting

Because the quadrupled Nd:YAG (4xNd:YAG) laser is readily available, money and time will be saved. However, this laser emits at only one wavelength (266 nm) and limits this laser link to one channel. To develop a multichannel capability for the quadrupled Nd:YAG laser, an attempt was made to use the Raman scattering process to shift UV radiation at 266 nm to other wavelengths in the solar-blind region.

An experiment was performed to determine the thresholds required to initiate Raman shift in gas cells (appendix G). The results indicated that Raman shifting in gas cells was not practical at the energy levels used in an ISRC UV laser system. Increasing the energy of the UV laser sufficiently to initiate Raman shifting requires such an increase in laser power that the system will likely be too large to be portable. In any case, too much light is self-defeating with respect to LPD.

5.2 PROTOCOL DEVELOPMENT

As part of developing test protocols (or requirements) for the various ISRC missions, fabricating some elements of the link to be tested proved necessary. The simplest and logical way to define requirements for a particular link is to test a link and record the advantages and deficiencies. Therefore, NRaD plans to develop and test stripped-down versions of the ISRC prototype links being developed by industry.

At this stage, the test protocols are in a qualitative form because detailed technical information on the prototype links and their test sites is, as yet, unavailable. As more information is developed, the test protocols (appendix A) will be updated. These requirements are expected to be quantified in time.

5.2.1 UV Laser Link

With MCSC funding, NRaD has acquired a 4xNd:YAG UV laser. This laser will be incorporated into a UV laser test link in preparation for developing test protocols such as the NRaD or the Mission Research prototypes.

Since both the Ti:S and 4xNd:YAG UV laser have emission at wavelengths of approximately 266 nm, the test requirements for both types of links will be identical, except for such factors as physical laser configuration. Therefore, the following efforts can be generalized for a generic UV laser link.

5.2.1.1 Omnidirectionality. As an UV laser is obviously directional and the Company Radio requires omnidirectionality, a study was performed on an optical device to channel UV laser radiation in all azimuthal directions. Appendix H indicates that a combination of an optical fiber bundle and breakout cone will be the best solution to achieve omnidirectionality.

Note that the analysis in appendix H can be applied, with some modifications, to the directional links, such as the LAN Backbone and the Wideband Link.

5.2.1.2 UV Propagation. The propagation characteristics of UV radiation in a communications configuration will be of major interest in developing test protocols for UV laser links. An understanding of the physical processes involved is a prerequisite for effective testing.

Propagation Model. The development of a theoretical model that can be simulated on a computer will provide the effort with a useful and adjustable tool (appendix I). This model can be executed to predict results of a test link configuration be used to correct the deficiencies in the model and improve future computer predictions.

Noise Suppression. The short pulse duration of a pulsed laser will suppress noise (section 3.1.3). By reducing the temporal bin size, we can spread out UV noise sources over a larger number of bins. This reduces the noise level at any particular bin to a few photons, while the laser pulse will result in ten or more photons in an ON bin.

To verify the above hypothesis, the 4xNd:YAG UV laser was used to emit UV pulses (2500 pulses per second) to a receiver 0.6 km away (appendix J). The laser pulses were detected, stored, and analyzed. Preliminary analyses confirm that laser pulse characteristics will considerably improve the signal-to-noise ratio of the laser link over that of UV lamp signals.

5.2.1.3 Electronics. The various electronics designed and fabricated for use with the UV laser link are discussed in appendix K. The control electronics for the transmitter end were simple, but the detection and recording electronics at the receiver end were complex and required several redesigns over the year.

5.2.2 UV Lamp Link

A voice link based on UV lamps was developed at NRaD. This link operates on AC power but can be rebuilt to operate on batteries. Such a mobile link will be useful in developing test protocols for a UV lamp link such as the Sparta prototype.

5.2.3 Development Plans

Further testing on the UV links (both lamp and laser) as well as simple IR and RF spread spectrum links will be performed in FY 93 to complete the development of the test protocols.

A quantified test protocols update is expected to be available at the end of FY 93. The Phase II contractors, who will be at about month 6 of a 12-month contract, will be invited to participate in refining these requirements. Upon finalization of the test protocols, the contractors shall incorporate the relevant requirements into their test plans. The Phase II link tests will be performed in the second quarter of FY 94.

5.3 CONTRACT DEVELOPMENT

During Phase I of the ISRC out-house development effort, solicitations were placed through the Small Business Innovation Research (SBIR) program and the Broad Agency Announcements (BAA). Out of the 34 responses to these solicitations, four contracts to perform concept development of ISRC links were awarded in FY 92 (appendix L).

One SBIR contract was awarded to Sparta, Inc., San Diego, CA. BAA contracts were awarded to GTE (Waltham, MA), Mission Research Corporation (MRC, Los Alamos, NM), and Titan Systems (San Diego, CA).

5.3.1 UV Laser Link

The MRC system is built about a quadrupled Nd:YAG UV laser (appendix D). During Phase I, MRC developed a portable laser package and a receiver package suitable for demonstration. Laser pulses that will theoretically result in a 4800-bps link were transmitted and received at a range of 0.5 km. However, as no modem was built during this phase, real data have not been transmitted through this link.

5.3.2 UV Lamp Link

The Sparta system is based on UV lamps (appendix E). During the Phase I study, Sparta proposed to develop surface discharge lamps for the UV source. These surface discharge lamps will be faster than gas or arc lamps and have a higher power-to-light efficiency. These lamp characteristics will reduce the size weight and power requirement of the system.

5.3.3 IR Laser Link

The Titan system is based on developing an IR laser diode emitting at a water-absorption band (appendix F). During the Phase I effort, Titan developed a laser diode capable of emission in a band centered at 1.335 μm and has a tuning range of ±0.013 μm. Laser pulses that will theoretically result in a 50-kbps link were transmitted and received at a range of 70 m. However, as a modem was not built during this phase, real data have not been transmitted through this link.

5.3.4 Spread Spectrum Link

The GTE system is based on adapting the Adaptive Sparsely Populated Rake (ASPARK) spread spectrum modem into an LPD link (appendix C). During Phase I, GTE modified the ASPARK testbed to transmit and receive the spread spectrum signal in the laboratory. A

multipath simulator was employed to demonstrate reconstruction of a multicomponent signal. Real data were transmitted through the hardwired link at a throughput of 16 kbps.

5.3.5 Contract Process

The four Phase I contracts listed above have all been completed as of this writing. These efforts have been evaluated and the selections for Phase II made.

5.3.5.1 Phase I Evaluation. Six NRaD personnel have participated in the monitoring and evaluation of these contracts. Table 1 correlates the evaluators to the contractors (and the technology used) that each one evaluated.

Table 1. Evaluation summary.

Contractor Technology	GTE RF DSSS	MRC UV Laser	Sparta UV Lamp	Titan IR Laser
Axford, Roy (844)	X			
Gookin, Debra (843)			X	X
Mirabile, Chuck (405)	X			
Moberg, Victor (842)	X			
Smaldino, John (033)		X	X	X
Yen, John (843)	X	X	X	X

5.3.5.2 Phase II Selection. These four contractors were ranked with respect to Phase I progress and Phase II potential. The recommendation was presented to the project sponsor (MCSC).

After due consideration of the available resources, the sponsor selected three contractors for Phase II. The Phase II contracts are to be 1-year efforts, with April 1994 as the expected completion date. Testing is planned for March 1994 before the final review and demonstrations.

5.3.5.3 Phase III Plans. Based on current resource projections, two Phase II contractors will be selected for Phase III. The selection will be based upon Phase II progress, potential of the technology, and Marine Corps needs.

The Phase III prototype link will be a full two-way link. Such a link will optimally need two distinct channels, so that the link will be assured of connectivity even when the two terminals transmit at the same time. Some link protocol will then determine which of the simultaneous transmissions will have priority.

5.4 MEMORANDUM OF AGREEMENT

The Marine Corps and the Army generated a memorandum of agreement (MOA) to cooperate in developing short-range tactical communications systems of interest to both. This MOA avoids duplication of efforts by allowing the Marine Corps and the Army to pursue different technologies and then share in the results.

The various efforts shown in the upper connected portion of figure 11 come directly under this MOA, while the other efforts are related to the program and will be asked to join in the MOA as required.

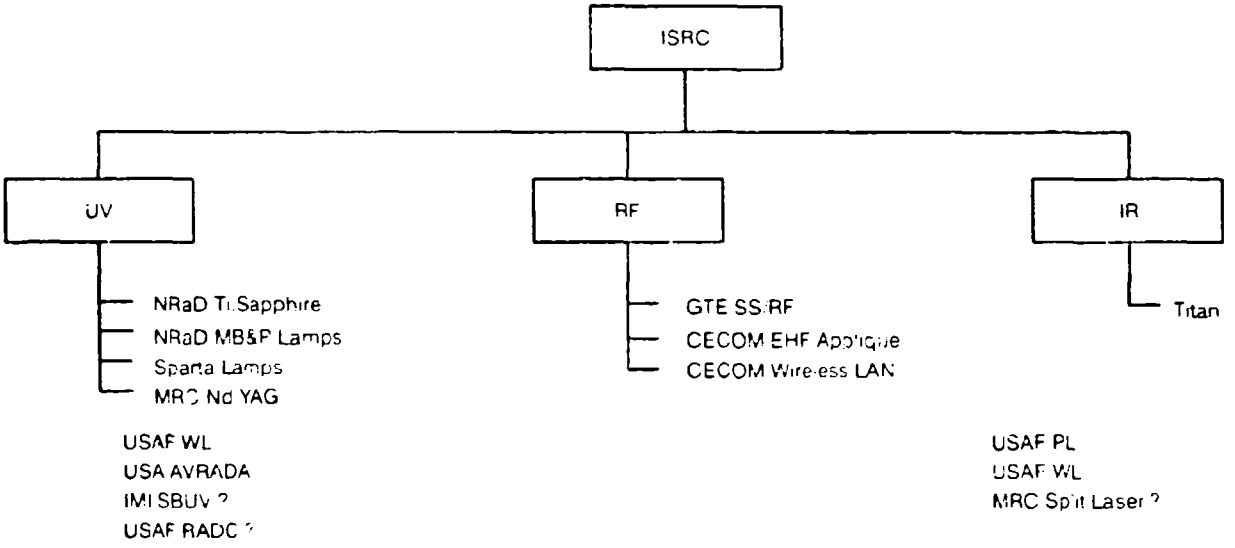

Figure 11. ISRC overview.

5.4.1 USA CECOM

The Army Communications Electronics Command (USA CECOM) at Fort Monmouth, NJ, has been involved in several efforts to develop tactical, LPD, short-range communications systems. CECOM has concentrated its efforts in EHF (or MMW) systems that uses the absorption properties of EHF radiation in the atmosphere in order to limit detection range.

5.4.1.1 EHF Applique. CECOM is funding the development of an EHF attachment to a UHF/VHF radio made by Hughes. This EHF Applique operates at 54 GHz (5.6 mm) in the FM mode for a maximum ideal operational range of about 4 km and detection range of about 8 km. Several units are to be delivered to the Army in FY 93.

5.4.1.2 Wireless LAN. CECOM is funding Rockwell and Chang Industries to develop LPD Wireless LAN systems based on EHF radiation. The Rockwell system uses 36-GHz EHF while the Chang system uses 54 GHz. Prototype units from each contractor are to be delivered to the Army in 1993.

5.4.2 United States Air Force (USAF) Wright Laboratory (WL)

The United States Air Force Wright Laboratory (USAF WL) at Wright-Patterson AFB, Dayton, OH, has initiated the effort to develop LPD communications systems for radio silence aerial missions.

5.4.2.1 UV Evaluation. USAF WL initiated an effort to evaluate the practicality and effectiveness of UV links for aerial operations.

5.4.2.2 UV Laser Diodes. USAF WL initiated an effort to develop UV laser diodes. Laser diodes emitting in the long-UV (325-400 nm) have been developed, and diodes in the solar-blind region can be expected in the next several years.

5.4.2.3 SBIR. USAF WL generated an SBIR solicitation AF93-162, "Aerial Refueling Communication Under Radio Silence Conditions," for technologies that will provide LPD capability intentionally.

5.5 MISCELLANEOUS

Several other organizations have expressed interest in LPD communications links for short-range communications.

5.5.1 IMI S.B.U.V.

The Israeli Military Industries (IMI) group indicated that a short-range communications system has been developed based on its S.B.U.V. technology. The current information indicates that the IMI link is not ready for demonstration and the project has been suspended.

5.5.2 United States Air Force (USAF) Phillips Laboratory (PL)

The United States Air Force Phillips Laboratory (USAF PL) at Kirtland AFB, Albuquerque, NM, has been developing IR communications systems. Although unintentional, these systems are short range because of their low power.

5.5.3 Special Operations

ISRC links have obvious applications for special operation forces. Contacts have been made with various activities and interest has been shown, but nothing concrete has yet developed.

6.0 RECOMMENDATIONS

6.1 TUNABLE UV LASER

Effort suspended on MCSC instruction. In addition to the cavity analysis shown in appendix B, NRaD will develop and submit a scientific paper on the progress to date.

6.2 TEST PROTOCOLS

Develop test links based on technologies being developed for the ISRC project in order to further develop test protocols. Specify and quantify the test requirements for each technology and update appendix A as required.

6.3 CONTRACT EFFORTS

Award and monitor the three contracts selected for Phase II. Work in conjunction with the contractors to finalize the test plans. Upon test completion, evaluate and select two contracts for Phase III.

6.4 MEMORANDUM OF AGREEMENT (MOA)

Continue cooperation and information sharing with USA CECOM. Invite other Army activities with similar interests and requirements to join in the MOA.

Make an effort to bring USAF WL into the MOA in addition to monitoring their tactical communications efforts. Include USAF PL and any other Air Force activities with similar interests and requirements to join in the MOA.

6.5 OTHER APPLICATIONS

The technologies developed for the ISRC missions are also suitable for applications such as covert insertions/extractions, surveillance, interdiction, and over-the-horizon amphibious operations.

7.0 REFERENCES

Fishburne, E. S., M. E. Neer, and G. Sandri. 1976. "Voice Communication via Scattered Ultraviolet Radiation, Report 274." Princeton: ARAP. ECOM-0115-F. Princeton, NJ.

Geller, M., G. B. Johnson, and R. L. Shimabukuro. 1983. "An Experimental Non-Line-of-Sight Communication System Using Ultraviolet Light." NOSC TN 1313* (Oct). Naval Ocean Systems Center, San Diego, CA.

Geller, M., and G. B. Johnson. 1985. "Non-Line-of-Sight Covert Ultraviolet Communication Link," *Proc. 1985 IEEE Mil. Comm. Conf.* **4**,95.

Geller, M., G. B. Johnson, J. H. Yen, and G. A. Clapp. 1986. "Short-Range UV Communication Links," *Proc. Tact. Comm. Conf.* **1**,60.

Hislop, A. R. 1982. "A Head-Worn 60-GHz Communicator for Short Range Applications." NOSC TN 1153* (Jun). Naval Ocean Systems Center, San Diego, CA.

Ippolito, L. J. 1981. "Radio Propagation for Space Communications Systems," *Proc. IEEE.* **69**,697.

Johnson, G. 1986. "An Ultraviolet Communication System." NOSC TR 1110 (Jun). Naval Ocean Systems Center, San Diego, CA.

Junge, D. M. 1977. "Non-Line-of-Sight Electro-Optic Laser Communications in the Middle Ultraviolet," NPS61-77-001. Naval Postgraduate School Thesis, Monterey, CA.

Jursa, A. S. 1985. *Handbook of Geophysics and Space Environment.* Air Force Geophysics Laboratory, Bedford, MA.

Kolosov, M. A., V. N. Pozhidayev, and L. V. Fedorova. 1976. "The Propagation of Ultraviolet Radiation in the Earth's Atmosphere and the Possibilities of Building Optical Communications Lines in the UV Band," *Rad. Eng. & Elec. Phys.* **21**,8.

Linford, G. J., and L. W. Hill. 1974. "Nd:YAG Long Lasers," *Appl. Opt.* **13**,1387.

Linford, G. J., E. R Peressini, W. R. Sooy, and M. L. Spaeth. 1974. "Very Long Lasers," *Appl. Opt.* **13**,379.

Neer, M. E., and J. M. Schlupf. 1978. "Solar Blind Ultraviolet Voice Communications, Report 374a." Princeton: ARAP, NESC Contract N00039-77-C-0278. Princeton, NJ.

*Technical notes are working documents and do not represent an official policy statement of the NCCOSC RDT&E Division. For further information, contact the author.

Neer, M. E., and J. M. Schlupf. 1979. "The Development and Testing of an Ultraviolet Voice Communication System, Report 394." Princeton: ARAP, NESC Contract N66001-78-C-0180. Princeton, NJ.

Nuyda, J. M. 1986. "CAINS Ultraviolet Covert Data Link Test Report." NAC TR-2386. Naval Avionics Center, Indianapolis, IN.

Patterson, W. L. 1988. "Effective Use of the Electromagnetic Products of TFSS and IREPS." NOSC TD 1369 (Oct). Naval Ocean Systems Center, San Diego, CA.

Reilly, D. M. 1976. "Atmospheric Optical Communications in the Middle Ultraviolet." MIT EECS Thesis, Boston, MA.

Ross, W. S. 1978. *An Investigation of Atmospheric Optically Scattered Non-Line-of-Sight Communication Links*. (Boston: MIT Res. Lab. of Elec.). US Army Research Office Contract DAAG29-88-C-0048.

Simmons, A. J. 1981. "EHF Propagation through Foliage." MIT Lincoln Laboratory, Lexington, MA.

Sunstein, D. E. 1968. "A Scatter Communications Link at Ultraviolet Frequencies." MIT EE Thesis, Boston, MA.

Thomson, J. J. 1992. "Split Laser Covert Communication Device." Mission Research Corporation White Paper, Torrance, CA.

Yen, J. 1987. "UV Communications Propagation Study." NOSC TR 1191 (May). Naval Ocean Systems Center, San Diego, CA.

Yen, J., and V. Moberg. 1988. "Medium Range Optical Scatter Communication Systems." NOSC TR 1223 (Mar). Naval Ocean Systems Center, San Diego, CA.

Yen, J. 1992. "Intentionally Short Range Communications (ISRC) Exploratory Development Plan." NRaD TD 2286 (Jun). Naval Command, Control and Ocean Surveillance Center RDT&E Division, San Diego, CA.

Yen, J., V. Moberg, and L. Gibeson. 1987. "Exposure to UV Radiation." NOSC TD 1187 (Aug). Naval Ocean Systems Center, San Diego, CA.

8.0 GLOSSARY

ASPARK	Adaptive Sparsely Populated Rake (spread spectrum modem)
BAA	Broad Agency Announcement
BER	bit error rate
BTP	birefringent tuning plate
Broadband	a broad spectrum of wavelengths
CAINS	Carrier Aircraft Inertial Navigation System
CBD	Commerce Business Daily
CECOM	Communications Electronics Command
CP	command post
DF	direction find
Directional	direction is within ±5 deg of the imaginary line between terminals
DRT	diagnostic rhyme test
DSSS	direct-sequence spread spectrum
Duplex	two-way channel
EHF	extremely high frequency
FIFO	first-in-first-out
FOV	field-of-view
FWHM	full-width-at-half-maximum
GPS	Global Positioning System
HMMV	high-mobility multipurpose vehicle
IMI	Israeli Military Industries
IR	infrared light ($\lambda \geq 700$ nm)
ISRC	Intentionally Short Range Communications
LAN	local area network
LLS	longitudinal light scatter
LOS	line-of-sight (direction within ±1 deg of the imaginary line between terminals)
LPAcq	laser pulse acquisition card
LPD	low probability of detection
LPI	low probability of intercept

LSL	Laser Systems Laboratory (Sparta, Inc.)
MAGTF	Marine Air-Ground Task Force
MCSC	Marine Corps Systems Command (Quantico, VA)
MMW	millimeter wave (with 1 mm $\leq \lambda \leq$ 10 mm, or 30 GHz $\leq \nu \leq$ 300 GHz)
MOA	Memorandum of Agreement
Multichannel	several communications channels
NCCOSC	Naval Command, Control and Ocean Surveillance Center (San Diego, CA)
Nd:YAG	neodymium-doped yttrium aluminum garnet crystal
NLOS	non-line-of-sight (no LOS between the transmitter and the receiver)
NOSC	Naval Ocean Systems Center
NRaD	NCCOSC Research, Development, Test and Evaluation (RDT&E) Division, San Diego, CA
Omnidirectional	signal sent in all directions azimuthally
PID	pulse identification
PMT	photomultiplier tube
PPM	pulse position modulation
PRR	pulse repetition rate
RENLOS	restricted envelope non-line-of-sight
RF	radio frequency
SBIR	Small Business Innovation Research
Semidirectional	signal sent into an azimuthal quadrant ($\pm$45 deg)
SFM	sum-frequency mixing
SHF	super high frequency
SHG	second harmonic generation
Simplex	one-way channel
SLOS	strictly line-of-sight (direction within $\pm$0.01 deg of imaginary line between terminals)
Ti:sapphire	titanium-doped sapphire ($Ti:Al_2O_3$) crystal
USMC	United States Marine Corps
UV	ultraviolet light (200 nm $\leq \lambda \leq$ 400 nm)
VUV	vacuum ultraviolet
WAN	wide area network

APPENDIX A

UPDATED ISRC TEST PROTOCOLS

1.0 INTRODUCTION

This appendix provides a single set of test protocols, or test requirements and procedures, that the ISRC links will have to satisfy. This appendix updates the test protocols that appeared originally in appendix A of NRaD TD 2286.

The test protocols at this stage are broad system requirements. The quantified test requirements and the test procedures will be further developed through FY 93. Phase II contractors will be given the opportunity to comment on these requirements and incorporate these requirements into their Phase II test plans.

The revised test protocols are expected to be published in the FY 93 report. However, the test protocols will be continuously refined as more technical information becomes available.

2.0 GENERAL REQUIREMENTS

The following ISRC general requirements apply to each ISRC link, although the quantitative requirements for these parameters are link specific.

2.1 LPD

Low probability of detection (LPD) is defined here to mean that the enemy has a low likelihood of detecting and direction finding our transmissions. A system that cannot be detected has an inherently low probability of intercept (LPI).

An LPD link with an operation range of X km must have a detection range of less than X+Y km.

The operational ranges of the ISRC links vary from 0.5 km to 5 km ($0.5 \text{ km} \leq X \leq 5 \text{ km}$). In general, an ISRC link must have a detection range of less than 5–7 km ($X \leq X+Y \leq 7$ km), preferably less.

2.2 NLOS

The non-line-of-sight (NLOS) characteristic is highly desirable because tactical operations tend to involve situations with various obstructions to line-of-sight. NLOS means that no single unobstructed line exists between the transmitter and the receiver (i.e., a structure lies between them). If complete NLOS is not achievable for a particular link, a partial requirement is that the link is viable when there is a misalignment of at least a minimum angle (e.g., such as 5 degrees).

2.3 TEMPERATURE

ISRC links must operate in temperatures ranging from 0 to 50°C.

2.4 SIZE, WEIGHT, POWER

The final (Phase III) communications system must be rugged and mobile in order to be mounted on a high-mobility multipurpose wheeled vehicle (HMMV) or similar Marine Corps

vehicle. Therefore, the total weight of the system shall not exceed 100 kg and the total volume cannot exceed 1 m^3. The system must function on the available power (100 A at 27 V) of the vehicle.

3.0 LOW-DATA-RATE LINKS REQUIREMENTS

In general, the Company Radio and the low-data-rate LAN backbone need to satisfy the same general requirements because of the similarities of data rate and operational configurations. The differences include the range, data format, and operational methods.

3.1 COMPANY RADIO

The Company Radio is characterized by very short range (≤0.5 km), omnidirectionality, low data rate, and mobility.

3.1.1 BER

The Company Radio is distinguished by a voice link that will tolerate a much larger bit error rate (BER). BER for a reasonable voice system is $\leq 10^{-2}$.

3.1.2 Data Rate

An adequate digital voice system would need at least 2400 bps link throughput. The diagnostic rhyme test (DRT) rating for this voice link should be ≥0.90 for good quality voice.

3.1.3 Omnidirectionality

The Company Radio needs to operate in an omnidirectional mode. The operator need not orient the system to communicate, since the positions of other terminals may be moving or unknown.

However, under conditions when some knowledge of another terminal's whereabout is available, some aiming to improve link connection (and reduce detectability) would be an useful additional asset. The Company Radio must be capable of omnidirectionality, but be allowed to operate directionally when circumstances permit.

3.2 LAN BACKBONE

The low-data-rate LAN Backbone is a short range (≤1.0 km), semidirectional, transportable data link.

3.2.1 BER

The uncorrected BER requirement for this link is $\leq 10^{-4}$. Error correction procedures shall be implemented to reduce corrected BER to $\leq 10^{-6}$ for reasons of clarity and redundancy.

3.2.2 Data Rate

The minimal data rate to connect a server computer to a terminal computer will be 2400 bps. However, higher data rates (such as 4800 bps or 9600 bps) will be a plus factor in evaluating the link.

3.2.3 Directionality

The low-data-rate LAN Backbone needs to operate in a directional mode in several different directions, although one at a time. The operator need not orient the system very precisely to communicate because the link can sustain an angular misalignment of at least 5 degrees. However, more precise aiming to improve link connection would be an additional asset.

3.2.4 LAN Software

Until a specific LAN operating system (such as MTS) is defined for the USMC, the Banyan VINES LAN software will be used to operate the LAN Backbone.

4.0 HIGH-DATA-RATE LINKS REQUIREMENTS

In general, the Wideband Link and the high-data-rate LAN (or WAN) Backbone need to satisfy the same general requirements because of the similarities of data rate and operational configurations. The differences include the range, data format, and operational methods.

4.1 LOS

These links can be directional because they are stationary when in operation and the positions of other terminals should be known. However, that may represent additional problems in acquisition and tracking (between moves). The high-data-rate links should be operated in a LOS mode in several different directions, although only one direction at a time.

4.1.1 Misalignment

By sustaining an angular misalignment of at least 1 degree, the system develops the capability to operate without very precise alignment. Link connectivity, despite misalignment, will be a valuable asset in terms of operational simplicity and personnel effectiveness. More precise aiming to improve link connection could be an additional asset available to the operator.

4.2 WIDEBAND LINK

The Wideband Link is a medium-range (3–5 km), directional, vehicle-mounted or fixed, and high-data-rate digital-data link.

4.2.1 BER

The uncorrected BER requirement for this link is $\leq 10^{-5}$. For clarity and redundancy, error correction procedures will be implemented to reduce corrected BER to $\leq 10^{-7}$.

4.2.2 Data Rate

The data link will require a minimum throughput of 2 Mbps to replace the throughput of lines connecting the command post to an antenna farm.

4.3 LAN/WAN BACKBONE

The high-data-rate LAN/WAN Backbone is a short-range (≤ 1.0 km), semidirectional, transportable data link.

4.3.1 BER

The uncorrected BER requirement for this link is $\leq 10^{-5}$. For clarity and redundancy, error correction procedures shall be implemented to reduce corrected BER to $\leq 10^{-7}$.

4.3.2 Data Rate

The link will require a minimum throughput of 2 Mbps to provide connectivity between a server computer and either a terminal computer or another server computer.

4.3.3 Software

Until a specific LAN operating system (such as MTS) is defined for the USMC, the Banyan VINES LAN software will be used to operate the LAN/WAN Backbone.

5.0 ENVIRONMENTAL REQUIREMENTS

Various environmental factors affect the ISRC links. However, because each link (and technology) is different, the impact of environmental factors varies. The following are some factors impacting upon the ISRC links.

5.1 OZONE

An ISRC link based on UV radiation is expected to operate in an urban environment, that is, the ozone concentration is between 30 to 100 ppb (Yen, 1987). A nominal ozone level of 50 ppb is to be expected in a test.

5.2 FOG

An ISRC link should be able to operate in thin fog (defined here as a visibility of 1 km). The definition of "thin fog" is imprecise because fog density depends on particulate density and size.

5.3 RAIN

An ISRC link should be able to operate in light rain (defined here as a rain rate of 1 inch/hour).

5.4 NOISE SOURCES

An ISRC UV link is expected to operate during daylight in the presence of noise sources such as arc-welding, flames, and explosions (at the same distance from the receiver as the transmitter). Specific source characteristics will be defined in the next publication.

An ISRC MMW or spread spectrum link is expected to operate during daylight in the presence of RF sources (at the same distance from the receiver as the transmitter) likely to exist in a battlefield.

An ISRC IR link is expected to operate during daylight in the presence of noise sources such as flames and explosions (at the same distance from the receiver as the transmitter).

5.5 FOLIAGE

The low-data-rate ISRC links are expected to operate in spite of foliage between the transmitter and the receiver. Precise definitions are unavailable as the test sites are unknown at this date, but will be defined in conjunction with the contractors.

5.6 OBSTRUCTIONS

The low-data-rate ISRC links are expected to operate in the presence of obstructions such as buildings that block the line-of-sight. More precise specifications for each prototype link shall be defined in conjunction with the contractors.

6.0 SPECIFIC PHASE II REQUIREMENTS

The various ISRC Phase II prototype links employ different technologies, which makes it impractical to apply one set of test criteria. Each link should be tested for its own strengths and weaknesses. Therefore, requirements will be delineated for each prototype link.

Each Phase II link will be a one-way link transmitting real data. Specific and quantifiable Phase II requirements are being developed and are expected to be included in the next report.

In addition to satisfying the specific mission requirements, a UV laser link, the UV lamp link, the MMW link, the IR link, and the spread-spectrum link must satisfy the maximum number of the system and environmental requirements (sections 2.0 through 5.0 in this appendix).

7.0 PHASE III REQUIREMENTS

The Phase III prototype link shall be a full two-way link that transfers real data outside the laboratory environment. Since the Phase III requirements will largely depend on Phase II results, only an outline will be given at this stage to start the development process.

7.1 MULTICHANNEL

The Phase III link must be able to communicate even when the two terminals transmit simultaneously. Ideally, two distinct channels will be provided to the link, so that the link will be assured of connectivity even in the event of simultaneous transmissions. Some link protocol will then determine which of the simultaneous transmissions will have priority. The ideal solution to the multichannel requirement is as follows:

(a) A UV laser that can be tuned to several wavelengths and filters that can discriminate between these wavelengths; (b) a set of UV lamps emitting at several wavelengths and optical filters that can discriminate between these wavelengths; (c) a set of distinct-frequency MMW/EHF antennas will satisfy the multichannel requirement; (d) an IR laser that can be tuned to several wavelengths and filters that can discriminate between these wavelengths; and (e) a set of distinct-frequency antennas or two orthogonal spread spectrum modems.

8.0 TEST PROCEDURES

The specific test procedures corresponding to each of the ISRC links will be developed during FY 93 and published in the first quarter of FY 94. These procedures will be based on inhouse testing of (simplified) links corresponding to the technologies used by the Phase II contractors.

Each prototype link shall satisfy the associated test requirements through the test procedures corresponding to that link type.

The initial draft of the complete test protocols will be distributed to the three Phase II contractors at the beginning of FY 94 (halfway through the contract). The contractors will be invited to participate in refining these test protocols. The Phase II contractors shall then incorporate these revised test protocols into their Phase II test plans to be carried out in the second or third quarter of FY 94.

9.0 REFERENCE

Yen, J. 1987. "UV Communications Propagation Study." NOSC TR 1191 (May). Naval Ocean Systems Center, San Diego, CA.

APPENDIX B

TUNABLE UV LASER

1.0 INTRODUCTION

During 1992, the following efforts were made to develop an intracavity-tripled titanium-doped sapphire (Ti:S or Ti:Al_2O_3) laser as a tunable ultraviolet (UV) laser (figure B-1). The goal was to provide the ISRC project with a tunable UV laser source operating at 250 pulses per second, with the UV power output substantial enough to be quantified.

This effort will contribute insight into and develop a scheme to upscale the design of a tunable UV source with greater power and efficiency, and will result in a database to increase the overall knowledge in the area of tunable solid-state lasers.

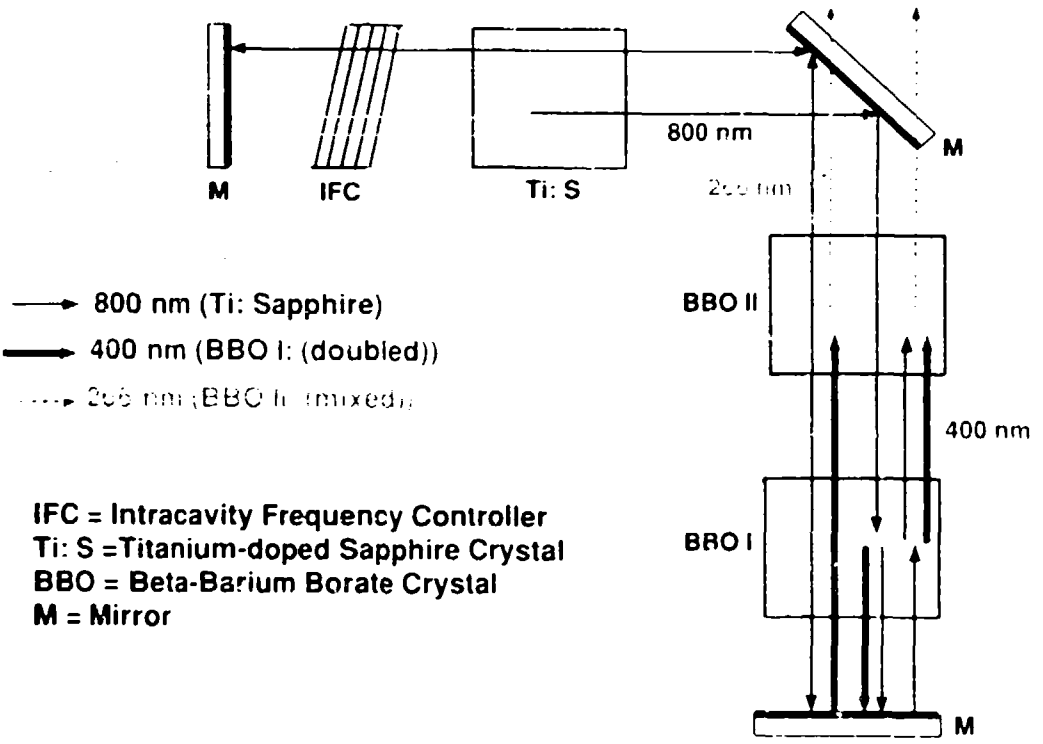

Figure B-1. UV converter: Ti:Sapphire tuning element.

2.0 BACKGROUND

Titanium-doped sapphire (Ti:S) lasers are a reliable and efficient alternative to tunable dye lasers in the IR spectrum (680–1050 nm). Combined with nonlinear crystals, the lasers can produce tunable sources in the blue, the UV, and even the vacuum ultraviolet (VUV) regions.

2.1 MISSION

A reliable and tunable UV source can be valuable in an ISRC tactical communications systems, where the proposed transmitting beam has a narrow linewidth and can be tuned over a wide range (260–280 nm). This would create separate channels of communication within the spectral band.

2.2 EXTRACAVITY METHOD

Several schemes exist to produce an UV tunable laser light by using nonlinear crystals and a Ti:S laser. The conventional way is to double the tunable IR light from a Ti:S laser cavity with a nonlinear crystal outside of the cavity, then mix the blue and IR outputs outside the cavity by using yet another nonlinear crystal to produce UV.

This extracavity method is not very efficient, unless the first crystal involved in the doubling process is itself in an external cavity matched to the Ti:S cavity. The same would be true with the second crystal involved in the IR and blue mixing process. This involves a complicated feedback system that has been demonstrated to yield a 50% conversion efficiency from IR to blue by using $LiIO_3$ and 5% from IR to UV by using LBO and BBO crystals (Nebel & Beigang, 1991). The choice of crystals is important, as will be shown later.

2.3 INTRACAVITY METHOD

A second scheme involves doubling the IR within the Ti:S laser cavity itself. Only two references were found of any experiment that used this scheme and only one that used a BBO crystal.

In one case, a 45% conversion efficiency from IR to blue was obtained by using a $KNbO_3$ crystal mounted in an oven for temperature tuning (Wu et al., 1990). In the other case, a 75% effective conversion efficiency from IR to blue was recorded, with a 5% efficiency from green to blue overall, by using a very thin BBO crystal (Ellingston & Tang, 1992). Theoretically, this method results in a simpler and more compact laser system, which is desirable for field equipments.

2.4 EXPERIMENTAL CAVITY

Therefore, the decision was to use an intracavity doubling and frequency mixing scheme as well as an L-shaped cavity (figure B-1), so that the IR would pass through the doubling crystal twice and the blue light would not pass back through to the Ti:S crystal.

This cavity consisted of three mirrors. The first mirror (M1) was a high reflector (HR) for the IR light produced by the Ti:S crystal centered around 800 nm. The second mirror (M2) was a high reflector for the IR light, but a high transmitter (HT) for both the blue light centered around 400 nm and the UV light centered around 266 nm produced by the sum-frequency mixing (SFM) process within the BBO II crystal. The third mirror (M3) was a high reflector for both the

IR light and the blue light produced by second harmonic generation (SHG) in the BBO I crystal. A birefringent tuning plate (BTP), used to select various wavelengths for the laser cavity, would ultimately create a tunable source of UV.

2.5 BEAM WAIST

The original mirror configuration was designed to produce a small beam spot, or waist, in the cavity near the Ti:S crystal. This waist, located at the mirror M1, would optimally produce a 180-μm waist. A small waist size of the cavity and the pump beam yields a lower threshold, and the overlap ratio of the two waists yields a higher efficiency. Having the pump waist near M1 and the laser cavity waist at the location of M1 would approximate the optimal configuration for an IR source, but the spot size also has an effect on efficiency for both SHG and SFM.

A waist near both the BBO crystals would also increase the efficiency of both blue and UV generation; but a too small waist would create a phase mismatch and decrease the conversion efficiency. Therefore, it was decided to have two waists in the cavity by using three curved mirrors from other experiments that had favorable results. A combined 50 mW of blue was produced from 1.5 W of green pump power, which is comparable to the efficiencies found in similar work (Ellingston & Tang, 1992).

2.6 NONLINEAR CRYSTALS

Two questions arose as to the type of crystals to be used. $KNbO_3$ and $LiIO_3$ are efficient doubling crystals for 800 and 400 nm, but not for mixing to produce UV. LBO and BBO are not as efficient for converting IR to blue, but can be used for frequency-mixing into the UV. LBO and BBO crystals also produce a better beam profile in doubling from IR to blue than $LiIO_3$, which is useful for frequency-mixing efficiency. Therefore, it was originally decided to use BBO for both doubling and frequency mixing due to its transparency range in the UV, its efficiency, and its SHG beam quality.

Table B-1, generated by Frank Hanson of the NCCOSC RDT&E Division, compared BBO, LBO, and KDDP crystals for both SHG (doubling to blue) and SFM (mixing IR and blue for UV). Note that a high d_{eff} (nonlinear optical coefficient) is related to a high-conversion efficiency. Also shown are the angular bandwidth B_{ang} and the spectral bandwidth B_{spec} Finally, a large walk-off angle results in poor beam quality. Not shown in the table is the transparency range, which is 160–2600 nm for LBO, 190–3300 nm for BBO, and 300–5400 nm for $LiIO_3$. Also not shown here is the damage threshold, which is dependent on wavelength.

Table B-1. Nonlinear crystals.

Crystal	Angle [deg]	d_{eff}	B_{ang} [cm*mrad]	B_{spec} [cm*A]	Walk-off [rad]
		SHG & 800 nm			
BBO I (oo–>e)	29.2	1.4	0.294	2.43	0.063
LBO I (zz–>yx)	33.7	1.03	1.13	4.185	0.0174
KDDP I (oo–>e)	27.7	0.25	0.63	0.01	0.031
KDDP II (oe–>e)	40.5	0.52	1.04	0.006	0.036
		SFM @ 800 nm & 400 nm			
BBO I (oo–>e)	44.3	1.15	0.152	0.67	0.086
BBO II (eo–>e)	55.4	0.53	0.222	0.72	0.069
LBO I (zz–>yx)	74.5	0.34	1.38	1.27	0.0099
KDDP I (oo–>e)	44.7	0.37	0.335	0.001	0.039
KDDP II (oe–>e)	58.1	0.48	0.537	0.001	0.034

3.0 APPROACH

The 5-step approach for developing a tunable UV laser cavity is described below.

3.1 PUMP SOURCE

The first step in the construction of a Ti:S laser cavity is locating a pump source in the green-to-yellow region of the spectrum. The Quantronix frequency-doubled Nd:YAG laser purchased in 1991 acted as a pump source.

3.2 CONVERSION TO INFRARED

The next step was the design and fabrication of a new Ti:S laser cavity to produce higher efficiency and a lower threshold in the IR fundamental.

3.3 DOUBLING TO BLUE

The third step was the design and construction of another Ti:S laser cavity by using nonlinear optics (BBO I) acquired in 1991. The blue light was maximized at the highest efficiency possible with the optics on hand.

3.4 MIXING FOR UV

The fourth step was an attempt to produce UV light by using a previously acquired crystal (BBO II). This also included a design of another Ti:S laser cavity that would incorporate custom optics, thereby increasing the efficiency for IR and blue production and UV throughput efficiency. Theoretically, this should increase the chances for SFM to produce UV.

3.5 WAVELENGTH TUNING

The final step was a demonstration of the tuning characteristics with the present cavity design by using a single BTP.

4.0 SETUP AND PROCEDURES

The experimental setup and the procedures followed are described below.

4.1 Nd:YAG PUMP

The pump source for the Ti:S laser was a green (532 nm), frequency-doubled, Nd:YAG laser from Quantronix (flashlamp pumped, doubled, and Q-switched). This laser has a maximum average power of 2.2 W at 2500 Hz and pulsewidth between 50 and 100 ns. This Quantronix laser was originally specified for frequency-quadrupled UV output with 200 μJ/pulse at 2500 pulses per second. The fourth harmonic crystal was removed and only the green output used.

Initial power measurements of the Quantronix laser made by the contractor showed that the maximum green output at 2.5 kHz of 4 W yielded 1.6 mJ/pulse of green light. With a quadrupler mounted, the UV power was measured to be 610 mW and yielded 244 μJ/pulse, which was within the required specifications. The output UV beam was elliptical with a beam divergence of 3-mrad horizontal and 2-mrad vertical.

Green power apparently dropped from 4 W to a little more than 2 W during the first week of operation.

4.2 CRYSTALS

Three Ti:S crystals, with 0.1% Ti^{+3} doping and various figures of merit, were used. Two BBO crystals were used: a type I BBO with a 30-degree cut and a type II BBO with a 56-degree cut.

4.3 OPTICS

An 8-inch focal length lens was used to focus the green beam into the Ti:S crystal. A half-wave plate and polarizing beam splitter were used to vary the intensity of the pump beam. The Ti:S crystal was cut at the Brewster angle and mounted with the appropriate tilt to allow only horizontally polarized light to lase. The mirrors varied greatly to obtain the most optimal cavity configuration. A single BTP was used to tune the optical frequency of the laser.

4.4 TI:SAPPHIRE

When using a sample of Ti:S and input power of 1.65 W, no IR lasing was achieved for the original cavity configuration: M1 = 100 cm radius of curvature (ROC), reflectivity (R) = 99.5% at 800 and 400 nm, M2 = flat, R = 99.5% at 45 degrees for vertical at 800 nm, M3 = flat, R = 99.5% at 800 and 400 nm. After switching M1 and M3 positions, laser output was achieved. Power output that comes from M3 and then passes through an IR filter was measured to be 3.7 mW.

When using the purchased Ti:S crystal with figure of merit 150:1 and doping of 0.1% for Ti^{+3} mounted in a large brass mount as a heat sink, 3.9 mW of IR was achieved for 2.2 W of green input. Assuming 0.5% transmission yielded 780 mW of calculated IR within the cavity, which is 35% efficiency from green to IR, the threshold pump power for the IR was 1.4 W.

The green pump was focused down too close to the surface of the Ti:S crystal, the surface sustained a burn mark, and the crystal had to be translated. Damage also occurred on the flat

mirror due to the IR beam waist. Therefore, care had to be taken as to the amount of pump power put into the cavity, so the process of alignment was slowed down. At this point, it was decided that to achieve blue light and minimal damage, the threshold for the IR would have to be reduced.

4.5 IR THRESHOLD

To drop the threshold for the IR, two parameters were changed. First, the cavity had to be shortened. Second, the mirror M3 had to be changed to a smaller ROC. This decreased the cavity waist which, along with decreasing the pump waist, lowered the threshold and increased the efficiency. This is due to the threshold power dependence on the summation of the squares of the pump and cavity waist radii and the dependence of the efficiency on the overlap of the pump and cavity mode volume.

4.5.1 Threshold Power

The threshold power is given by

$$P = E_c \, (F_p/S) \, L \, (W_o^2 + W_p^2) \, ,$$

where E_c is the coupling efficiency, F_p is the pump frequency, S is the emission cross section, and L is a loss factor, which includes upper state lifetime, crystal length, and figure of merit. W_o and W_p are the waist radii for the cavity and pump beam, respectively.

4.5.2 Laser Slope Efficiency

The laser slope efficiency is given by

$$E_s = P_{ov} \, E_c \, (F_o/F_p) \, L_s \, ,$$

where L_s is another loss term, F_o is the cavity frequency, and P_{ov} is an overlap parameter of the fraction of the absorbed pump power that overlaps the cavity mode volume (Harrison et al., 1991).

4.5.3 Tradeoffs

Several references can be found concerning the tradeoff between energy density and phase mismatch at small spot sizes to achieve the highest efficiencies within nonlinear optics and how that tradeoff is also dependent on crystal length (Beausoleil, 1992). Most of the literature suggests a small spot size (Skripko et al., 1991).

4.6 BLUE CONVERSION

With a shortened cavity, threshold was reduced to 800 mW. After inserting the BBO type I crystal, a flicker of blue with 1.5-W pump power was observed. The placement of a 30-cm ROC mirror in position M1 and flat in position M3, or flat back at M1 position and 30-cm ROC at M3, yielded no blue

However, by using a new 30-cm ROC, R>99% mirror for 800 nm and flat, R = 99.9% mirror for 800 nm, lasing was achieved at 400-mW threshold pump power. Blue light was observed at

500-mW pump power. After separation through a prism, ar average of 10 mW of blue light was observed with 1.6-W green pump power.

By using a ray-tracing program, various cavity config irations were modeled to obtain a better insight into what was happening. The best configuration from these trials was used with the two 30-cm ROC mirrors and one 25-cm ROC mirror coated for 45 degrees, which were available at the time. Note that M3 was not coated to reflect blue, so about half of the blue light was wasted. The threshold for IR was around 300 mW and about 350 mW for blue. Blue output power was between 10 to 15 mW with input green power of 1.5 W. Therefore, no significant change happened with a new configuration.

For a 2-W green input, about 25 mW of blue was obtained. Using 1.5 W of green pump power and another sample of Ti:S with a higher figure of merit resulted in an IR threshold of less tha 250 mW and output of 25 mW of blue light from each mirror (M2 and M3).

4.7 WAVELENGTH TUNING

Placing a BTP within the cavity resulted in a tuning range from 427 nm down to 395 nm with peak power around 417 nm. The cavity had to be realigned each time that the frequency was changed. Maximum divergence for both blue and IR was measured to be 2 to 3 mrad.

5.0 RESULTS

The results of this effort have been the generation of intracavity-double Ti:Sapphire laser given a green pump beam input of 1.5 W at 2.5 kHz. The tunable blue output has approximately 5 mW split into two directions. The threshold for blue was slightly above 250 mW of green pump power. The tuning range was demonstrated to be from 395 nm to 427 nm.

Attempts to mix internally to obtain UV light resulted in no detectable output. The current laser cavity configuration design was found to be inadequate. Other laser mirrors available in the laboratory were used to produce a tunable blue laser source, but many losses in efficiency occurred due to nonoptimal coatings on the mirrors. Some of these mirrors had been acquired for other NRaD projects. Similar mirrors with the proper coatings were ordered, but they were not yet physically incorporated into the design at the time that the effort was suspended by the sponsor.

6.0 PLANS

Evaluation by experienced NRaD laser scientists indicates that an endeavor of this magnitude on the leading edge of the present laser technology will take considerably more time, money, and expertise.

6.1 OPTICAL ANALYSIS

More rigorously detailed designs need to be made to ensure the optimal cavities. Mirror curvature, cavity length, and angle of incidence all play a part in an optimal configuration to be determined. The spot size in the crystals affects the efficiency of the laser in a nontrivial manner.

All of the above factors have to be looked into as part of a rigorous approach to this particular effort, since there is little previous work involving internal SHG and none involving internal

SFM for Ti:S lasers. Internal processes will, in theory, result in higher power outputs with the least customized optics, but are more difficult to implement.

6.2 PROPOSED CAVITIES

Proposed efforts include the design and testing of both intracavity and extracavity frequency mixing configurations for a Ti:S laser cavity. Each configuration proposed will include BBO crystals for both intracavity SHG to produce blue and SFM to produce UV. Four new mirrors that should improve the chances of obtaining UV have already been ordered. Other mirrors that have more promise (although a higher cost) are under consideration.

6.2.1 New L-Cavity

The first proposed configuration (figure B-2) is similar to the configuration shown in figure B-1, except that the mirrors are curved to improve beam quality. The radii of curvature of the mirrors are similar to those used previously at NRaD. The mirror coatings will be customized to accommodate this particular effort.

The pump beam, as well as the cavity IR and UV beams, is p-polarized. The blue beam is s-polarized. The blue beam is represented by the dashed lines and the UV beam is represented by the dotted line. Type I and II BBO crystals (the same crystals previously used) are cut to 30 and 55 degrees, respectively. Two Ti:S crystals, also available, are cut at the Brewster angle, allowing only the correct polarization to lase. This configuration would create two waists (approximately 120 μm in size) near the middle of each leg as before; however, with the correct coatings there will be less losses in the cavity.

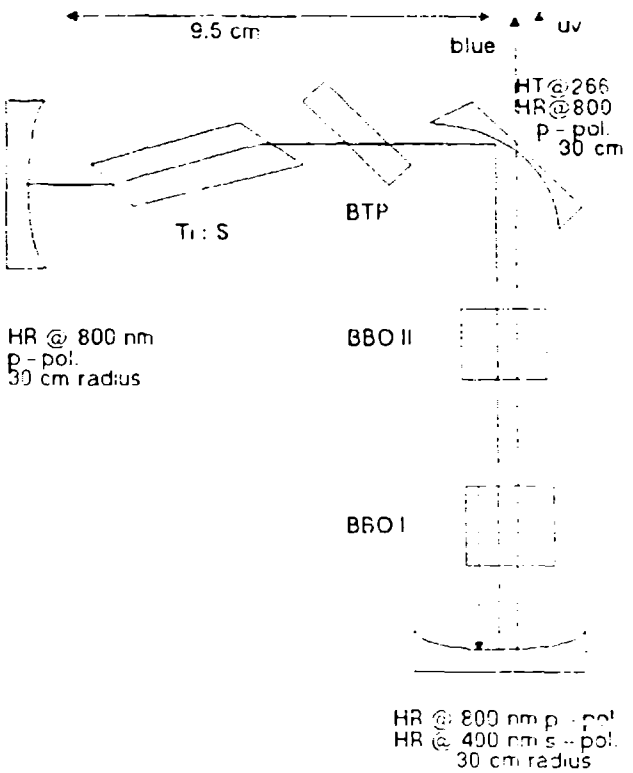

Figure B-2. New L-cavity.

6.2.2 Small Angle Cavity

The second proposed configuration (figure B-3) has more curved mirrors, which at the same cavity length would create smaller spot sizes and may increase the efficiency. The coating of the second mirror will allow a smaller incidence angle, thereby decreasing the astigmatism of the cavity mode between the S and T planes. This astigmatism affects the beam quality vital to SHG and SFM processes.

6.2.3 External Cavity with BBO I

The third proposed configuration (figure B-4) is similar to the figure B-2 configuration, but here the SFM is done by a more efficient BBO I crystal external to the Ti:S cavity.

One percent of the IR light is transmitted through the third mirror. The second mirror transmits the blue light that is mixed with IR light, which will have the same polarization after passing through a half-wave plate.

This proposed configuration includes the basic cavity design known to produce blue light, along with other components that have not yet been acquired.

6.2.4 External Cavity with BBO II

The fourth proposed configuration (figure B-5) is similar to the third configuration, except that the SFM is made with a BBO II crystal external to the Ti:S cavity. While SFM with BBO II crystal is less efficient than with BBO I, the geometry is simpler with less optical components and losses. Also, the BBO II crystal is already available.

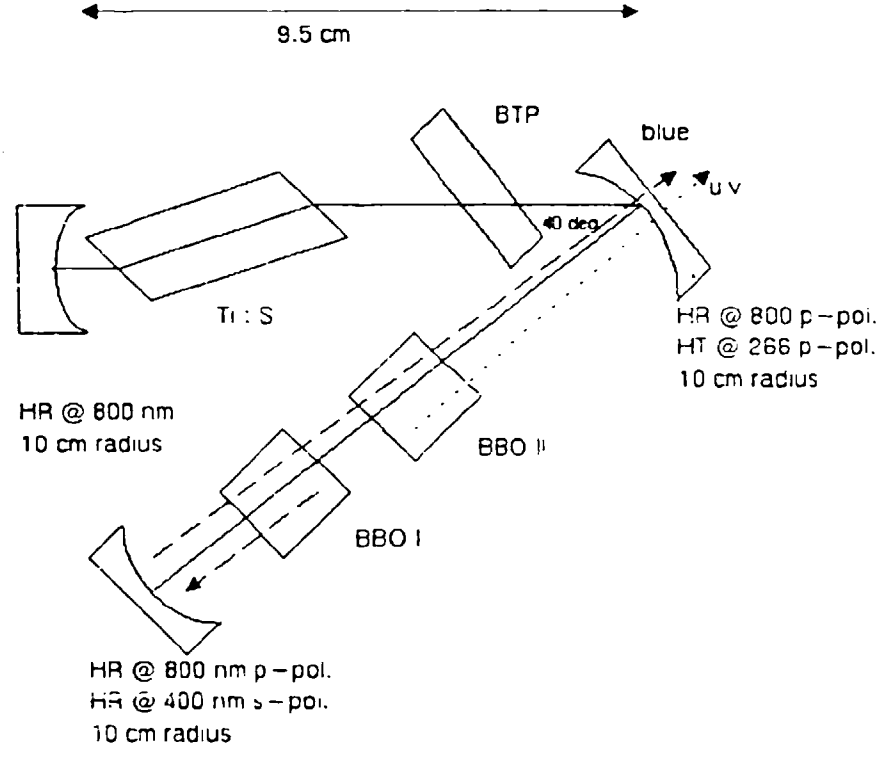

Figure B-3. Small angle cavity.

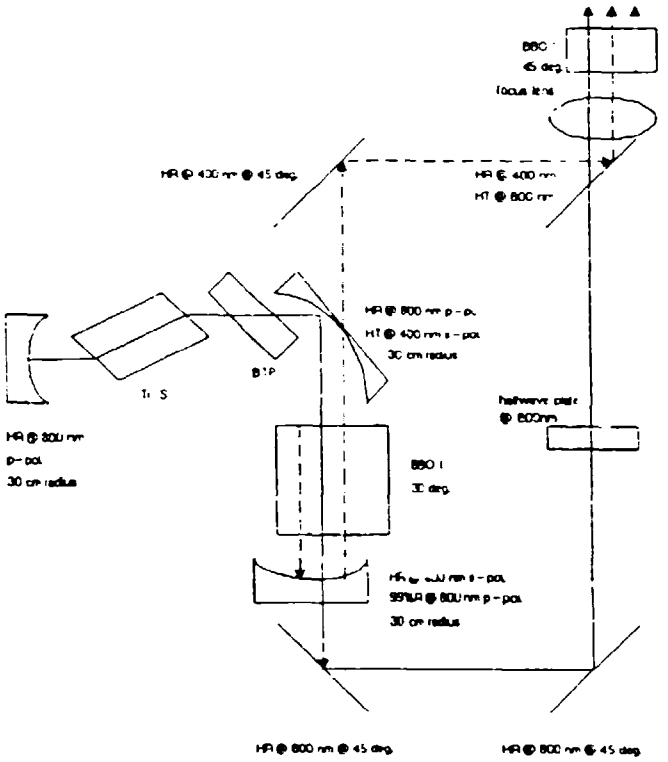

Figure B-4. External type I sum-frequency mixing.

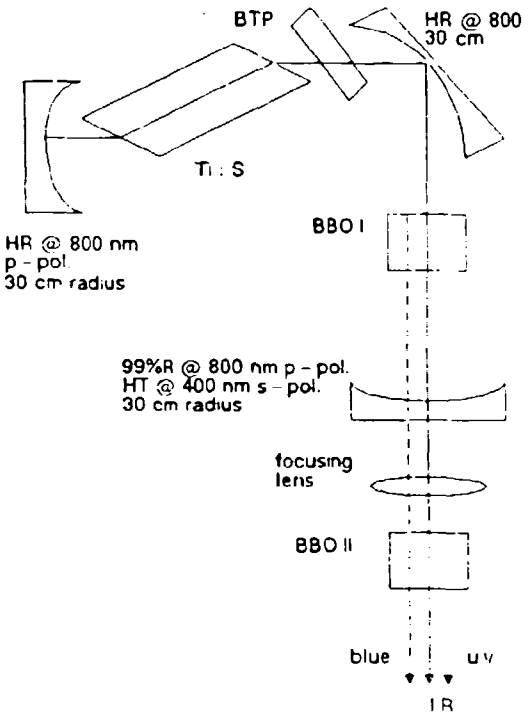

Figure B-5. External type II sum-frequency mixing.

APPENDIX C

GTE PHASE I OVERVIEW

1.0 BACKGROUND

The ISRC project solicited thr ugh the Broad Agency Announcements (BAA) for technologies that can provide LPD tactic l communications.

Three contracts were awarded under the BAA solicitation N66001-92-X-6005. This appendix is a brief summary of a BAA contract effort; a more detailed discussion will be included in a following ISRC report.

1.1 OBJECTIVE

The GTE Government Systems Corporation in Waltham, MA, proposed to develop a short-range, LPD, tactical communications system based on spread spectrum techniques in order to satisfy the ISRC requirements. GTE will deliver a design for the proposed link upon the completion of the contract.

1.2 CONTRACT DATES

The BAA contract N66001-92-C-6010 was awarded to GTE on 30 April 1992. The kickoff meeting was held on 21 May 1992 in Needham, MA. The quarterly review was held on 30 July 1992. The final review and demonstration was held on 28 October 1992.

2.0 APPROACH

The proposed GTE link was developed from GTE's Adaptive Sparsely Populated Rake (ASPARK) spread spectrum modem that was developed with GTE internal funds.

The GTE-proprietary extremely wideband direct-sequence spread spectrum (DSSS) technique would spread the RF signal over a wide bandwidth (100 MHz), thus reducing the RF power spectral density so that the signal will be hidden in the noise. The receiver, which knows where to look in the spectrum, can then reconstruct the signal.

2.1 FREQUENCY

GTE's proposal to use the Military L-Band (1.35 to 1.85 GHz) as its propagation medium was based on its operating license, as well as the propagation range, power required, antenna size, bandwidth requirements, and expected environments.

A tradeoff study on the best frequency to be used for any particular scenario will be performed as part of a Phase II effort.

2.2 MULTIPATH

The ISRC mission environments will likely involve many obstructions that result in multipath components spread over a few microseconds. While multipath effects (fading due to

interference) were problematical for ordinary communications systems, these effects can be exploited for cluttered environments such as cities and forests.

The GTE system identifies the indirect components, recovers the information in those components, and then integrates them together with the direct component into a total received signal. By recovering information in the strongest (3 to 5) indirect components, the direct component signal can be enhanced rather than degraded by multipath effects.

2.3 NLOS OPERATION

The ISRC missions may require operations without a direct component, that is, no line-of-sight between two terminals of a link. By the use of the indirect path components, GTE proposed to communicate in a non-line-of-sight (NLOS) mode. The indirect components arise from reflections off various surfaces in the region between the two terminals, such as buildings, foliage, or natural structures.

2.4 WIDE BANDWIDTH

In the DSSS scheme, the signal is spread with a pseudorandom key over a 100-MHz band at a low power level so that the signal hides in the noise. Even at a data rate of 2 Mbps, the signal can be spread into the extremely wide band employed by the GTE system. This unique wide bandwidth of the ASPARK was one of the major reasons the GTE proposal was selected for contract award.

The wide bandwidth results in very low signal strength at any one frequency, thus creating a small signature for detection by an enemy. This provides the system with its LPD characteristic.

3.0 RESULTS

The final review and demonstration was held on 28 October 1992 at the GTE plant in Needham, MA. The final review was attended by John Yen and also by Chuck Mirabile, who represented the project sponsor.

3.1 TECHNICAL

The study and adaptation of the DSSS technique, from which GTE adapted the ASPARK modem for this effort, went well. The GTE progress for the contract met all the initial milestones. A government reservation regarding the engineering support (more effort needed in building reliable equipment) appeared to be resolved.

3.1.1 Vulnerability Analysis

The vulnerability study made of the proposed link indicated that the LPD characteristic is very good. In a classified appendix to the Phase I final report, vulnerability to feature extraction detectors was analyzed. The GTE system implemented countermeasures that reduced feature detector effectiveness below that of radiometers.

3.2 SATELLITE TERMINAL DEMONSTRATION

The Portable Satellite Terminal (POST™) demonstration (figure C-1) showed the viability of the DSSS scheme as the POST™ system uses the same DSSS technology as the ASPARK. Two

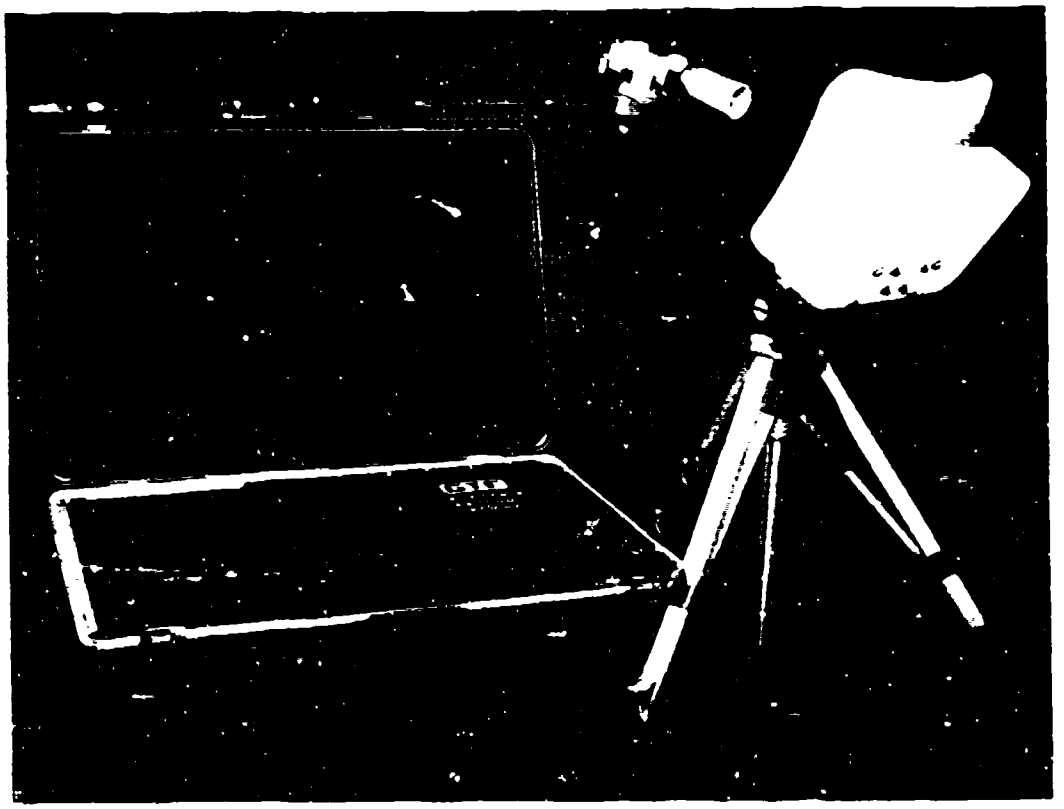

Figure C-1. Portable satellite terminal (POST™).

POST™ terminals at the Needham plant were linked through a satellite over the Pacific Ocean. Voices and faxes were sent through the link at a data rate of 16 kbps.

3.3 LABORATORY DEMONSTRATION

A laboratory demonstration with the RF/simulator breadboard (figure C-2) and the ASPARK modem (figure C-3) was performed. During the demonstration, an image (250 kBytes or 2 Mb) was transmitted through a multipath simulator (several cables of length 500 meters connected in a series, resulting in path lengths of x, x+500, x+1000 meters). This demonstrated the ASPARK adaptation's capability to reconstruct three multipath components into a coherent signal. The image was transferred at a data rate of 16 kbps, with 2 errors during the 2 minutes of transmission (corresponding to $1x10^{-6}$ bit error rate).

3.4 PHASE II PLANS

GTE has provided the Government with an ISRC Phase II Program Plan that covers the work to be performed during a Phase II effort.

Figure C-2. GTE RF/simulator.

Figure C-3. GTE ASPARK modem breadboard.

4.0 CONCLUSIONS

The GTE system is based on a mature technology and has a relatively low risk in developing the prototype link into fieldable equipment. The GTE system also has a high data rate and can also support all three USMC missions.

While its NLOS capability remains unresolved, the multipath aspects of the GTE system may provide NLOS capability.

5.0 ACKNOWLEDGMENTS

John Lovell of GTE Government Systems Corporation, the principal investigator for this effort, can be reached at (617) 455-3606. Any questions regarding the ISRC project should be addressed to John Yen at (619) 553-6502.

APPENDIX D

MRC PHASE I OVERVIEW

1.0 BACKGROUND

The ISRC project advertised through the Broad Agency Announcements (BAA) for technologies that can provide LPD tactical communications.

Three contracts were awarded under the BAA solicitation N66001-92-X-6005. This appendix is a brief summary of a BAA contract effort; a more detailed discussion will be included in a following ISRC report.

1.1 OBJECTIVE

The Mission Research Corporation (MRC) in Los Alamos, NM, proposed to develop a short-range, LPD, tactical communications system based on UV radiation propagation. MRC would study UV sources, such as lamps and lasers, and determine the optimal source to use in the proposed link. MRC would deliver a design for the proposed link upon the completion of the contract.

1.2 CONTRACT DATES

The BAA contract N66001-92-C-6007 was awarded to MRC on 6 April 1992. The kickoff meeting was held on 22 May 1992 in Los Alamos, NM. The quarterly review was held on 4 August 1992. The final review and demonstration was held on 5 November 1992.

2.0 APPROACH

The MRC link is based on the transmission characteristics of UV radiation in the atmosphere, which absorb the radiation exponentially and scatter UV photons efficiently. The solar-blind region of the electromagnetic spectrum offers a unique low-noise spectral region in which to operate a link with a very low signal, such as scattered UV light.

2.1 OZONE LAYER

The fact that ozone absorbs UV radiation in the 220–285 nm band combined with the ozone layer in the upper atmosphere results in a spectral region virtually free of natural solar background. The low background enables the detection of the small number of photons from an UV signal, which were much smaller than the noise level for other types of radiation.

2.2 ABSORPTION

Ozone absorption in the lower atmosphere also reduces the UV signal exponentially, resulting in a very short range for UV transmissions. The signal will not be detectable a few kilometers beyond the operational range, thus the link will be LPD.

2.3 SCATTERING

The scattering (Rayleigh for molecules and Mie for aerosols) characteristics of UV radiation in the atmosphere also diffuse a region around the transmitter with UV photons. Because of the

low background, such scattered photons can be detected and used so that, under some conditions, a non-line-of-sight (NLOS) link will exist.

2.4 TECHNICAL OBJECTIVES

MRC proposed to study further the phenomena associated with UV propagation and to develop a more effective UV source in support of designing a Phase II system.

2.4.1 Modelling

MRC used a computer propagation model to predict the effects of various parameters of the atmosphere on the UV signal and then compared these predictions with actual data.

2.4.2 UV Source Comparison

MRC compared UV lamps and UV lasers to determine the optimal source to use in the proposed UV link. The MRC study concluded that a UV laser would provide a better source and the Government representatives concurred.

2.4.3 UV Laser

MRC subcontracted with Big Sky Laser to develop and fabricate a compact transmitter package based on a quadrupled Nd:YAG laser. The laser will be air-cooled with a closed-cycle water cooling system.

2.4.4 Modulation

The laser outputs 600 pps, which is too slow for voice throughput. Therefore, MRC proposes to use an 8-ary pulse position modulation (PPM) to obtain an effective throughput of 4800 bps. The system can be upgraded to 9600 bps.

2.4.5 UV Receiver

MRC developed an effective UV filter and subcontracted with Barr Associates to fabricate it. The resultant filter has very good transmission characteristics in the solar-blind region.

3.0 RESULTS

3.1 TECHNICAL RESULT

MRC put together a UV laser package no bigger than an oscilloscope. The package included the laserhead, drivers, fans, and water cooling unit (figure D-1). The only external hardware was a 28-VDC power supply. The receiver package is compact and already runs on a battery.

3.2 DEMONSTRATION

The demonstration, a totally NLOS test, was performed at a range of 0.5 km on a cliff behind a large building. MRC did not have the modem (to be made in Phase II) to control laser output, so only a 600-Hz laser pulse train that was detected by their prototype receiver was sent out. The receiver detects the UV photon and determines whether there is a laser pulse and then displays results on oscilloscope.

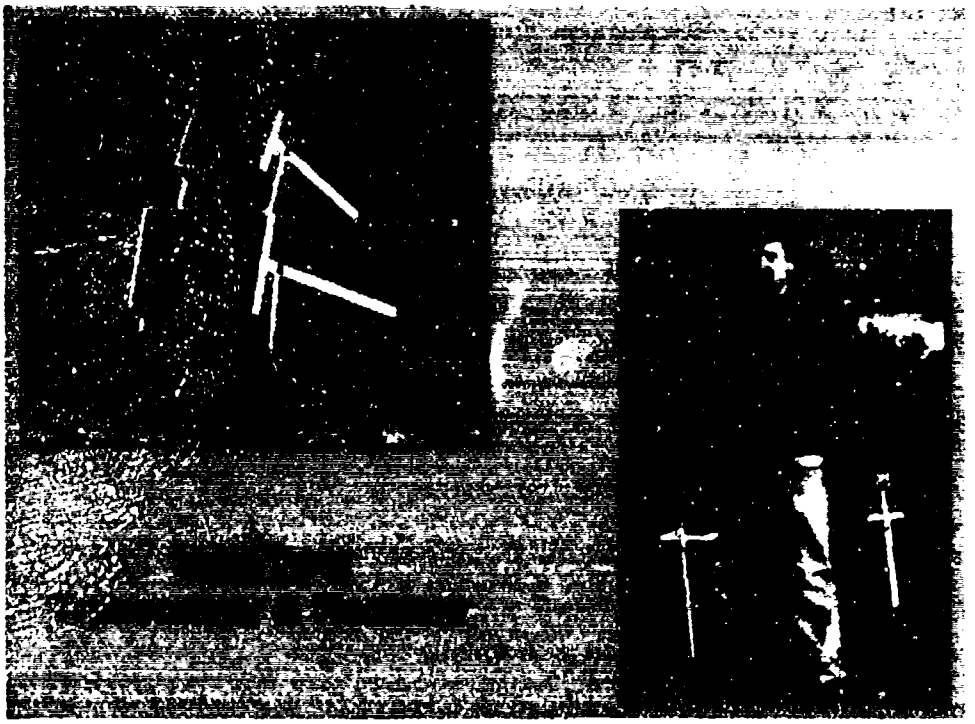

Figure D-1. MRC SBUV hardware.

3.3 PHASE II PLAN

MRC has provided the Government with a BAA Phase II Proposal that covers the work to be performed during a Phase II effort.

4.0 CONCLUSIONS

The MRC progress in Phase I is impressive. The small transmitter and receiver packages indicate a good prospect for a fieldable demonstration unit.

5.0 ACKNOWLEDGMENTS

Barry Charles of MRC, the principal investigator for this effort, can be reached at (505) 662-2133. Any questions regarding the ISRC project should be addressed to John Yen at (619) 553-6502.

APPENDIX E

SPARTA PHASE I OVERVIEW

1.0 BACKGROUND

The USMC and the ISRC project solicited through the Small Business Innovation Research (SBIR) for technologies that can provide LPD tactical communications.

One contract was awarded under SBIR solicitation N91-308. This appendix is a brief summary of the SBIR contract effort; a more detailed discussion will be included in a following ISRC report.

1.1 OBJECTIVE

Sparta, Incorporated, of San Diego, CA, proposed to develop a short-range, LPD, tactical communications system based on ultraviolet (UV) lamps. Sparta will evaluate various UV lamps and incorporate the optimal one in the link design. Sparta would deliver a design for the proposed link as a deliverable for the contract.

1.2 CONTRACT DATES

The SBIR contract N66001-92-C-7007 was awarded to Sparta on 30 January 1992. The kickoff meeting was held on 11 March 1992 in San Diego, CA. In May 1992, Sparta was granted an extension of the contract to 6 November 1992. The quarterly review was held on 25 August 1992. The final review and demonstration was held on 3 November 1992.

2.0 APPROACH

The proposed Sparta link is based on the transmission characteristics of UV radiation in the atmosphere, which absorb the radiation exponentially and scatter UV photons efficiently. The solar-blind region of the electromagnetic spectrum offers a unique low-noise spectral region to operate a link with a very low signal, such as scattered UV light.

2.1 OZONE LAYER

The fact that ozone absorbs UV radiation in the 220–285 nm band combined with the ozone layer in the upper atmosphere results in a spectral region virtually free of natural solar background. The low background enables the detection of the small number of photons from a UV signal. This number was much smaller than the noise level for other types of radiation.

2.2 LPD

Ozone absorption in the lower atmosphere also absorbs the UV signal exponentially, resulting in a very short range for UV transmissions. The signal will not be detectable a few kilometers beyond the operational range. Thus, the link will be LPD.

2.3 NLOS

The scattering characteristics of UV radiation in the atmosphere also make possible a region around the transmitter that the UV photons permeate. Because of the low background, such

scattered photons can be detected and used so that, under some conditions, it is possible to have a non-line-of-sight (NLOS) link.

2.4 UV RENLOS

The Sparta Laser Systems Laboratory (LSL) has developed the UV restricted envelope non-line-of-sight (RENLOS) voice communications system based on UV propagation (figure E-1). This system, based on arc lamps, has been tested in the San Diego area.

2.5 DPPM

Because of the relatively low repetition rate of UV lamps, Sparta proposed to use the differential pulse position modulation (PPM) to increase the data throughput to a 4800-bps data rate.

2.6 TECHNICAL OBJECTIVES

Sparta proposed to study further the phenomena associated with UV propagation and to develop a more efficient UV lamp source in support of designing a Phase II system.

2.6.1 Modeling

A computer propagation model was used to predict the effects of various parameters of the atmosphere on the UV signal and compared these predictions with actual data. Also studied was the practicality of an omnidirectional system.

2.6.2 Surface Discharge Lamp

Sparta developed a surface discharge UV lamp that is more efficient and faster than the gas or arc lamps (figure E-2). Faster lamps would allow a greater data throughput and carry out more ISRC missions. Higher lamp efficiency would reduce the power requirement, thus the size and weight.

3.0 RESULTS

3.1 TECHNICAL RESULT

The technical brief was done well, with adequate discussions on the surface discharge lamp, propagation modeling, and battery power. All the initial contract objectives were satisfied. Some Government reservations regarding the safety of the proposed system were discussed and should be addressed later.

3.2 DEMONSTRATION

The Sparta surface discharge lamp was not available at the final review. Progress seemed to be reasonable considering that Sparta received only $50K for the initial SBIR effort. On the following day, Richard Morton showed the surface discharge lamp just received from MA, but the lamp could not be run as no lamp driver was sent.

3.3 PHASE II PLAN

Sparta has provided the Government with a Sparta Phase II ISRC Plan that covers the work to be performed during a Phase II effort.

Figure E-1. SPARTA prototype voice communicator.

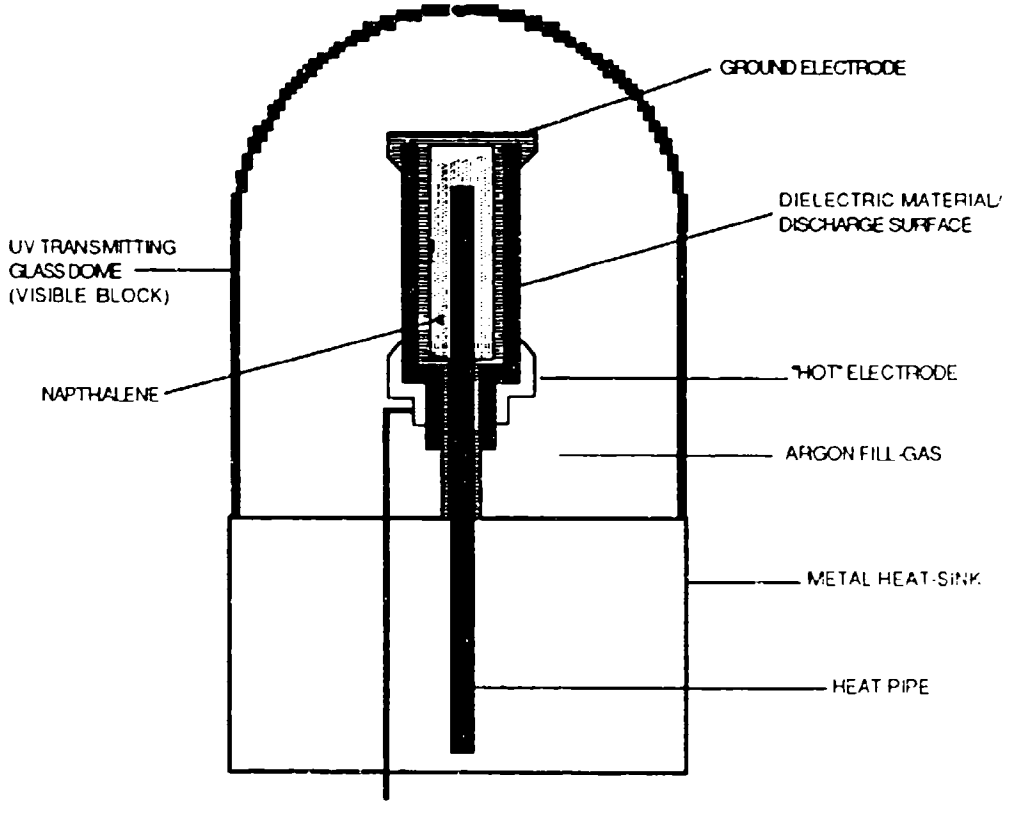

Figure E-2. SPARTA UV surface-discharge source.

4.0 CONCLUSIONS

The Sparta system is based on a relatively mature technology and can be applied toward the ISRC missions that use lower data rates.

5.0 ACKNOWLEDGMENTS

Richard Morton of the Sparta Laser Systems Laboratory, the principal investigator for this effort, can be reached at (619) 455–1650. Any questions regarding the ISRC project should be addressed to John Yen at (619) 553–6502.

APPENDIX F

TITAN PHASE I OVERVIEW

1.0 BACKGROUND

The ISRC project advertised through the Broad Agency Announcements (BAA) for technologies that can provide LPD tactical communications.

Three contracts were awarded under the BAA solicitation N66001-92-X-6005. This appendix is a brief summary of a BAA contract effort; a more detailed discussion will be included in a following ISRC report.

1.1 OBJECTIVE

The Titan Systems Group in San Diego, CA, proposed to develop a short-range, LPD, tactical communications system based on an infrared (IR) laser diode array that emits in the water absorption band about 1.39 μm. At the end of the contract, Titan would deliver a design for the proposed link.

1.2 CONTRACT DATES

The BAA contract N66001-92-C-6005 was awarded to Titan on 14 May 1992. The kickoff meeting was held on 3 June 1992 in San Diego, CA. The quarterly review was held on 3 August 1992 in Albuquerque, NM. The final review and demonstration was held on 6 November 1992 in Albuquerque, NM.

2.0 APPROACH

The proposed Titan link is based on the transmission characteristics of IR radiation in the atmosphere where water vapor absorbs the radiation exponentially.

2.1 ABSORPTION

Water vapor has many absorption bands in the atmosphere where the attenuation coefficient increases by many orders of magnitude. By selecting a wavelength (centered at 1.39 μm) on the edge of one of these bands, Titan proposed to build a link that was attenuated a short distance beyond the operation range. By being on the edge of the band, Titan could then vary the range by changing the wavelength.

2.2 LASER DIODE

Titan proposed to build an InGaAsP laser diode that could be tuned to emit at a wavelength between 1.32 and 1.35 μm. The subcontractor, David Sarnoff Research Center, was to fabricate a tunable laser diode with center wavelength of 1.335 μm and tuning range of ±0.013 μm.

2.3 TUNING

The laser wavelength is tuned by varying the temperature of the diode. To obtain the wavelength range, the diode temperature must be controllable in the range between −20° to +50° C.

To keep the wavelength stable, the temperature must be stable. The wavelength gradient of the laser diode is about 0.3 nm/deg C, so that the temperature must be maintained in a 6°C range for the wavelength to remain within ±1 nm.

2.4 MODULATION

The laser diode has the potential of being modulated at rates of up to 15 MHz, although a practical rate of a few megahertz is more likely. This high potential data rate will more than satisfy the ISRC data rate requirements and indicates that this system should be targeted toward the missions needing higher data rates.

Titan currently uses a pulse generator to modulate the laser diode and envisions using a pulse position modulation (PPM) scheme to code actual data.

2.5 RECEIVER

Titan proposed to use an InGaAs photodiode behind an interference filter and focusing lens as the receiver of the link. All parts are commercially available.

2.6 POWER CONSUMPTION

The proposed Titan link's power requirement, on the order of 500 W, is well within the power specification listed in the BAA solicitation.

2.7 ANGULAR SPREAD

The laser diode was designed to emit at a large angular spread, on the order of 10 degrees. This, coupled with a wide field-of-view detector, will alleviate some of the difficulties associated with aligning LOS systems. However, because of the weak molecular IR scattering characteristics and the natural IR background, the Titan link will have a low probability of ever operating in the NLOS mode.

3.0 RESULTS

3.1 TECHNICAL

The technical briefing, with the IR laser diode subcontractor (Sarnoff Research Center) participating, was well done. The laser diode characterization was performed well, although a question remains as to the reason for "rabbit ear" vertical output profile. Titan will make more measurements to confirm.

Government reservations about the ability of Titan to maintain diode temperature stability indicate that Titan and Sarnoff should further investigate other methods of temperature control during Phase II.

3.2 DEMONSTRATION

Titan demonstrated an IR link outdoors during the final review. All hardware was powered by AC lines. The laser diode (figure F-1) was pulsed at a rate of 50 kHz. The receiver was set up about 70 m away (figure F-2). Since no modem was built (part of Phase II), no real data were sent through the link. This link is strictly LOS. When someone walked into the beam path area between the transmitter and receiver, the link was lost.

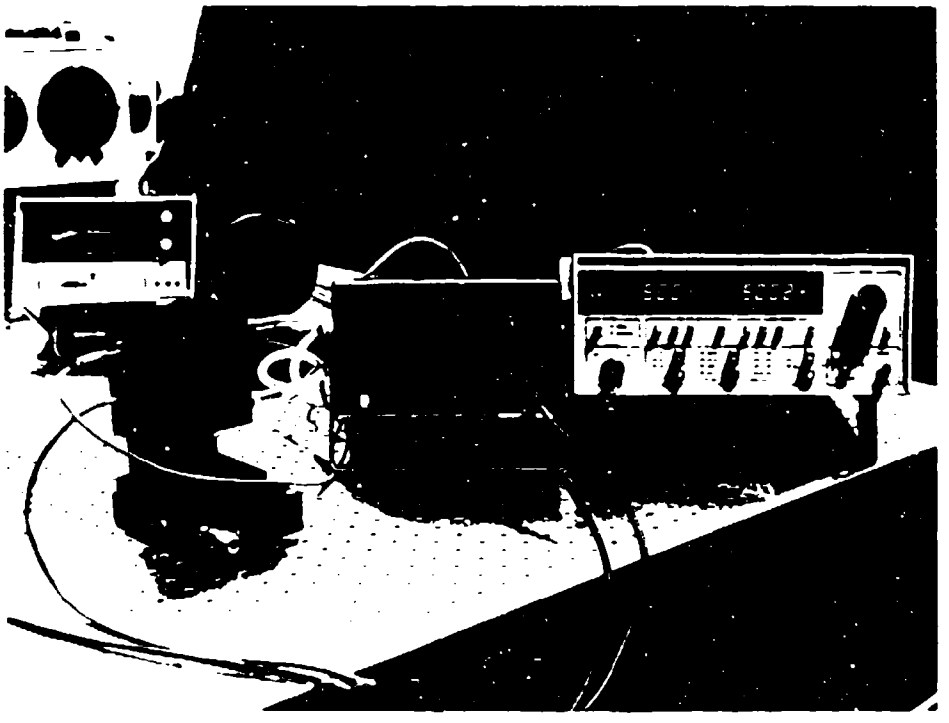

Figure F-1. Titan IR laser diode.

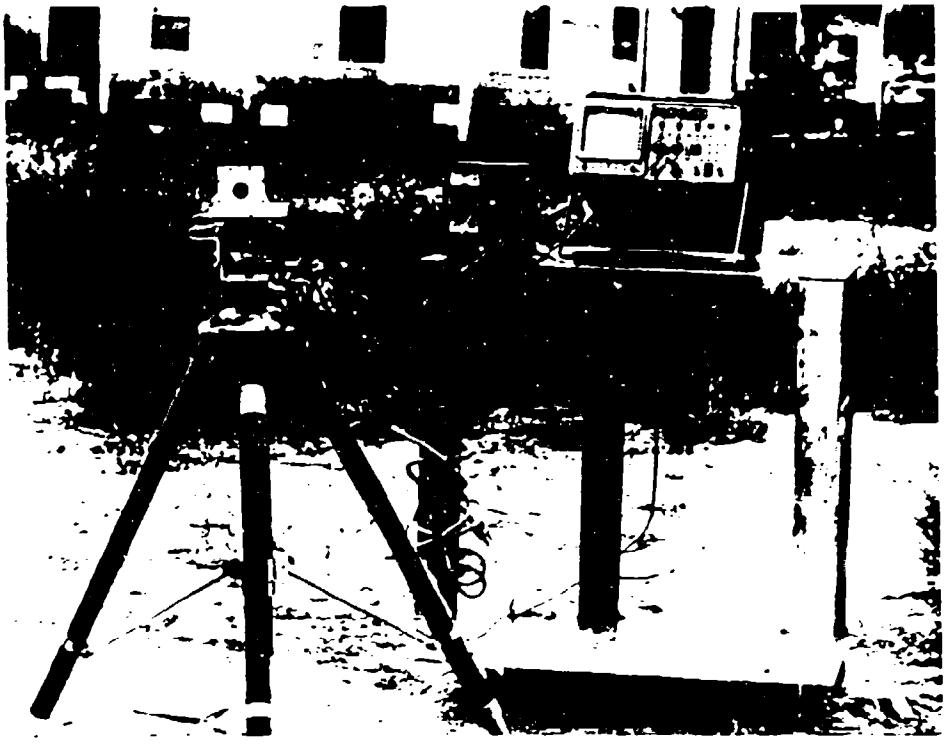

Figure F-2. Titan receiver.

3.3 PHASE II PLAN

Titan has provided the Government with a plan for Phase II of Short-Range Infrared Laser Communication. The plan covers the work to be performed during a Phase II effort.

4.0 CONCLUSIONS

The Titan system has the potential of providing a high-data-rate link, on the order of 2 Mbps, to support high-data-rate ISRC missions, although the LOS limitation of the Titan IR link is unfortunate.

5.0 ACKNOWLEDGMENTS

Jeffery Puschell, the principal investigator for this effort, can be reached at (505) 764–5315 in Albuquerque, NM. Any questions regarding the ISRC project should be addressed to John Yen at (619) 553–6502.

APPENDIX G

RAMAN SHIFT EXPERIMENT

1.0 INTRODUCTION

This is a summary of the work performed on Raman scattering for the ISRC project. The ISRC project proposed to use an UV laser for very short-range tactical communications. UV light is selected for this application because of the strong attenuation of UV radiation by the atmosphere. Having a tunable laser to adapt to changing atmospheric conditions will be highly desirable.

1.1 RAMAN SHIFTING

A possibility for a tunable UV laser will be the use of a quadrupled Nd:YAG laser that produces light at 266 nm and shifts its frequency by using the Raman effect. Hydrogen gas (H_2), one of the most effective Raman scattering materials, has a rotational Stokes shift at 582 cm^{-1} and vibrational Stokes shifts at 4160 cm^{-1}. This gives rotational lines at 270.183 nm, 274.5 nm, 278.96 nm, etc., and a vibrational line at 299.1 nm. Any of these lines will be within the solar-blind region (220–300 nm) in which UV communication operates.

1.2 EXPERIMENTAL REQUIREMENTS

The purpose of this experiment was to determine whether one can get efficient conversion to separate individual lines within the region of interest to the ISRC project. The ISRC laser was expected to produce about 200 μJ of UV energy per pulse 50–100 ns long. The laser used in the experiment had a pulsewidth of 5–7 ns. Since the Raman conversion threshold roughly scaled inversely with pulse length, one needed to see a Raman shift threshold at less than 20 μJ in this experiment for the effect to be useful when using the ISRC laser.

2.0 VIBRATIONAL SHIFT

2.1 SETUP

This section describes the setup for the first phase of this experiment. The laser light was changed to circular polarization by using a quarter-wave plate, then focused into a 2-m hydrogen tube by using a 0.5-m focal-length lens. The output from the cell was sent into an integrating sphere coupled directly into the spectrometer.

2.2 RESULTS

A 4-mJ threshold was obtained at 800 mTorr and a 2.5-mJ threshold was obtained at 1500 mTorr. While increasing the pressure was expected to reduce the threshold, it could not even begin to approach the desired 20-μJ threshold required for ISRC.

2.3 MODIFICATION

Since almost all of the Raman conversion occurred at the point where the beam was focused, the 2-m-long Raman cell was unnecessary. Therefore, the threshold at 1500 mTorr was later reexamined using a 1-meter cell. Although the energy was not calibrated, the threshold was clearly still about 3-4 mJ.

3.0 ROTATIONAL SHIFT

3.1 SETUP

This experiment attempted to lower the threshold for the rotational Raman shift by making two passes through a 1-m cell. The results were never completely calibrated on this phase of the experiment, so the energies mentioned here were only approximate.

3.2 RESULTS

At 1500 mTorr, the threshold was about 1.5 to 2.0 mJ, with the first vibrational shift dominating. Initially, this was a surprise because circular polarization of the light should favor rotational shifting.

3.3 CELL PRESSURE

Steve Bowman (Bowman et al., 1989) of the Naval Research Laboratory (NRL) found that in a two-cell system, the cell pressure during the first pass needs to be less than one atmosphere [1] Otherwise, enough of a seed of vibrational Stokes would be formed that would dominate in the second pass, since the vibrational Stokes has a much higher gain once it is initiated. Reducing the pressure of the single-cell, 2-pass system to 550 mTorr is necessary to get significant rotational Raman shifting. At that point, the threshold was about 4 mJ, which is higher than that for vibrational shifting.

4.0 CONCLUSIONS

Raman shifting in a gas medium is unlikely to result in a practical tunable UV laser system suitable for ISRC. Raman shifting in solids is intriguing and should be investigated if Raman shifting is to be pursued, but does not fall under the limited scope of this experiment.

5.0 ACKNOWLEDGMENTS

This experiment was performed by Maureen O'Brien of NCCOSC RDT&E Division. This work was completed using the equipment and assistance of Frank Hanson, also of RDT&E Division.

6.0 REFERENCES

Bowman, S. R., B. J. Feldman, J. M. McMahon, A. P. Bowman, and D. Searl. 1989. "Laser Techniques and Frequency Conversion for a Neodymium-Based Blue Communication Transmitter," *OSA Proc. Tunable Solid State Lasers*, **5**, 108.

1 Bowman, S. R., NRL, private communication, 1993

APPENDIX H

LONGITUDINAL LIGHT SCATTERERS

1.0 INTRODUCTION

The purpose of the ISRC Company Radio development program is to demonstrate a propagation-limited system for very short-range communications. This system would have the advantage of a very low probability of detection (LPD) outside its intended range.

One candidate system is based on an UV laser. For that system to work, each laser pulse must be spread out in all directions along the horizontal. This study will examine several schemes for such a longitudinal light scatter (LLS) and recommend a course of action.

1.1 LASER PARAMETERS

The current study assumes a quadrupled Nd:YAG laser emitting at a wavelength of 266 nm. The parameters of the laser in question are expected to be the following:

Beam width	0.2 mm
Beam divergence	2.5 mrad
Energy per pulse	200 μJ
Pulse width	50-70 ns
Pulse rate	≈3 kHz

1.2 OPTICS

At this wavelength, only pure UV-grade silica can be used for the optical components. Because diamond tooling is not accurate enough, specialized components must be ground and polished.

1.3 CONFIGURATION

To lessen the eye safety problem and to ensure efficient propagation of the beam, the UV light must be sent vertically upward at least five meters. The UV light will then be scattered azimuthally. Schemes to accomplish this will be discussed in the following sections.

2.0 VERTICAL CHANNEL

Essentially, two ways that can bring the UV light up five meters to the LLS are propagation (1) through an enclosed tube or (2) through an optical fiber.

2.1 TUBE

In the enclosed tube design, light is reflected upward by using a 45-degree mirror. Because of the eye safety problem, the light path must be enclosed by a UV absorbing or reflecting tube. The LLS assembly will be attached to the top of the tube if the tube is rigid enough; if not, the assembly will be bound to a rigid pole. Given a 2.5-mrad divergence and a 5-m beam path, the spot size will still be only 1.25 cm. This should not be a problem for the LLS.

The most likely problem is that the pole must be rigid to prevent misalignment of beam optics, but lightweight enough to be practical in the field. Guidewires are not considered practical for anchoring it to the vehicle and the system must be able to function in high winds. For instance, if the structure should tilt by even 1 degree, an unacceptable 8.73-cm misalignment would result. Therefore, this design was ruled out.

2.1.1 Losses

This system would have the lowest losses. Transmission through the air in the tube is about 98.3% (based on attenuation of 3.5 km^{-1} from Yen, 1992). One mirror is needed to direct the light upward, with a typical loss of 10% for UV optics. Thus, the total transmission up the tube would be 88%, provided that adequate alignment of this system is possible.

2.1.2 Costs

Costs involve one 45-degree mirror and the fabrication of the 5-m rigid tube. As this was not deemed a feasible approach, a detailed costing was not pursued.

2.2 OPTICAL FIBER

The second and perhaps only practical approach is to bring the beam upward by using an optical fiber.

2.2.1 Losses

At high intensities, around 1 MW/cm^2, two photon processes can excite the band gap of the fiber.[1] This nonlinear effect can cause very high losses. Assuming the minimum pulse width of 50 ns, the ISRC laser delivers 4 kW/pulse. At the beam waist, this is 12.7 MW/cm^2.

To reduce the intensity to 1 MW/cm^2, the beam must be at least 0.712 mm wide. The beam can be expanded by using a simple biconcave lens or a beam expander and a 1-mm fiber. Five meters would cost about $850 (at $170/m) for the basic silica-clad fiber. A plastic clad 1-mm UV fiber costs $25/meter, but it would be suitable only for testing purposes and not for field applications. Fibers shift around in the plastic cladding and become unreliable.

The expected 300–400 dB/km loss in the cable varies from batch to batch for each manufacturer.[1] The quality of the UV glass that the fiber manufacturers start with is very unpredictable. Figuring reflection losses of 4% at each end of the fiber (see Oriel catalogue), the minimum 10% loss for the expanding lens, and 400 dB/km for the fiber (T = 0.63), the total transmission will be 52.3% to the LLS (58.7% if a 300-dB/km cable is obtained). This is about 60% of the transmission expected from the tube (section 2.1).

2.2.2 Configuration

For the field version of this system, the 5-m pole would be assembled from sections with the LLS bolted onto the top section. The pole, when assembled, would have a slot on the side into which the fiber fits. This would protect the fiber from the elements.

2.2.3 Costs

A 20x beam expander costs about $900 from Oriel. Other quotes have ranged to nearly double. The fiber would cost $50. The total cost would be about $2000.

[1] Theriault, G., Computer Sciences Corporation, private communication, 1992.

3.0 LLS ALTERNATIVES

At the top of the vertical channel, a LLS is needed to direct the UV light to all azimuthal directions.

3.1 INTEGRATING SPHERE

One LLS design uses an integrating sphere with a series of azimuthal exit ports along the equator of the sphere. An integrating sphere is a sphere with a small entrance port that is painted internally with a highly reflective diffuse scatterer. Upon entering the sphere, light reflects and ultimately appears to come from all directions.

3.1.1 First Reflection

The first reflection within the sphere is simply reflected at the top in all directions. The energy leaving the sphere on the second reflection is proportional to the angle intercepted by the output windows from the top of the sphere. Starting with the first reflection, light is scattered from all directions within the sphere.

Let: S_0 = surface area of integrating sphere
S_1 = surface area of exit ports
S_2 = surface area of entrance port

R = reflectivity of paint within sphere

w = width of output port window (assumed to be continuous about the the sphere's equator)

Rs = radius of sphere
a = aperture for input port

$$S_1' = S_1/S_0 = w/(2.0 * Rs)$$
$$S_2' = S_2/S_0 = (a/4.0 * Rs)^2 \approx 0.0$$

On each reflection, the energy going out the windows is proportional to S_1' times the energy remaining in the sphere. It can be shown that the output energy from the sphere is

$$E = \lim_{N \to \infty} S_0' R \left[\pi^{-1} + C(1 - A^{N-1})\right]$$

$$\approx S_0 R \pi^{-1} \left[1 + \pi C\right], \qquad (1)$$

where $N = 0$ for the initial reflection at the top of the sphere
$A = R(1 - S_1')$
$C = R(1 - S_1'\pi^{-1})/(1 - A)$.

3.1.2 Reflectivity

The output energy is plotted in figure H-1 for a variety of reflectivities. The efficiency is heavily dependent on the reflectivity of the sphere and the size of the output port. Manufacturers

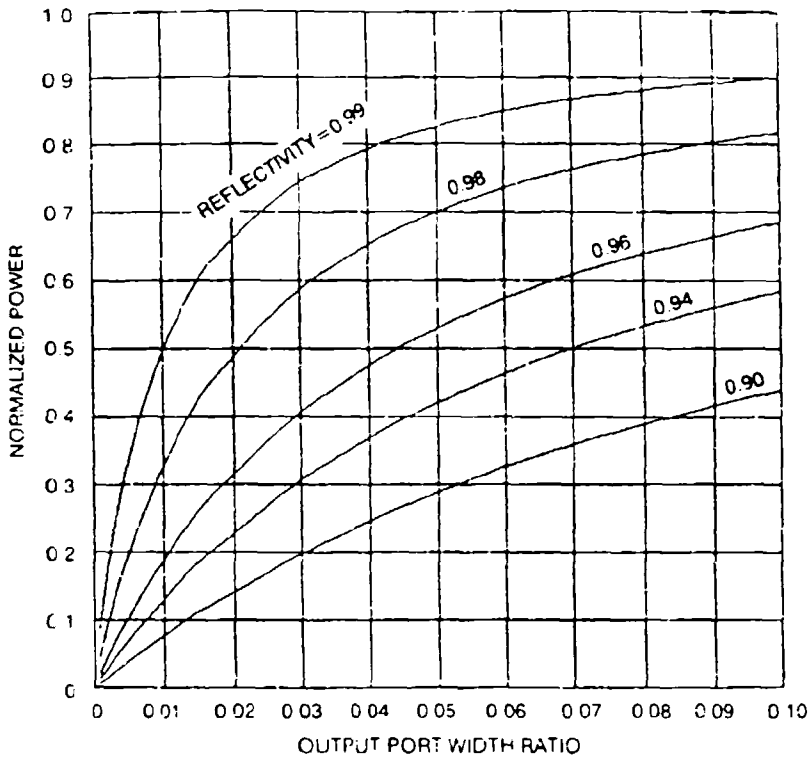

Figure H-1. Integrating sphere output power.

have estimated reflectivities for their spheres to be from 0.93 to 0.96 at 266 nm. A carefully applied paint (Grum & Lyckey, 1968) had a reflectivity of 0.96 at this wavelength. A reasonable choice for reflectivity of 0.95 with an S_1 of 0.05 has an output of 47% of the input energy (for an 8-inch sphere, this would correspond to a window at the equator 0.4 inch wide).

The output of the sphere would be in all azimuthal directions, so one would figure about half of the output energy would go into the ground. Another fraction would be lost to the sky. Some of this will scatter back to the receivers. The majority of light collected at the receivers will be scattered (Yen, 1992).[2] Because more of the light is initially directed upward than in other LLS designs, more will be lost to upward scattering. Because of the lack of directionality of the output of the sphere, a 24% efficiency for the parameters above must be considered an upper limit. If this is combined with the loss due to transmission of the fiber, this would give a maximum system efficiency of 12%.

3.1.3 Subsequent Reflections

Assuming the mean number of reflections of the light within the sphere is equivalent to the number of reflections it takes for the output energy to reach half of the limiting value above,

$$S_o' R\pi^{-1}[1 + \pi C] = S_o' R\pi^{-1}[1 + \pi C(1 - A^{N-1})]$$

$$N = 1 + LOG_e [(1 + (\pi C)^{-1})] / LOG_e (A) . \qquad (2)$$

[2] Yen, J., NCCOSC RDT&E Division, private communication, 1992.

Equation 2 is plotted in figure H-2. For the $R = 0.95$, $S_2 = 0.05$ sphere given above, the mean number of reflections is 4.99. This should be enough to make the light within the sphere look fairly isotropic. It also means that the time spreading is insignificant within the sphere. For the example of the standard 8-inch sphere, the spreading is 0.678 ns.

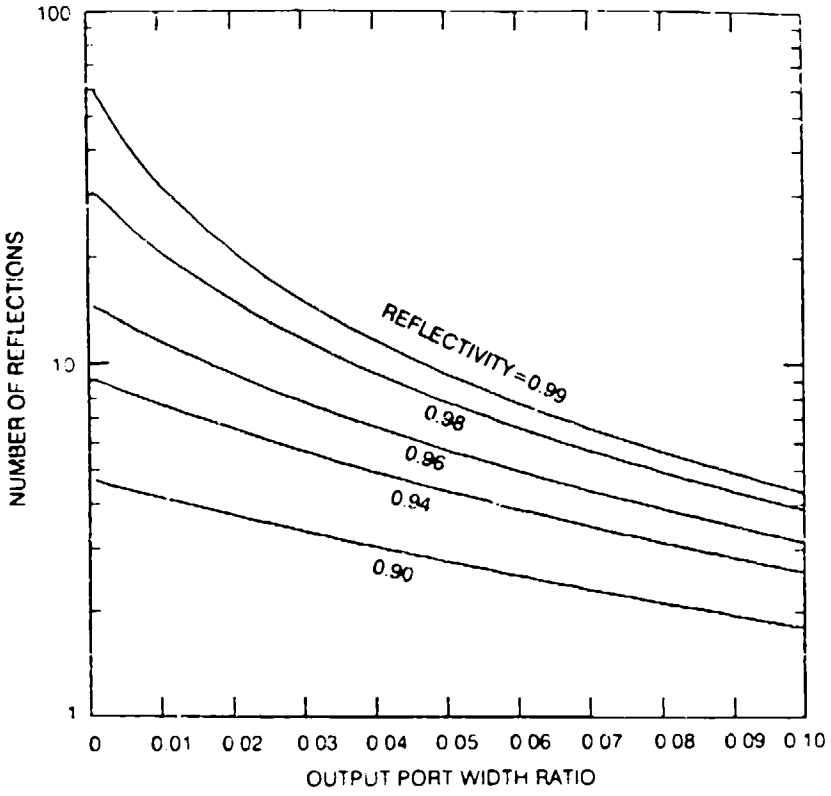

Figure H-2. Number of reflections.

3.1.4 Supplier

Labsphere is the only company that could make a customized sphere for our application (other companies selling integrating spheres referred us to Labsphere). The sphere would be made from Spectralon SRM-990, a material that is tough and hydrophobic (unlike most UV paints for integrating spheres). The material reflectance varies between 0.95 at 250 nm and 0.985 at 300 nm. The sphere could be easily fabricated with the window at a higher latitude than the equator, say 10 degrees. Efficiency would raise substantially by greatly lowering losses to the ground and by raising the mean launch angle. The cost would be about $4400.

3.2 REFLECTIVE CONE

In this design, a reflective cone is placed in the beam path to scatter the light horizontally. The reflective cone would be at a 45-degree angle (or at a 35-degree angle to direct the beam upward by an amount equal to the beam divergence from the fiber).

3.2.1 Reflective Coating

The efficiency of the cone itself would be equal to its reflectivity, which is about 95%. However, any good UV aluminum coating degrades rapidly, especially in a moist atmosphere. This

could be alleviated by hermetically sealing the cone in a fused silica cylinder and attaching the cone to the top of the cylinder. The optical fiber could be introduced though a metal base with a SMA feedthrough.

3.2.2 Configuration

The several designs that could be envisioned for the sealed container are the following: (1) repurge the container with nitrogen gas periodically; (2) assemble the container in a nitrogen environment; (3) fill the container only once and then completely seal. The most versatile design would be to have a purging valve on a removable metal base for the fiber. A metal ring could be epoxied to the base of the glass cylinder onto which a metal base for the fiber is screwed. An o-ring would be used to seal the system (figure H-3). The 5-m pole of the vertical channel would be attached to the metal base.

Assume that there is a 35-degree cone, a 1-mm fiber with a 20-degree divergence, and a 1-inch distance between the fiber and the cone. Reasonable dimensions for the cone would then be a height of 5 mm and a base of 7 mm. The glass cylinder would need to be 7.5 mm high and would have a diameter of at least 7.5 mm.

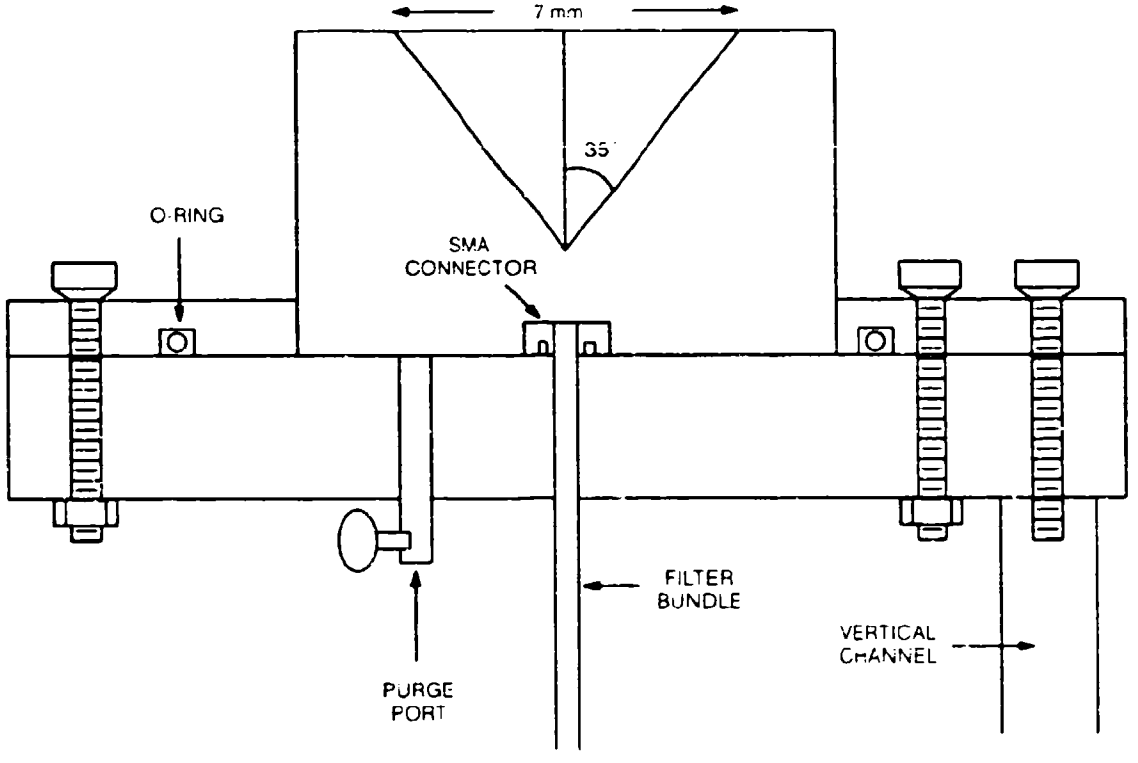

Figure H-3. Reflective cone.

3.2.3 Suppliers

Laser Power Optics of Del Mar, CA, would build the reflective cone with diamond turning. The company indicated that once their machine was set up to produce one optic, it would be cost effective to turn out several cones. Laser Fiber Optics is willing to work on an actual cost basis.

This gives us a good amount of support for $5K or less. Several runs and some experimentation with coatings would be included. As machine time is about $100/hour, this is more than what we need.

A quote from Rocky Mountain Instrument Company for a polished glass cone with an aluminum evaporate was $850. The apex on this optic would be sharp to 0.01 inch.

3.2.4 Errors

Two problems are anticipated with this design. The first is its possible sensitivity to the positioning of the reflective cone with respect to the beam. The second is the lack of sharpness of the apex of the cone, causing light to be downward scattered from the most intense part of the beam.

These two errors are not additive and whichever one covers the larger area dominates. In fact, it is easy to see that the positional error dominates, as it cannot be easily adjusted and diamond turning produces a very precise apex.

3.2.4.1 Apex Error. In the calculations below, use a normalized radius where

$r = r'/\sigma$
$\sigma = \sigma_0 2^{1/2} = 0.7071$ mm at the output of the fiber
r' = is the actual radius of rounded apex area in mm
σ' = is the beam radius in mm ($1/e^2$ point).

The loss due to rounding of the apex is then

$$E = \int_0^{2\pi} \int_0^{r} \exp(-x^2)\, x\, dx\, d\theta \;/\; \int_0^{2\pi} \int_0^{\infty} \exp(-x^2)\, x\, dx\, d\theta$$

$$E = 1 - \exp(-r^2) \tag{3}$$

$$r = [-LOG_e\,(1 - E)]^{1/2}\,, \tag{3'}$$

where x is the position on the cone furthest from the angle of interest (figure H-4).

To get a 5% loss for a 1-mm diameter beam, the apex rounding would have to cover a 0.16-mm radius. Thus, it is clearly not a serious problem.

3.2.4.2 Positioning Error. To find the effect of position error, x_0, on intensity radiated into a given angle, θ (figure H-4), the following equation was integrated numerically:

$$E = 2\theta^{-1}\exp(-x_0^2) \int_0^{\infty} \int_0^{\theta} \exp[-r^2 - 2x_0 r\cos(\theta)]\, r\, dr\, d\theta\,. \tag{4}$$

Results for the fiber are shown in figure H-5. If the cone is an inch away from the fiber and σ is 2 mm, the beam is then 2.82 mm wide at the cone. Table H-1 shows the maximum errors and why the reflective cone will not work. It is unlikely that the cone could be aligned to fractions of a millimeter above the fiber in this configuration.

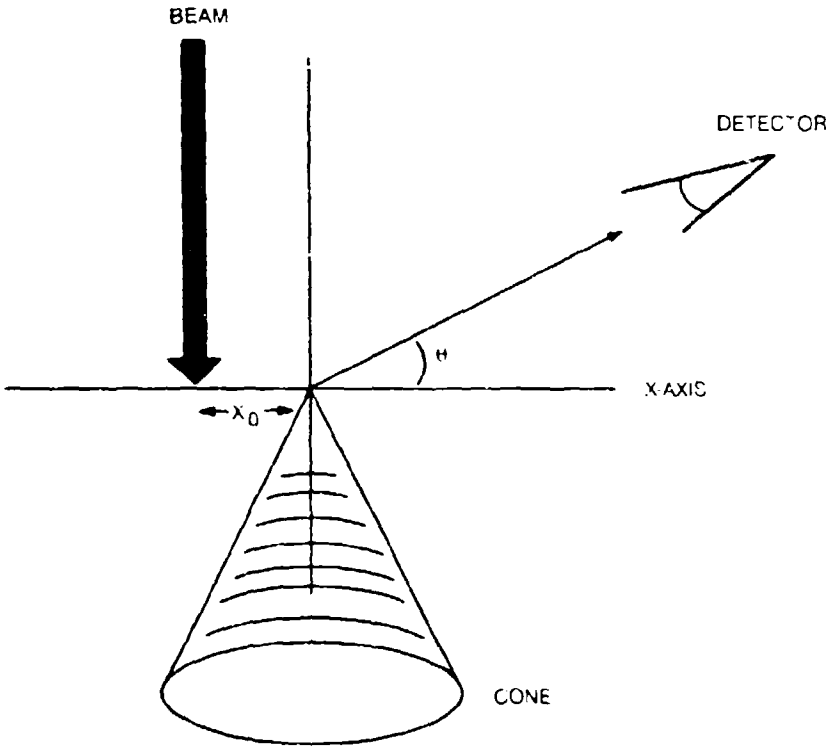

Figure H-4. Beam/cone configuration.

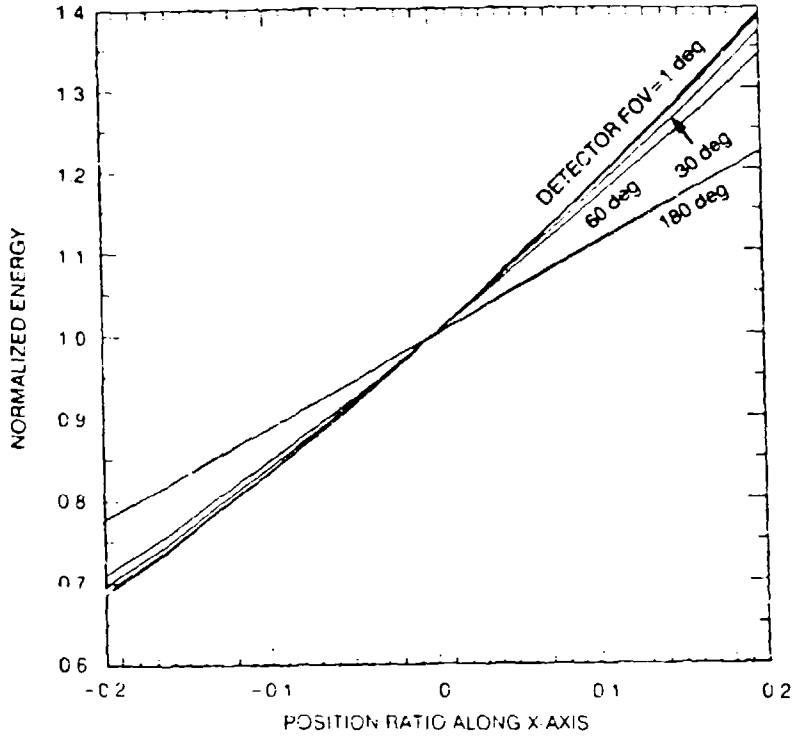

Figure H-5. Positional errors.

Table H-1. Errors due to position.

Loss (%)	x	x' (mm)
5	–0.0287	0.0574
10	–0.0584	0.1168
20	–0.121	0.242
50	–0.362	0.724

3.3 FIBER BUNDLE

In this design, the laser beam is expanded and coupled into a UV-grade silica fiber bundle.

3.3.1 Loss

The energy transmitted through the system is expected to be

$$T = PF\, T_f\, (r_o/r_c)^2\, (1 - R_f)^2\, T_c\, BF\,, \tag{5}$$

where PF ≡ packing factor = 0.72

T_f ≡ transmission through fiber = 0.6 for 5.5 m at 400 dB/km

r_c/r_o ≡ cladding to core ratio = 1.1

R_f ≡ reflection at each end of fiber ≈ 0.04

T_c ≡ transmission through beam expander = 0.9

BF ≡ beam fraction to $1/e^2$ intensity = 0.8647.

Substituting the values listed above in equation 5, the transmission is then 25.6% for a 200-μm fiber with 220 cladding. The larger the fiber, the less the loss from the r_c/r_o ratio. Fibers come in r_c/r_o ratios of 1.1 and 1.2. The 1.2 fiber is made by using high-quality silica needed for UV. The use of this larger cladding fiber will reduce the total transmission down to 21.5%.

Not much can be done about the theoretical 75% packing factor in a fiber bundle. In principle, the fibers could be heated and fused closer together. In practice, that is very difficult to accomplish.[3] The bundling process is more likely to result in a lot of breakage of expensive fiber.

The divergence out of the fibers is approximately 20 degrees. Therefore, angling them upward 20 degrees from the horizontal would lower some of the loss to the ground and reduce the potential eye danger.

3.3.2 Alignment

This system should be relatively simple to align, as the critical procedures can be performed on the laser platform. A potential difficulty is the UV fiber degradation, which gradually reduces transmission through the fiber. Another difficulty is that 25% of the UV energy goes into the region between the fibers, which can cause considerable problems.[4]

General Fiber Optics has observed two possible solutions: either by using a reflective mask (not trivial) or by using reflective epoxy (recommended). Several epoxies have been used and

3 Orazi, R. J., NCCOSC RDT&E Division, personal communication, 1992

they should be experimented with further. If an epoxy fails to prevent damage or the end is damaged for any reason, the fiber could be sent back and reterminated with a different epoxy for about $70. Of course, the fiber bundle must be made longer than the minimum requirements so that it can be reterminated a number of times.

3.3.3 Structure

In a typical fiber bundle, the first layer has one fiber with each succeeding layer having a multiple of 6 more fibers than the previous layer (table H-2). In practice, a packing fraction of 0.72 is realistic.

Table H-2. Fiber bundle.

Layers	Total # of fibers	Maximum packing fraction
1	1	1
2	7	0.7778
3	19	0.76
4	37	0.7555

As a candidate system, consider a 19-fiber bundle with r_o = 200 μm and r_c = 220 μm. Let Lmax = # of layers in the fiber. The radius of the bundle is r_o *(2*Lmax-1). The radius of the bundle is then 1.1 mm, thus requiring the beam width (0.2 mm) to be expanded 11 times. As stated, this would be expected to transmit 25% of the light.

In table H-3, a number of typical cable bundles are examined with respect to the layer number (L), relative intensity (I_r), relative density (D_r, which is the product of I and the number of fibers in the layer), and the coverage angle per fiber (θ). An estimate is made of the relative intensities of the light in each fiber of the bundle. From that estimate, determine the angular distribution for laying out the cable bundle that will result in the most even distribution of energy about the horizon.

Table H-3. Bundle comparison.

L	I_r	D_r	θ
		7-Fiber Cable	
1	0.897	0.897	96
2	0.411	2.467	44
TOTAL:		3.364	
		19-Fiber Cable	
1	0.96	0.96	29.68
2	0.726	4.357	22.44
3	0.527	6.328	16.3
TOTAL:		11.644	
		37-Fiber Cable	
1	0.98	0.98	21.4
2	0.85	5.096	18.58
3	0.52	6.245	11.37
4	0.23	4.14	5.03
TOTAL:		16.47	

[6] Burke, G. General Fiber Optics, personal communication, 1992.

3.3.4 Angular Output

For the center fiber, the relative intensity is calculated exactly. For the fibers in the outer layers, the intensity for the entire fiber is approximated by the value at its center. The intensity for the center fiber is given by:

$$I = r^{-2}[1 - \exp(-r^2)] , \tag{6}$$

where $r = 2^{1/2}(2L_{max} - 1)^{-1}$.

The intensities for the fibers in the outer layers are

$$I = \exp(-x^2) , \tag{7}$$

where $x = 2^{1/2}\,(2L - 2)/(2L_{max} - 1)$.

The angular output of this system will not be uniform. However, because each fibers $1/e^2$ points are 40 degrees apart, the light cones of each fiber frequently intersect each other. A certain amount of nonuniformity in the angular distribution should not matter because the light at the receiver is most likely scattered light anyway.

3.3.5 Cost

A 200-μm core bundle costs about $5 per fiber-meter ($3 per fiber-meter for 100 μm). A 6-m, 19-fiber bundle will thus cost $570. At the breakout side of the bundle, polishing each fiber and mounting it in a hypodermic needle will cost about $15–$20 per fiber (≈$380 total). In addition, a jacket for the cable will be needed. Total cost will be about $2400 for the bundle.

The cone holding the breakout end can be machined in-house. The cone will be machined with slots to align the hypodermic needles and clips to hold them in place. A cover over the top of the cone will protect the fibers from the elements (figure H-6).

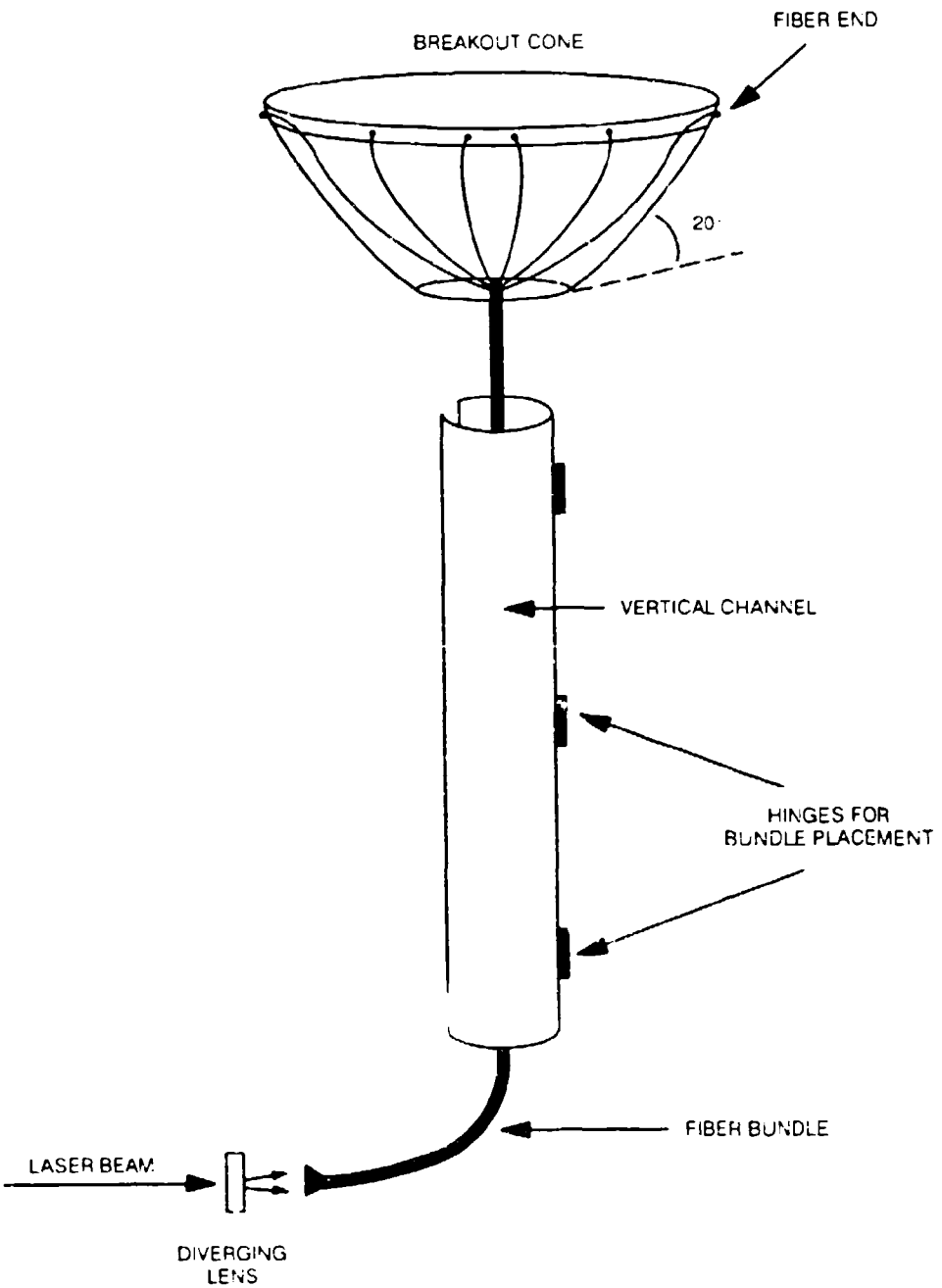

Figure H-6. Fiber bundle configuration.

4.0 CONCLUSIONS

The only two practical designs are the fiber bundle and integrating sphere. Of these two, the fiber bundle has the best efficiency (25% versus 12–24% for the sphere) and it is the most cost-effective ($2.4K versus $5.4K). The integrating sphere is probably more rugged and has a more even angular distribution (but this may not be a significant effect because of scattering). The sphere will most likely be easier to handle in the field, because the fiber ends are fragile and can only be protected so much by the top housing. In either case, careful handling will be needed for the 5-m section of fiber.

Overall, the fiber bundle design seems the best. However, the modal effects caused by propagation of UV light through the optical fiber may result in signal degradations. The degree of degradation in optical fibers should be further analyzed before any device fabrication the includes optical fibers.

In both of these systems, the only alignment necessary is in coupling the light into the fiber(s).

5.0 ACKNOWLEDGMENT

This analysis was performed by Maureen O'Brien, NCCOSC RDT&E Division.

6.0 REFERENCES

Grum, F., and G. W. Luckey. 1968. "Optical Sphere Paint and a Working Standard of Reflectance," *Applied Optics*, 7, 2289.

Yen, J. 1992. "Intentionally Short Range Communications (ISRC) Exploratory Development Plan." NRaD TD 2286 (Jun). Naval Command, Control and Ocean Surveillance Center RDT&E Division, San Diego, CA.

APPENDIX I

UV PROPAGATION MODEL

1.0 BASIC MODEL

The modeling work was an updated and improved version of the Schlupf model (Schlupf, 1982). Some familiarity with this model is assumed.

1.1 SCHLUPF MODEL

Some of the features of the Schlupf model are the following:

1. Calculation of direct beam and first-order scattering. First-order scattering is done by breaking the transmitter signal into a set of weighted "beams." These beams are formed in layers about the central axis of the transmission. Each layer contains two more beams than the previous one. Each transmitter beam's vector length is incremented by an amount corresponding to the desired time accuracy. The received energy from that path increment is calculated and summed into a time bin corresponding to the total path length.

2. A laser pulse is assumed to have a Gaussian distribution in time. The receiver signal is convolved with this shape.

3. Aerosol scattering with Neer-Sandri phase functions and an option to input a phase function from an input file. The aerosol extinction coefficient can exponentially decrease with height. A second exponential coefficient can be used once a cloud layer is reached. The operator inputs the ground-based values of the aerosol absorption and scattering coefficients because these are highly variable (their sum typically varies from 0.2 to 2 km^{-1}).

4. The use of an accurate wavelength-dependent ozone (O_3) absorption coefficient.

5. Rayleigh scattering dependent on wavelength, temperature, and pressure. But for most cases, the scattering is more significant for wavelengths above 230 nm (figures I-1 and I-2), so there is little value in looking at varying temperature and pressure for wavelengths above 230 nm.

The Schlupf model does not include oxygen (O_2) absorption (which is important at wavelengths below 250 nm), higher order scattering, or the effect of obstacles in the path. Schlupf treats the ground as a perfect absorber.

1.2 NRAD MODEL

The NRaD model computer program is written in MicroSoft FORTRAN 5.1 for use on an IBM-compatible PC (80486). It is intended to model UV scattering in the 200- to 300-nm range. However, all discussion and results will be given for 266 nm, which is the current case of interest for the ISRC project.

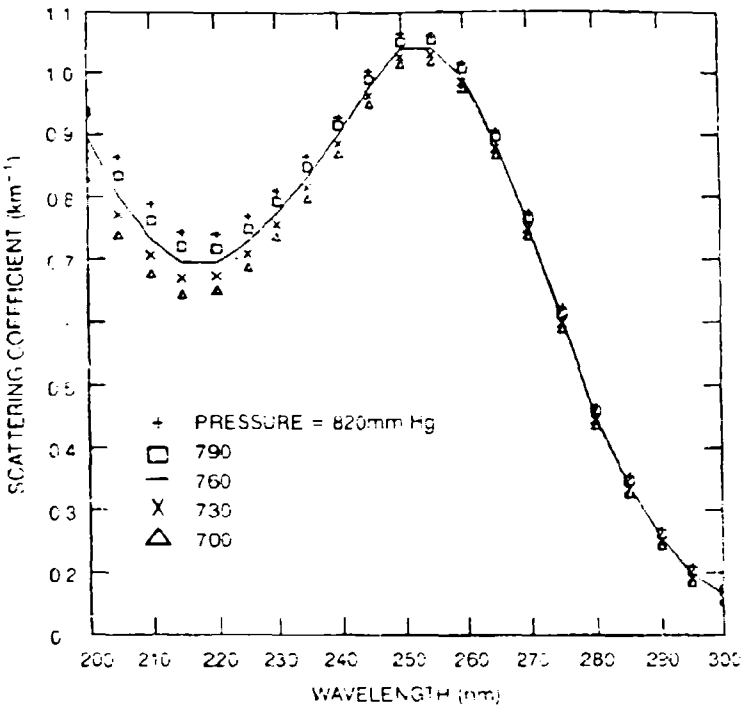

Figure I-1. Pressure variation.

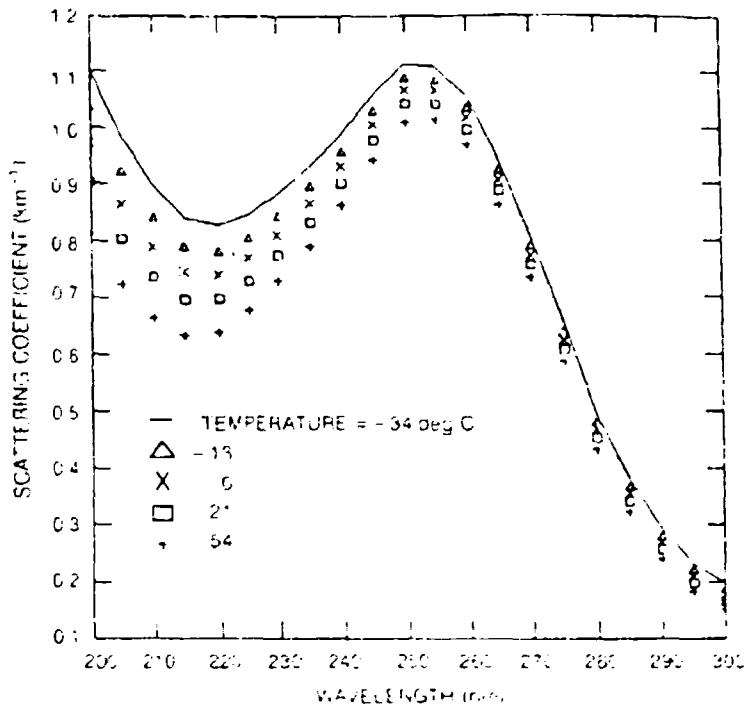

Figure I-2. Temperature variation.

1.2.1 Second-Order Scattering

Improvements to the model include the addition of the second-order scattering effects, the LOWTRAN aerosol phase functions, and the ability to include walls (or barriers) near the receiver. O_3 scattering has not yet been included in the model. This is planned for the near future, because it is needed for dealing with wavelengths below 250 nm, but it does not affect current work at 266 nm.

Second-order modeling is done in an analogous manner to the first-order scattering. In this model, the receiver as well as the transmitter is broken into a series of weighted beams. Each beam is incremented by a path length corresponding to the desired time resolution. All combinations of paths with less than a maximum path length (determined by the path's attenuation) are examined.

1.2.2 Beam Distribution

The Schlupf model convolved the laser beam with a Gaussian function in time. In the previous NRaD model, the laser signal was treated as instantaneous. The received laser signal function is saved to file and can then be convolved with the actual time signature of the laser in the plot programs. In the current NRaD model, the laser signal is expected to be a 70- to 1[illegible] square wave signal. Should this not be the case, one can go back to the original calculated data and reconvolve it with the true laser time signature.

2.0 MODEL PARAMETERS

The following parameters are used in the NRaD computer model of the test link.

2.1 ORIENTATION

The 266-nm transmitter laser is 0.5 km away from the receiver, at a height of 20 m above the receiver, and pointed horizontally toward the receiver. The laser beam has a 2-mrad (half-angle) divergence.

The receiver orientation is toward the transmitter (180-degree orientation). Its field-of-view (FOV) is 90 degrees (45-degree half-angle) and has a 1 COSINE distribution.

2.2 ATTENUATION

The aerosol phase function used was LOWTRAN model #7 (maritime 80% humidity). An aerosol absorption of 0.01 km^{-1} was used, making the extinction coefficient almost totally dependent on the scattering coefficient. Cloud effects were not included in this simulation.

The model was executed for a variety of environments and transmitter elevation angles. Ozone levels were varied from 25 to 125 parts per billion (ppb). San Diego ozone levels do not usually go above these values, with 50 ppb being a good average for the Point Loma local environment. The aerosol scattering coefficient was varied from 0.3 to 1.2 km^{-1}.

The unscattered laser beam is only 10 m across at the receiver position, so that the beam is [illegible] the receiver. [illegible] only scattered light is received.

2.3 EXECUTION

It was more efficient to run the first- and second-order scattering problems separately for a variety of reasons. For instance, it is useful to look at their results separately. Also, different accuracies in time and number of transmitter beam layers are needed. Finally, computation times for first- and second-order scattering differ significantly. In fact, the computation time would be prohibitive if the small time step required in the first-order scattering were to be used for the second-order case.

3.0 RESULTS

In this problem, the results were dominated by first-order scattering. The integrated energy from the first-order scattering was always at least an order of magnitude larger than the second order and occurred within a much shorter time interval.

3.1 FIRST-ORDER

For first-order scattering, a time step of 0.25 ns was used in a 4-layer transmitter beam model. This many layers was not really necessary for such a small beam divergence. In fact, one can get fairly reasonable results by using the 0-layer model (figure 1-3).

3.1.1 Pulsewidth

The pulsewidth as a function of transmitter elevation angle can be calculated from simple geometric arguments and is plotted in figure 1-4. The pulsewidth goes up slowly from 22.5 ns at 0-degree elevation to 116 ns at 90-degree elevation. After that, it increases rapidly. However, the received energy dies off approximately exponentially with time.

3.1.2 Absorption

The single-scattering energy is very heavily dependent on ozone levels, as would be expected. This is plotted in figure 1-5 for a variety of elevation angles.

3.1.3 Scattering

Surprisingly, varying the aerosol scattering coefficient, K_{scat}, had almost negligible effect (figure 1-6). This would not be true in general, but is just a singular characteristic of the particular beam path being modeled currently.

3.1.4 Range

By increasing R, the propagation distance, K_{scat}, became significant. For the propagation channel under consideration, increases in K_{scat} were balanced by corresponding increases in the coefficient for the aerosol phase function. A typical first-order calculation was completed in a few minutes. If one used 0-layer laser beam, which was really quite accurate, the calculation took only seconds.

3.2 SECOND-ORDER

Second-order scattering took much longer to calculate—on the order of one to two hours per curve. Of course, the greater the number of receiver beam layers and the shorter the time step, the greater the accuracy of the model.

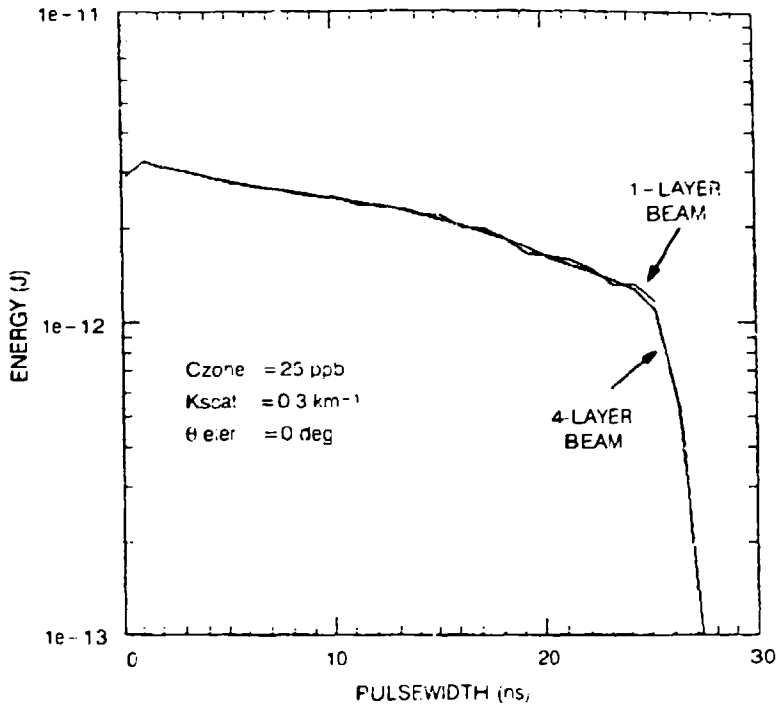

Figure 1-3. First-order scattering.

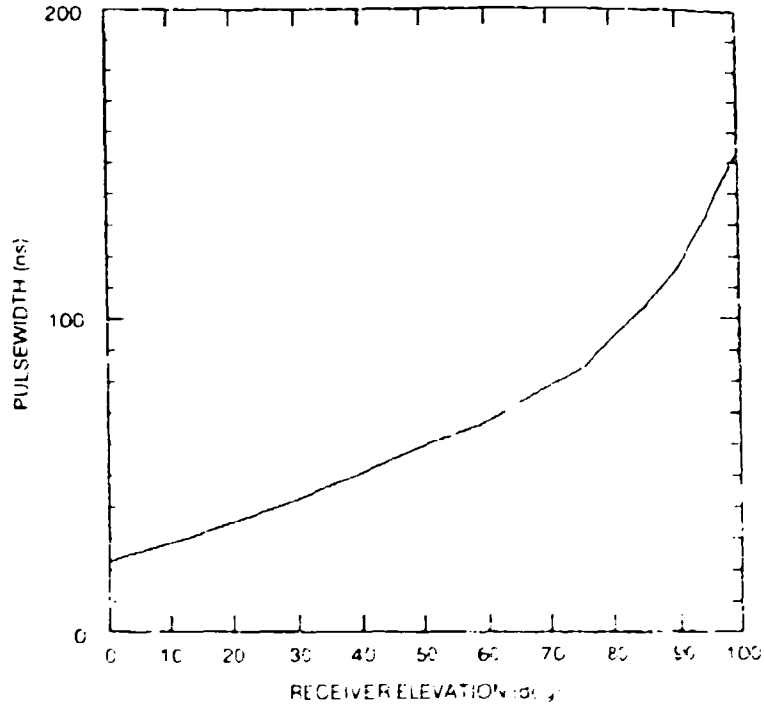

Figure 1-4. Single-scattering pulsewidth

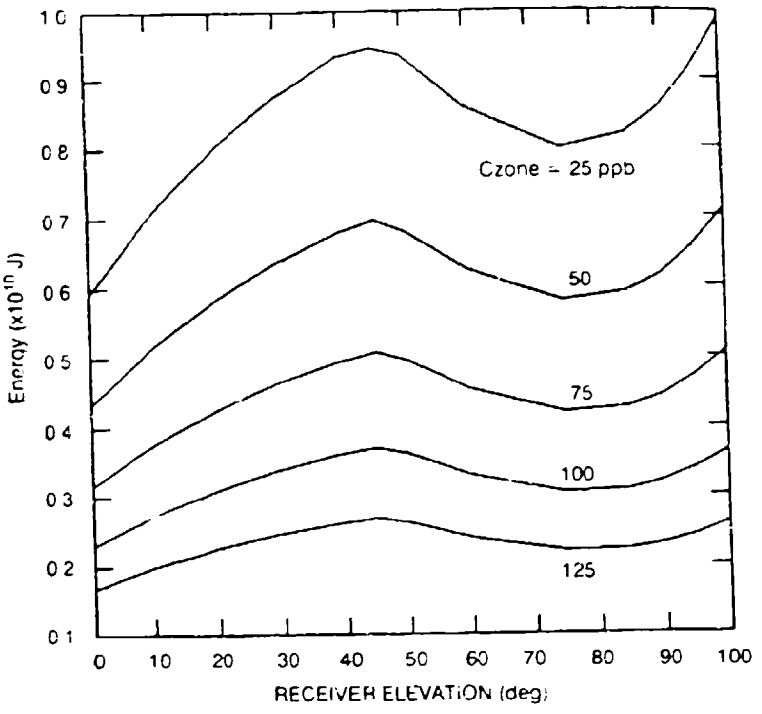

Figure 1-5. Single-scattering energy.

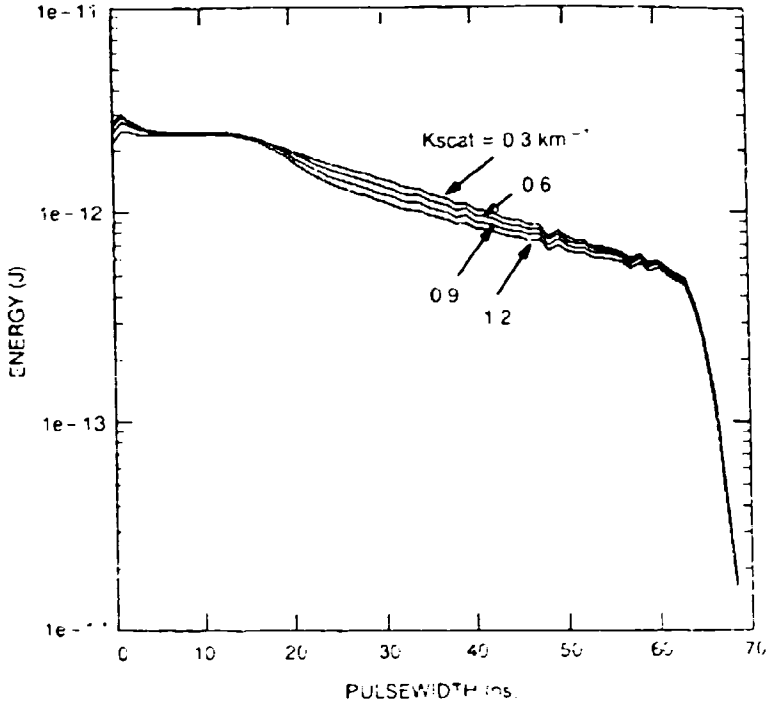

Figure 1-6. Scattering coefficient variations.

3.2.1 Model

A time step of 10 ns with a 4-layer receiver provided a sufficient model of the situation. The transmitter was modeled with one beam, which was quite adequate because of its low divergence.

3.2.2 Attenuation

Again, the effect of ozone level variations seemed to be much more significant than that of the aerosol scattering coefficient. A plot of the effect of K_{scat} at 0-degree receiver elevation and an ozone level of 25 ppb is shown in figure I-7. One can see that the higher the K_{scat}, the narrower and more intense the second-order scattering pulse becomes. The effect of ozone variation for 0-degree elevation is shown in figure I-8. Figure I-9 shows the effect of receiver elevation angle on the peak energy received.

3.2.3 Pulsewidth

It is difficult to characterize the pulsewidth due to the second-order scattering, because it drops off slowly. Figure I-10 shows the full-width-at-half-maximum (FWHM) as a function of the ozone level. In reality, the pulsewidth is the point at which the detector is receiving an average of 1 photon within a 100-ns time interval.

As it turns out, the experimental pulsewidth was on the order of 5 μs (appendix J), which indicates that the energy in the second-order scattering was large enough to be observed by the receiver. A 5-μs pulsewidth indicates that the ozone level for that day was on the order of 75 ppb.

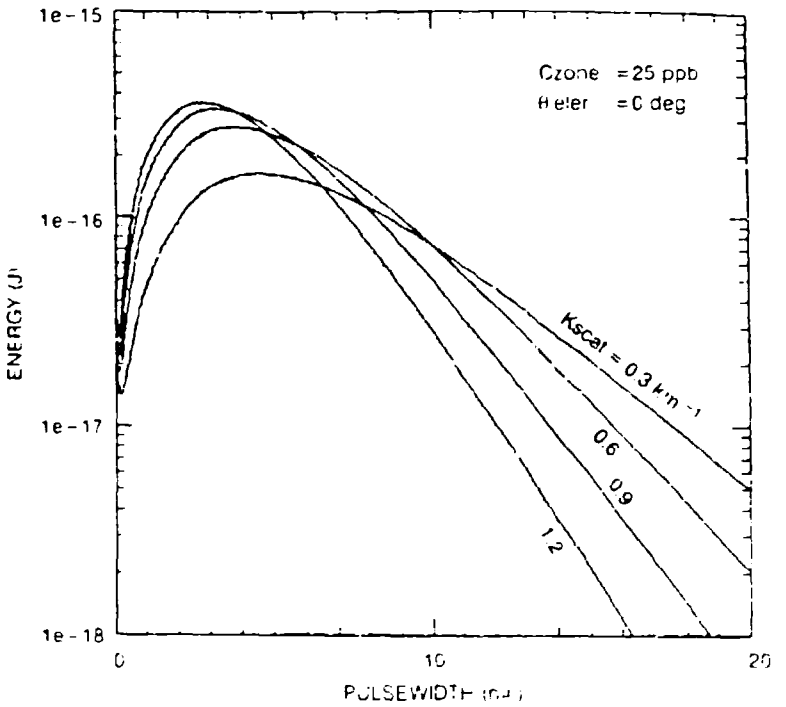

Figure I-7. Second-order effects: scattering

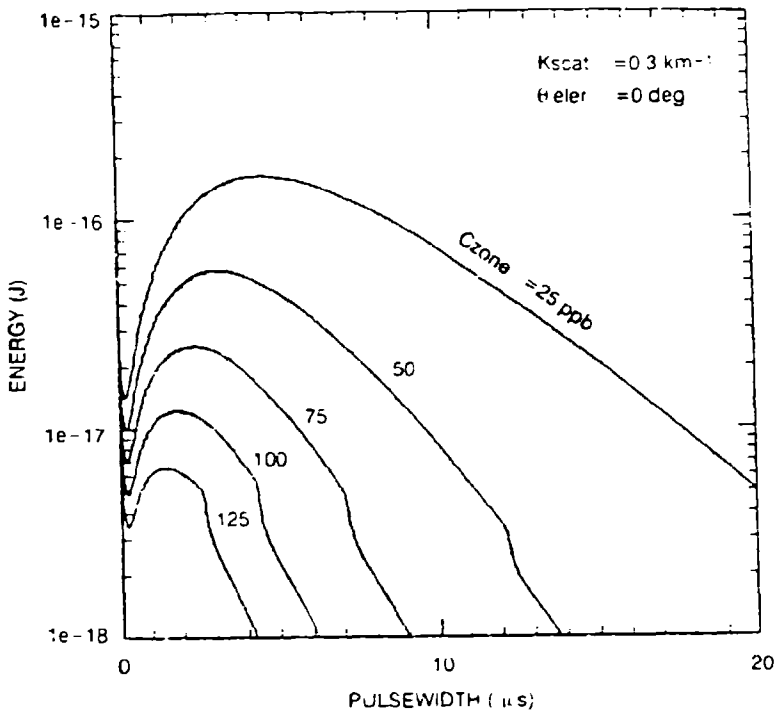

Figure 1-8. Second-order effects: ozone.

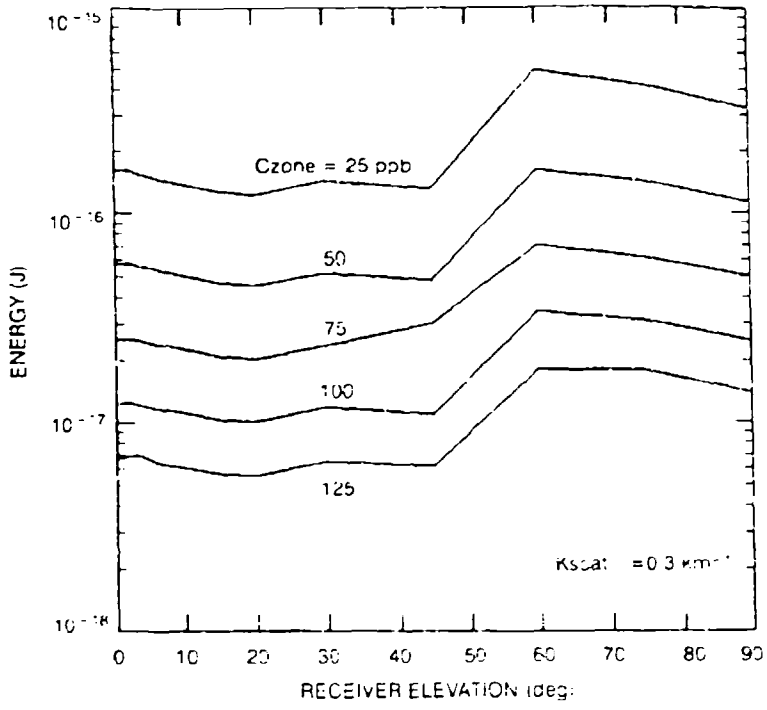

Figure 1-9. Second-order effects: elevation angle.

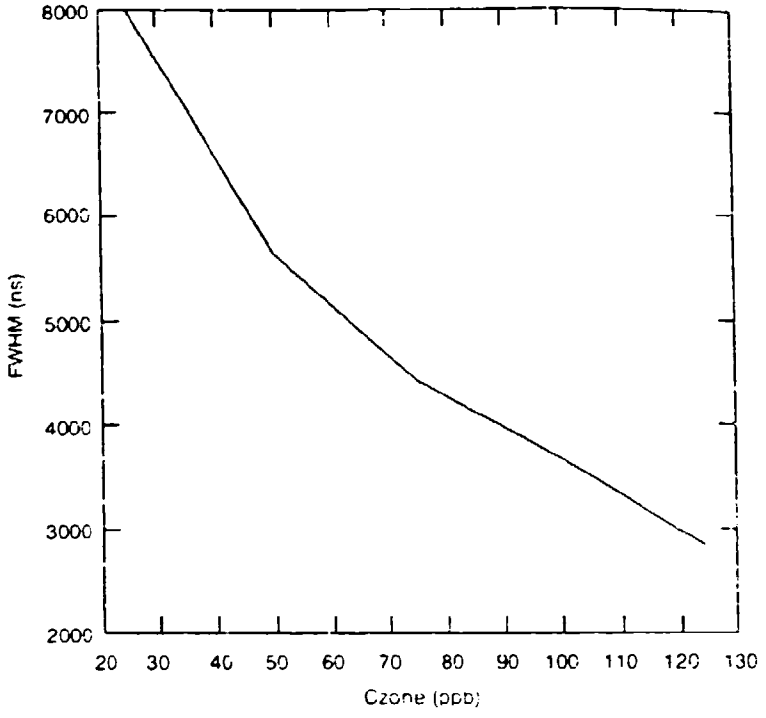

Figure 1-10. FWHM vs ozone.

4.0 PROGRAM NOTES

4.1 UNITS

Units used in the program are in degrees, kilometers (km), and nanoseconds (ns) unless otherwise noted. All angles are converted to radians.

4.2 GEOMETRY

The line between the transmitter and the receiver defines the x-axis. Orientation is measured from the positive x-axis in the xy-plane. Elevation is measured from the xy-plane, not from the z-axis.

4.3 BEAM LAYERS

Zero beam layer means that the transmitter is modeled by one beam at its center. Each successive beam layer has two more beams than the previous layer. The program allows for up to 10 layers.

4.4 BEAM DIVERGENCE

The beam divergence is measured in milliradians (mrad) from the center of the beam.

4.5 ENVIRONMENTAL FACTORS

The following environmental factors (corresponding units) are included in the computer model: time step (ns), wavelength (nm), ozone (parts per million, ppm), pressure (mm Hg).

temperature (deg F), cloud height (km), aerosol absorption coefficients (km^{-1}), aerosol scattering coefficients (km^{-1}), and aerosol phase function models from LOWTRAN.

4.6 AEROSOL PHASE FUNCTION

Aerosol phase function types 1 through 26 are the standard LOWTRAN types with wavelength dependence included. Types 100 and 101 are the SciTec types used in the Schlupf model. Table I-1 summarizes these aerosol phase function types.

In general, at the wavelengths of interest, light will be scattered strongly in the forward direction. For the low humidity types, lower wavelength implies more forward scattering bias (up to an order of magnitude at 0 degree). The phase function is wavelength-independent for wavelengths greater than 300 nm. The phase function is wavelength-independent for humidities of 80% and above.

Table I-1. Phase function types.

Type	Environment	Relative Humidity (%)
1	Rural	0
2	Rural	70
3	Rural	80
4	Rural	99
5	Maritime	0
6	Maritime	70
7	Maritime	80
8	Maritime	99
9	Urban	0
10	Urban	70
11	Urban	80
12	Urban	99
13	Oceanic	0
14	Oceanic	70
15	Oceanic	80
16	Oceanic	99
17	Tropospheric	0
18	Tropospheric	70
19	Tropospheric	80
20	Tropospheric	99
21	Stratospheric	—
22	Aged Volcanic	—
23	Fresh Volcanic	—
24	Radiation Fog	—
25	Advective Fog	—
26	Meteoric Dust	—
100	SciTec	—
101	Neer-Sandri	—

4.7 WALLS

Walls, used to block scattering to the receiver, are defined about the receiver with the following factors (figure 11):

1. the number of walls obscuring receiver;
2. an elevation angle as seen from the receiver to the top of the wall; and
3. two orientation angles as seen from the receiver defining the azimuthal angle range blocked by the wall.

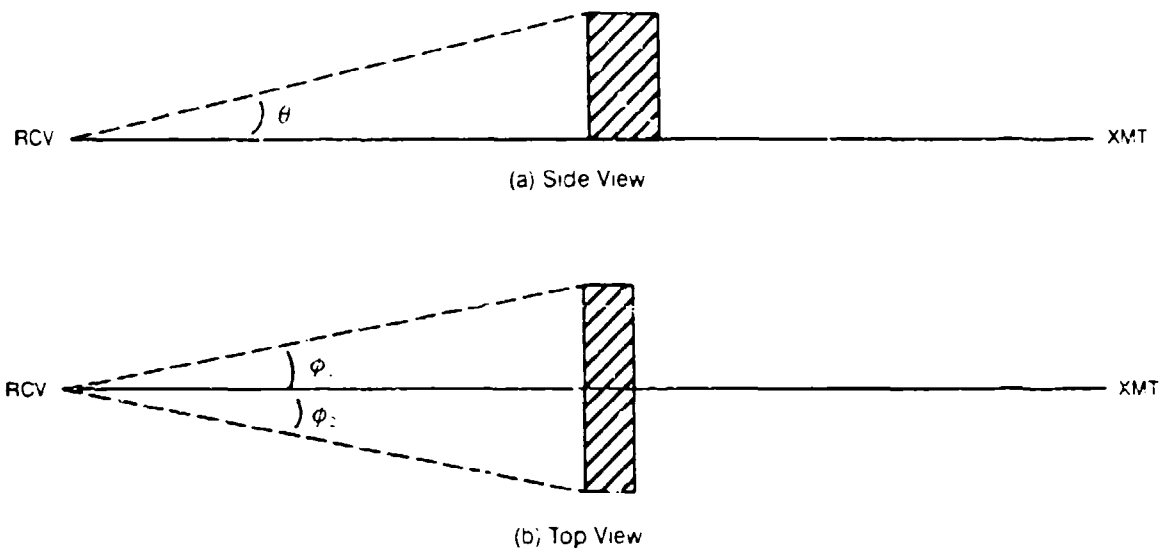

Figure 1-11. Wall definitions.

5.0 ACKNOWLEDGMENT

Maureen O'Brien, NCCOSC RDT&E Division, was responsible for the UV propagation model development.

6.0 REFERENCE

Schlupf, J. May, 1982. *Computation of Radiation Scattered from Pulsed Ultraviolet Beamed Sources*, SciTec Report TR-82-006.

APPENDIX J

LASER LINK DATA AND ANALYSIS

1.0 BACKGROUND

In the mid-1980s, the Naval Ocean Systems Center conducted extensive tests of an UV Communications (UV Comm) link in the Point Loma area of San Diego, CA (Yen, 1987). This 780-m link consisted of an UV transmitter and an UV receiver (figure J-1). A building and a hill in between made this configuration completely non-line-of-sight (NLOS).

1.1 UV COMM SIGNAL DESCRIPTION

The UV Comm transmitter continuously sent out 600 pulses per second, with each time period (representing a "symbol" of two bits) of 1667 μs subdivided into four "bins" of 417 μs each (see figure J-2 for the symbol meanings).

The lamps were turned on during the "00" bin and off in the other bins (01, 10, and 11). Turning the lamps on in any one particular bin represented a 2-bit symbol, corresponding to the bin being sent out. The above represented a 1200-bps pulse position modulation (PPM) scheme.

1.2 SIGNAL CHARACTERISTICS

The solar-blindness of the sensor meant that the UV Comm link did not have to contend with solar noise. Figure J-3 showed the received signal from the UV Comm link with the dots where the "ON bins" should be.

Because the number of UV photons per bin was small, the everyday Gaussian distribution must be replaced with the Poisson distribution. The Poisson distribution was designed to describe a small number of discrete occurrences. The effect of Poisson statistics could be clearly seen in the random pulse heights, but all the "ON bins" were still clearly higher than than noise and each symbol was then correct.

1.3 NOISE CHARACTERISTICS

It should be noted here that the high background (1 UV photon/bin) (figure J-3) was due to the presence of the small LOS UV source. Several manmade UV sources exist, such as burning fuel and arc welding. Burning fuel results in a relatively constant level of UV photons that can be handled by the use of the proper algorithm and sufficiently intense signal pulses.

Arc welding is a more serious problem, as can be seen in the following discussion. Figure J-4 shows the received signal 50 ms after the time period shown in figure J-3, when some arc welding spikes appeared. The arc-welding produces short but very intense bursts of UV radiation, that seriously interfere with the UV signal. Signal-processing schemes can be developed to handle this type of random interference.

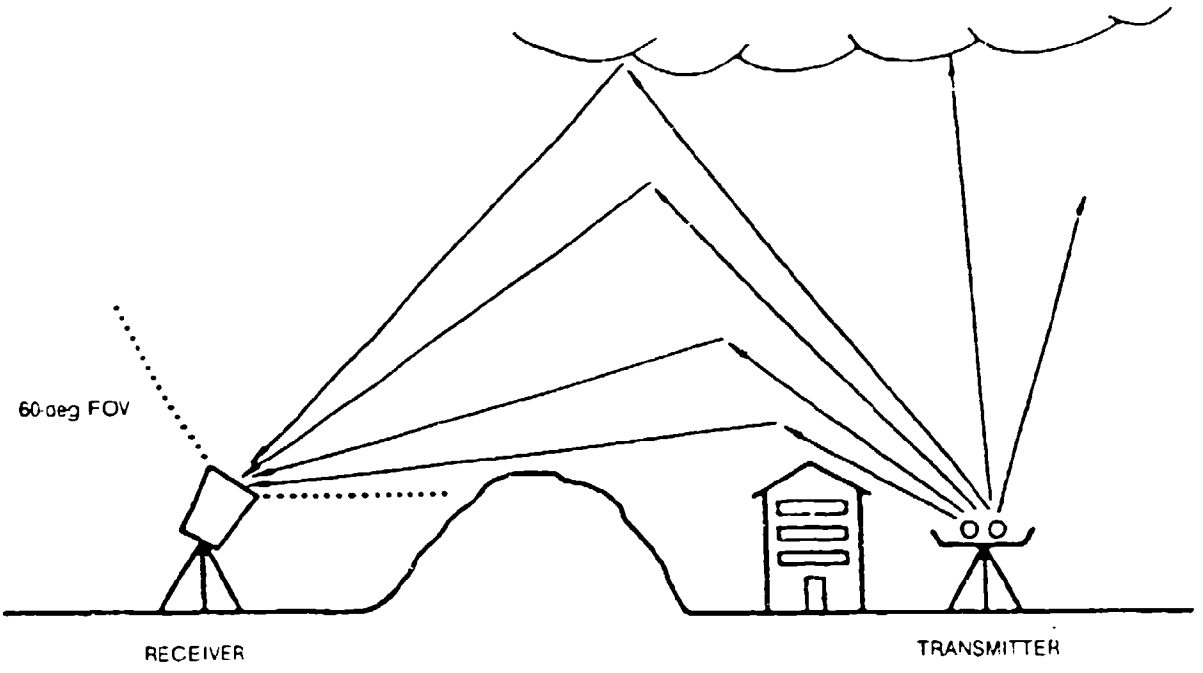

Figure J-1. UV Comm configuration.

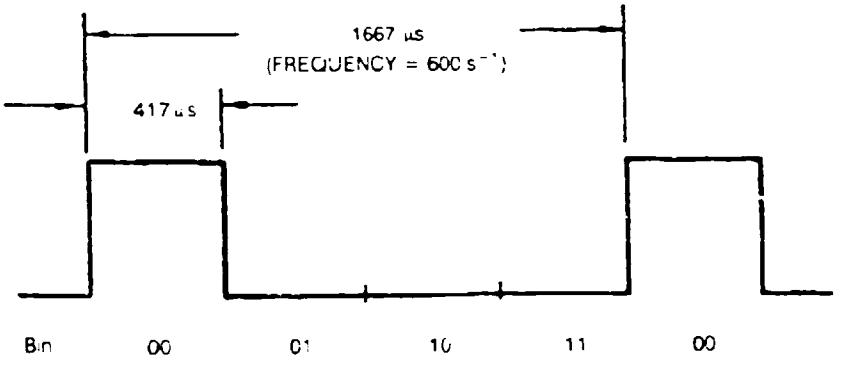

Figure J-2. UV Comm signal format.

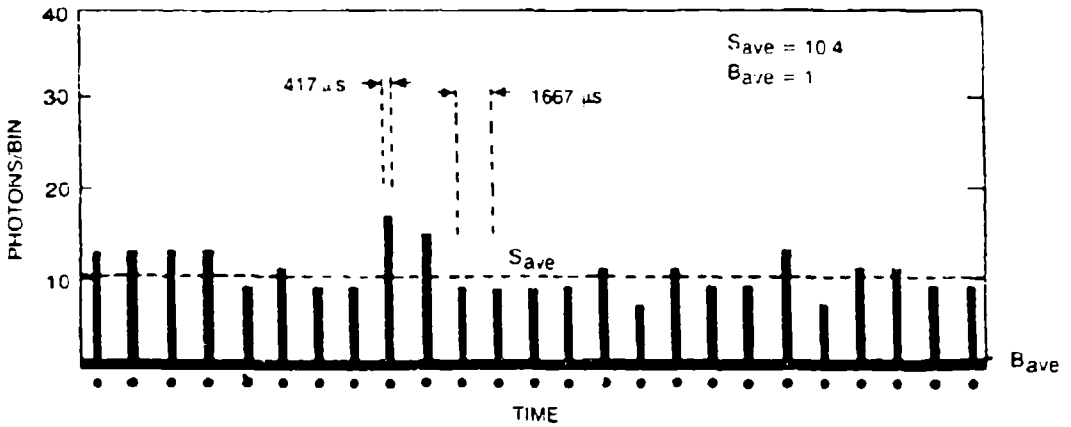

Figure J-3. UV Comm signal (Poisson).

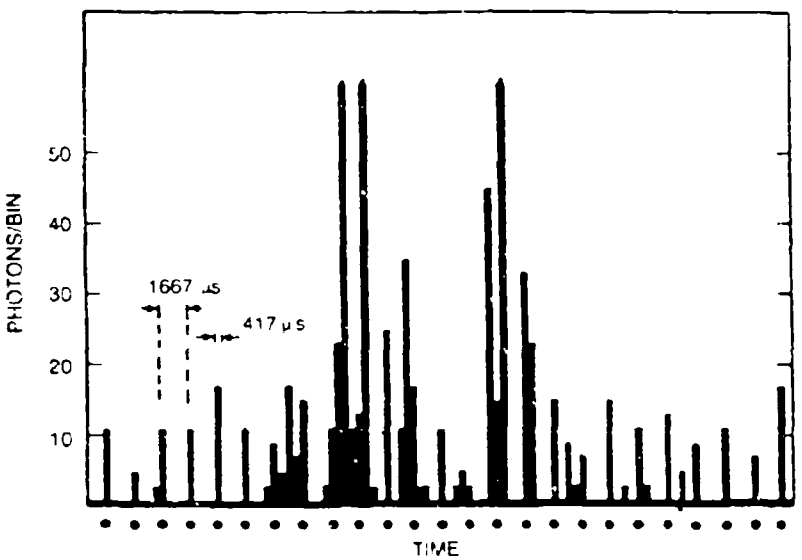

Figure J-4. Arc welding noise.

2.0 UV LASER

An alternative to signal processing for solving the random noise problem noted above is the use of a pulsed laser as the UV transmitter.

2.1 LASER PULSEWIDTH

A Q-switched, pulsed, UV laser (such as 4xNd:YAG) emits very short light pulses, on the order of 100 ns or less. While a UV pulse travels from the transmitter to the receiver, it encounters various atmospheric scattering components and is scattered. Therefore, the received signal will be a "stretched" pulse, with pulsewidth of several μs (appendix I).

2.2 NOISE SUPPRESSION

Laser pulses allow the reduction of the temporal bin size, or the receiver integration time, so that UV noise sources can then be spread out over a larger number of bins. This reduces the noise level at any particular bin to a few photons, while the laser pulse will be concentrated in one or two bins, resulting in ten or more photons in an ON symbol. Therefore, the use of laser pulses should suppress UV noise sources.

A numerical comparison with the UV Comm system described above indicates considerable improvement in the signal-to-noise ratio of the laser system. With much smaller bin sizes (5 μs versus 416 μs), most UV noise sources are expected to have time characteristics of longer duration and to be spread out over these 83 bins to resemble a DC source. The laser "pulse" in the ON bin would then be easily distinguishable from the semiconstant noise, resulting in a higher signal-to-noise ratio.

3.0 TEST LINK

A quadrupled Nd:YAG UV laser was set up as the transmitter of a test link in order to verify the above hypothesis that the use of short laser pulses will suppress noise.

3.1 TRANSMITTER

The 4xNd:YAG laser emits UV pulses at a rate of 2500 pulses per second with per pulse energy of about 150 μJ, for a total power output of about 0.4 W. The beam divergence (half-angle) was about 2 mrad.

The laser beam was directed out of the laboratory by two mirrors placed in a beam pipe (figure J-5). The loss from the two reflections was about 10%.

3.2 CONFIGURATION

The beam was directed horizontally toward a receiver situated on the roof of a building about 0.6 km away. The transmitter site was about 20 m higher than the receiver site (figure J-5), so the beam should pass near and above the receiver. Given the beam divergence, the diffraction-limited, scattered beam radius near the receiver site should be less than 2 m. Therefore, all the UV photons detected at the receiver site are scattered photons.

3.3 RECEIVER

The receiver consisted of the UV Comm photomultiplier tube (PMT) and electronics package, a data-collection PC board (appendix K), a PC hard disk for data storage, an oscilloscope for realtime observations, and a printer for oscilloscope tracings.

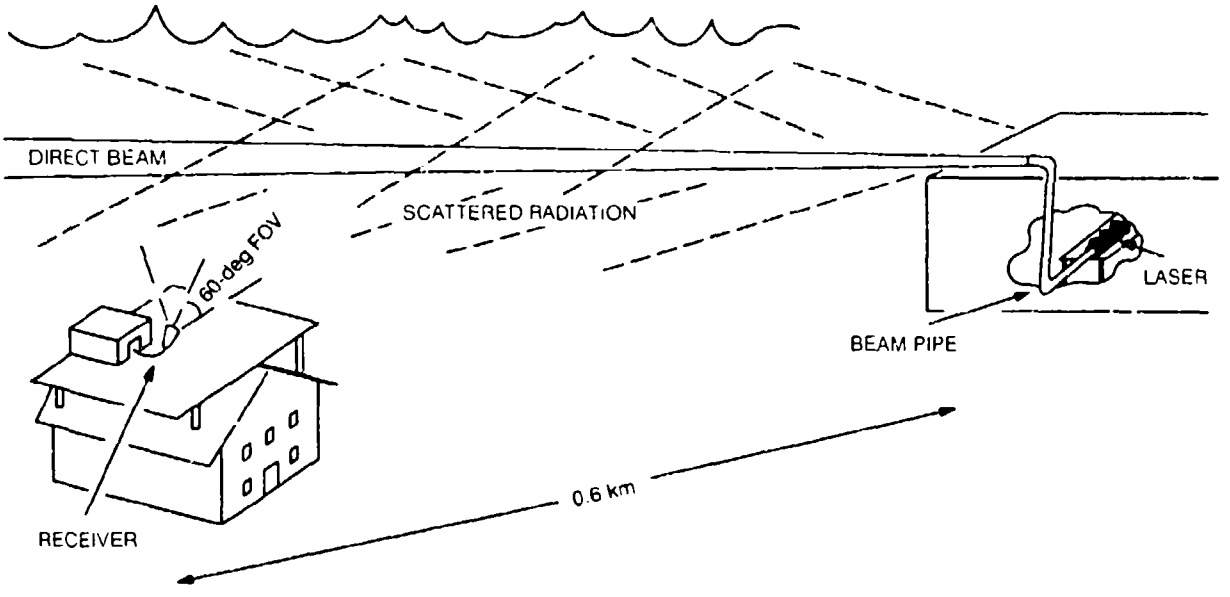

Figure J-5. Laser link configuration.

The data collection system was capable of recording all data at 100-ns intervals for about 30 seconds per run. One bit is recorded for each 100-ns interval; 1 indicates the presence of a photon and 0 otherwise. The SCSI hard disk is capable of storing data from 12 runs.

The detector was aimed about 15 degrees from vertical and oriented in the azimuthal direction of the transmitter. Also colocated at the receiver site was a small UV light (pen ray) for generating UV noise.

4.0 RESULTS

The laser pulse trains were detected and stored at the receiver site. Some preliminary analysis was performed there. Finally, UV noise was added to the test link pen ray as the noise source.

4.1 OSCILLOSCOPE TRACINGS

Although stored data were checked, most of the preliminary analysis was from the oscilloscope displays (and tracings) discussed below.

4.2 NOISE

By turning on a small UV light (pen ray) near the receiver, the area around the receiver was flooded with UV photons to simulate UV noise.

The noise levels shown in the tracings (figure J-6) are on the order of 10^5 UV photons per second. This noise level, equivalent to about 40 photons per 417-μs bin, would have made the UV Comm link untenable, because only about 10–20 UV photons were expected in an ON bin.

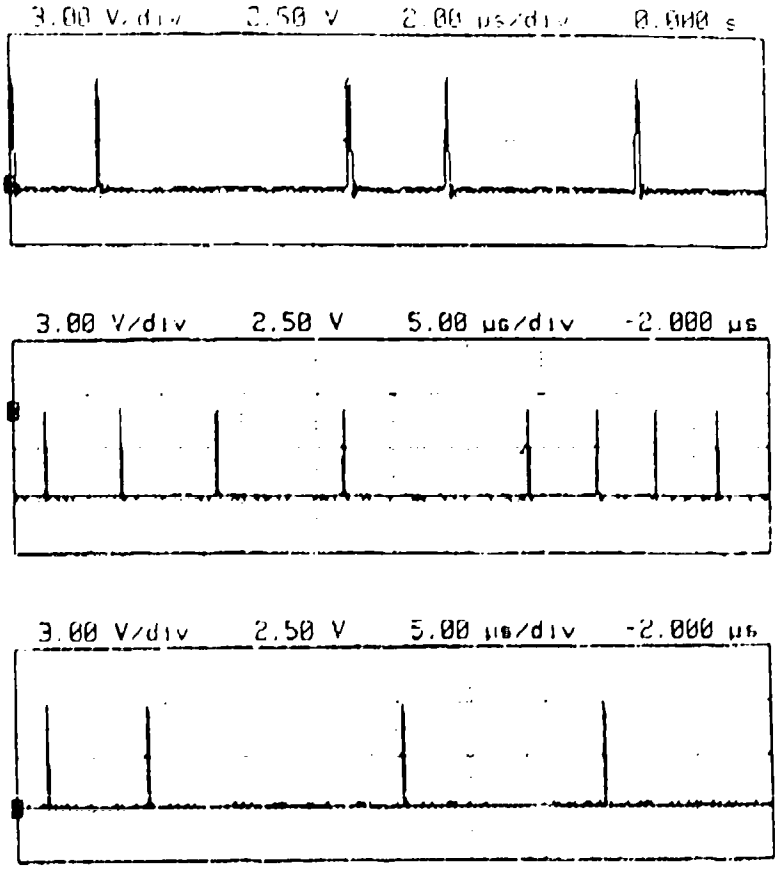

Figure J-6. Examples of noise.

Note that while the UV photons from the pen ray arrive in a random fashion (Poisson distribution), the photons constituted more of a semiconstant noise source than a "spiky" noise source like arc welding.

4.3 LASER PULSE WITHOUT NOISE IN CLEAR WEATHER

During the first test series, the weather was clear, dry, and sunny, with little variations. The result is an environment with a relatively small number of scatterers. The laser link test results confirm that the pulsewidth, which is a function of scattering strength, showed relatively small variation (figure J-7).

4.4 LASER WITH NOISE IN CLEAR WEATHER

Next, the pen ray was turned on while the laser was running. This noise, as expected, does not overwhelm the UV laser signal (figure J-8). The laser pulses are quite distinctive among the noise photons. Thus, one can conclude that the use of the UV laser pulse is conducive to suppressing noise of this type.

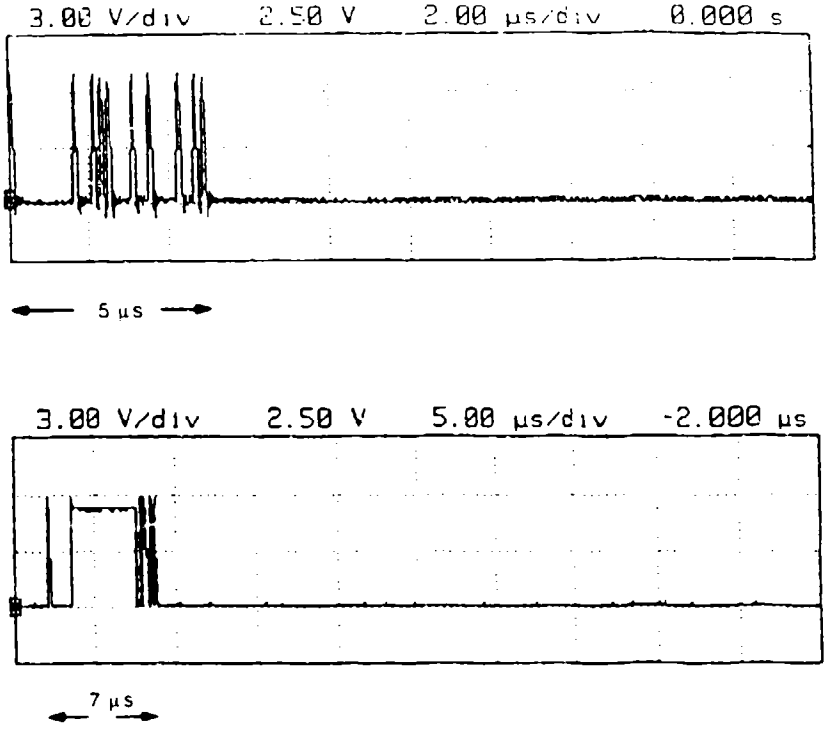

Figure J-7. Laser pulse example.

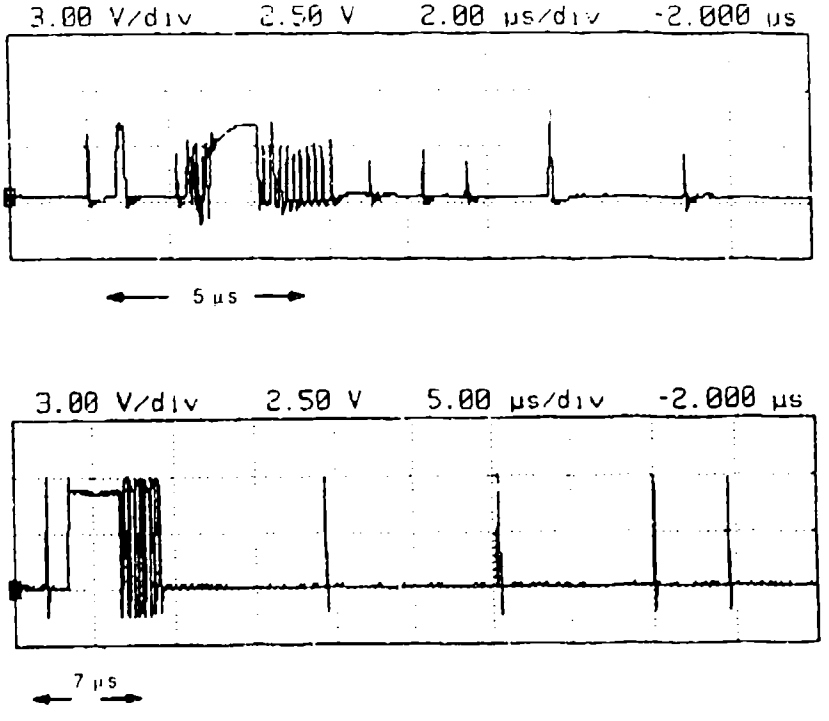

Figure J-8. Laser pulse with noise.

4.5 LASER PULSE WITHOUT NOISE UNDER OVERCAST

The second test series was conducted under a heavy overcast. The humidity (and aerosol concentration) was high. The received pulses varied considerably, with the pulsewidth varying from 3 μs to 8 or 9 μs (figure J-9). Even though the number of photons captured in a received laser pulse is considerable, the Poisson distribution for small discrete occurrences still applies. Therefore, considerable variation occurs in the pulsewidths of the detected laser pulses.

4.6 LASER PULSE SIGNATURE

The Q-switched, 4xNd:YAG laser used for the testing has a pulsewidth of less than 100 ns. The configuration shown in figure J-5 favors detecting single-scattered photons in the forward direction. Therefore, in the first 100 ns of the laser pulse, so many UV photons reached the PMT at almost the same instant of time that the PMT behaved in a peculiar way.

As can be seen in figures J-7 through J-9, the oscilloscope sees a pulse, then nothing for about 2 μs, and finally a compact group of pulses. This particular signature can be useful in determining a real laser pulse in situations with more noise.

This characteristic signature effect differs from what is generally called PMT saturation, where a steady stream of a few million photons hits and overloads the PMT. Although the total number of photons is large, it is equivalent to only a few photons per microsecond. The PMT can well handle a photon every 100 ns for short periods of time, but it overloads when the large photon flux continues for too long. The recovery from this type of saturation is on the order of several milliseconds.

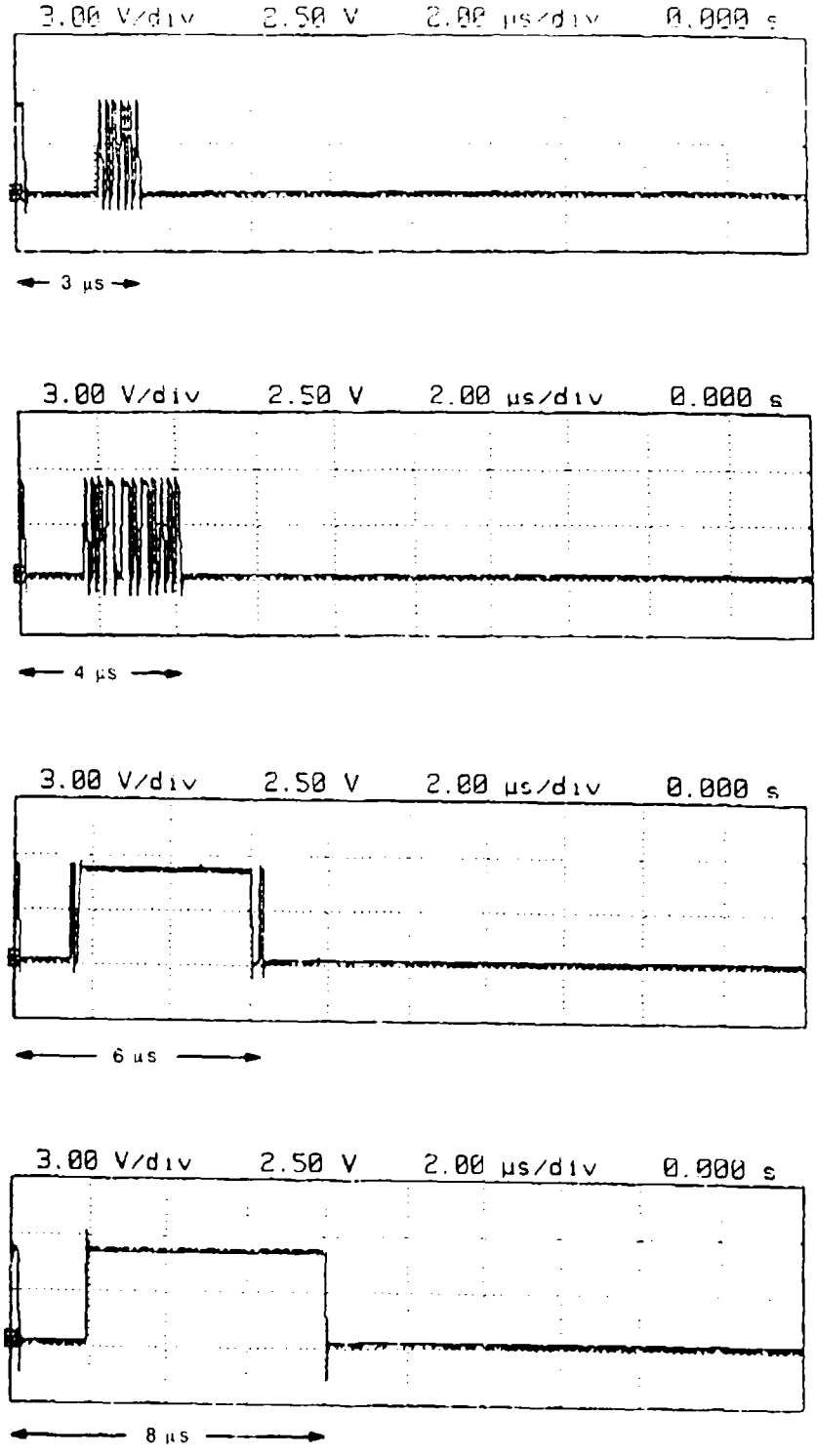

Figure J-9. Overcast examples

5.0 TEST DATA

A computer software package was developed in parallel with the data recording hardware (described in appendix K) to record and analyze the test data.

5.1 DATA DESCRIPTION

This section describes UV laser data taken by a PMT and stored for further analysis on an IBM-compatible personal computer. The 266-nm UV laser was pulsed at about 2500 Hz. The signal was received by a PMT about 0.6 km away from the transmitter. Probably only scattered data would be received in that configuration (figure J-5).

The data were digitized at 100-ns intervals and taken over periods of 1633.6 μs. Each of these periods was identified by a pulse identification (PID) number. Each file consisted of 16,384 of these data-taking periods (PIDs), resulting in 26.76 seconds of data. Because each data acquisition was initiated by a synchronization pulse, the process slowed down somewhat to cover a longer period in realtime. This was necessary because finite time is needed to read the data from the acquisition board and store it to a RAM disk.

5.2 DATA STORAGE

Because of the limited amount of RAM (36 MB) available for creating a RAM disk, it was decided to make individual runs that generate 32-MB (33,554,432 bytes) files. After each run, that file is copied onto a 400-MB hard disk; thus, 12 runs are possible before permanent storage must be arranged.

Twelve files of data were taken on 16 December 1992 and another 12 files were taken on 17 December 1992 (table J-1). The time spans over which the data files were taken were short. The first series (16 December) was taken over a 20-minute time period and the second series (17 December) was taken over a 38-minute time period.

5.3 TEST CONDITIONS

The weather was clear and dry on 16 December. In contrast, 17 December was cloudy and humid, resulting in a lot of moisture in the air. The fast-moving clouds overhead meant that some propagation variability would be expected in the data as a result. Neither day had rain or fog. Data were taken both days with and without noise from a small UV light (The UVP Company Pen Ray).

On 16 December, experiments were performed by turning the laser on and off during data runs. There was also a file of noise-only data.

Because the data are digitized in 100-ns increments, it is convenient to present it in "counts" of 100 ns rather than microseconds (μs).

5.4 PULSE IDENTIFICATION

Valid pulses are considered to be those with the signature described in section 4.6. Some "fadeout" periods occurred where the characteristic signature was missing (table J-1).

Table J-1. Data files summary.

File	Date	Time	Noise	Laser	Comment
16-0	16 Dec 92	09:02:59	No	ON	
16-1	16 Dec 92	09:04:35	Yes	ON	Fadeout
16-2	16 Dec 92	09:07:09	No	ON/OFF	
16-3	16 Dec 92	09:08:11	Yes	OFF	
16-4	16 Dec 92	09:09:39	No	OFF/ON	
16-5	16 Dec 92	09:11:11	Yes	ON	
16-6	16 Dec 92	09:13:02	Yes	ON/OFF	
16-7	16 Dec 92	09:14:25	High	OFF	
16-8	16 Dec 92	09:16:04	Yes	OFF/ON	
16-9	16 Dec 92	09:17:43	No	ON	
16-10	16 Dec 92	09:20:53	No	OFF/ON	
16-11	16 Dec 92	09:22:08	No	OFF/ON	
17-0	17 Dec 92	09:02:09	No	ON	Fadeout
17-1	17 Dec 92	09:09:38	High	ON	Fadeout
17-2	17 Dec 92	09:15:25	Yes	ON	Fadeout
17-3	17 Dec 92	09:25:50	No	ON	
17-10	17 Dec 92	09:29:21	No	ON	
17-11	17 Dec 92	09:30:07	No	ON	
17-12	17 Dec 92	09:31:24	No	ON	
17-13	17 Dec 92	09:32:34	Yes	ON	
17-14	17 Dec 92	09:33:55	No	ON	Board Waving
17-15	17 Dec 92	09:35:06	No	ON	
17-16	17 Dec 92	09:36:35	No	ON	
17-17	17 Dec 92	09:37:46	No	ON	

6.0 SUMMARY

In the link tests described above, the raw data have also been stored onto a hard disk. Because of the fine resolution (one bit per 100 ns) and the amount of computer memory available (36 MB), the maximum recording time per run was only about 27 seconds. The size of the hard disk used limited a test series to only 12 runs. However, even with these limitations, one test series can record up to about 800,000 laser pulse events.

6.1 LASER STABILITY

The analysis of the time between laser pulses indicates that the laser's internal clock is generally stable. More importantly, the analysis implies that the UV laser can be made to lase at certain times, within a few microseconds, and well within the expected bin size (say 10 μs) of a laser link. Therefore, a laser link based on PPM and a bin size of 10 μs will be feasible.

6.2 PULSEWIDTH

In general, the detected laser pulses have pulsewidths ranging from 3 to 10 μs, with an average of about 6 to 7 μs. This indicates that a bin size of 10 μs can be used to define UV laser link modulation/demodulation schemes. With a bin size of 10 μs, a laser pulse is unlikely to cover

more than two of these bins, and concatenating results from two successive bins is relatively easy.

The unusual laser pulse signature noted in section 4.6 makes the pulsewidth calculations unreliable. Until this phenomenon is resolved, the pulsewidths remain in doubt. Possible explanations include electronic processing error, PMT overload, and stretching due to atmospheric scattering.

Further, it is difficult to be more specific about the pulsewidths because variations in the test data are not extensive to date. When more data are available, a more detailed analysis will be performed and reported.

6.3 NOISE

In general, the noise is distributed randomly, although there is some clustering of noise photons with an average of a few photons per 10-μs bin. Thus, a noise is unlikely to be mistaken for a laser pulse and vice versa, given a noise source such as an UV lamp.

However, a possibly more spiky noise source, such as arc-welding, must be tested to determine whether the UV photons thus generated are more clustered in the time regime discussed above.

6.4 CONCLUSIONS

Preliminary analyses confirm that UV laser pulse propagation characteristics can improve the signal-to-noise ratio of a laser signal considerably over that of UV lamp signals. Therefore, a laser link can tolerate much higher noise levels than a lamp link, but the tolerance limit is as yet undetermined.

6.5 RECOMMENDATIONS

a. Perform more laser link tests and collect propagation data under different conditions.

b. Further study the effects of environmental factors on the UV laser pulse propagation characteristics.

c. Further characterize the UV laser pulse propagation through the atmosphere in the presence of different noise sources.

d. Establish what level and type of noise an UV laser link can tolerate.

7.0 ACKNOWLEDGMENTS

The link tests described above have been performed by LeRoy Gibeson, Pete Poirier, and John Yen of NCCOSC RDT&E Division, with the assistance of Charles Saylor of SDSU. The data analysis programs have been developed by Maureen O'Brien, also of the RDT&E Division.

8.0 REFERENCE

Yen, J. 1987. "UV Communications Propagation Study." NOSC TR 1191 (May). Naval Ocean Systems Center, San Diego, CA.

APPENDIX K

ISRC ELECTRONICS

1.0 INTRODUCTION

One of the efforts of the ISRC project was the development of an UV laser link for tactical communications.

1.1 REQUIREMENT

A primary uncertainty of UV laser communications was the limited knowledge of the propagation characteristic of the laser pulse at the communication range. Thus, the characterization of the UV laser pulse propagated to this distance defines the requirement.

1.2 ASSETS

The two available photomultiplier tubes (PMTs) used for previous UV projects were housed with solar-blind filters and associated electronics. These electronics provided amplification and shaping for each photon event, which resulted in a single 70-ns electronic pulse per photon event.

IBM-compatible PCs have been acquired as terminals for the ISRC data link. These computers possess a 80486 processor, 4 megabytes (MB) of memory, and a 130-MB hard drive. It was decided to develop the characterization procedure within the constraints of the PCs' Industry Standard Architecture (ISA) data bus.

2.0 APPROACH

Previous methods of counting photon events with a counter (with a time base of a second) were impractical because of the very short duration of the laser pulse (50 to 100 ns) and the limited expected scattering effect (on the order of 2 to 10 μs). Ideally, capturing the laser pulses in realtime with as high a resolution as possible was desirable.

2.1 RESOLUTION

The available PMT units had an output pulse of 70 ns per photon event and a recovery of approximately 30 ns, which determined that a 100-ns resolution was attainable. This resulted in the maximum count of 1 photon event per 100 ns, or 10^7 counts per second.

2.2 THROUGHPUT

Capture of the 10 megabits per second (Mbps) serial data (assuming serial to parallel conversion) required an input-to-computer (PMT-to-hard disk) throughput of 1.25 Mbps (or 625 kilowords per second or 10 Mbps ÷ 16). The initial throughput testing was conducted with commercially available products.

2.3 STORAGE

The storage requirement was set at 400 MB, which would allow for about 330 seconds of realtime data collection. This is equivalent to approximately 760,000 laser pulses.

The hard drive selected was an SCSI Seagate ST1480N with an internal data rate of 17 to 25 Mbps and a spindle rotation of 4400 RPM (versus the normal 3600 RPM).

In memory-to-disk throughput tests, data rates approaching 2 Mbps were attained. Although this data rate was greater then the 1.25 Mbps required, it did not involve the handling of data from an input port.

2.4 INPUT TESTING

The input testing was performed with a National Instruments AT-DIO-32F parallel I/O card with a conservative data rate specification of 1 Mbps. It was hoped that with a double-buffer, interrupt-driven driver, a higher data rate could be achieved. However, pushing the PC's ISA bus speed beyond the designed specification of 8 MHz (1 Mbps data rate) proved to be unreliable.

A decision was made to design a PC data-capture board that would capture a window of data centered around each laser pulse. This would redefine the throughput data rate requirement to [(windowsize ÷ 8)* pulse rate]. Assuming a nominal realtime capture window of 100 µs, the required data rate would drop to 0.307 Mbps, which is well within the capability of the PC. This also has the advantage of increasing the capacity of the hard disk to greater than 3 million pulses captured over a 20-minute test period.

Figure K-1 is a block diagram of the Laser Pulse Acquisition (LPAcq) card.

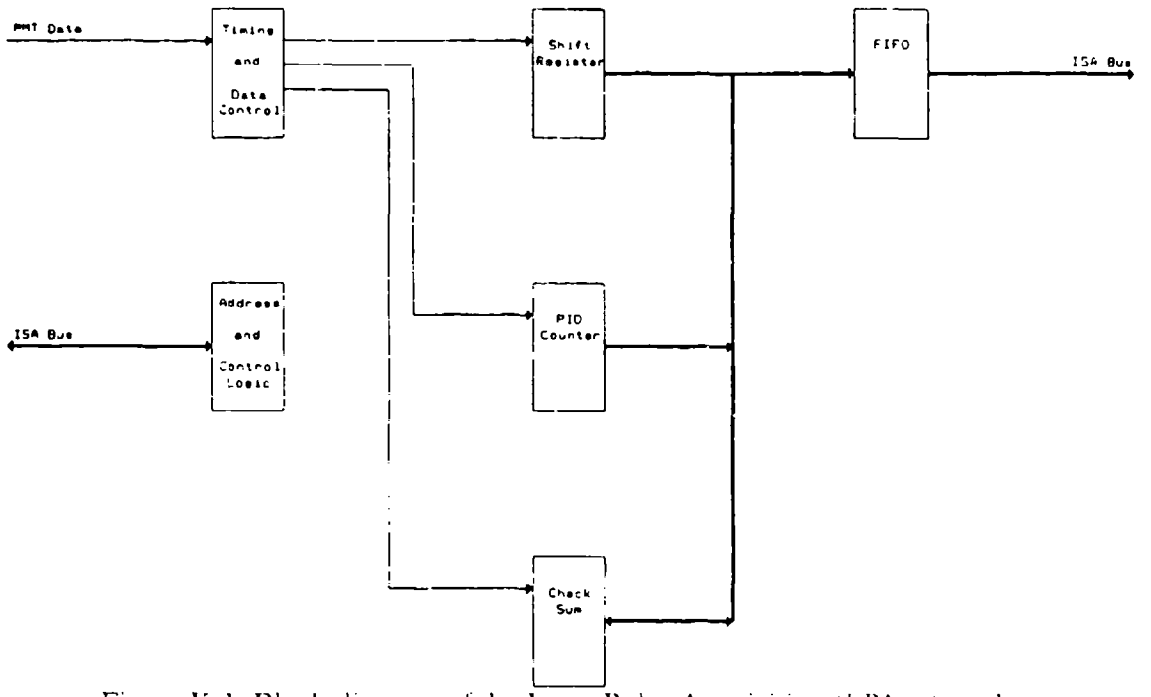

Figure K-1. Block diagram of the Laser Pulse Acquisition (LPAcq) card.

2.5 SYNCHRONIZATION

A means of synchronizing the data capture window with the laser pulse was required for the test link because of the continuous nature of the laser pulse train. Three methods were evaluated: a direct land line over existing underground wiring, Global Positioning System (GPS) receivers available from another project, and a microwave link.

2.5.1 Land Line

The direct land line proved to be unreliable due to the suboptimal condition of the available wiring and inherently undesirable for future use in field (portable) testing.

2.5.2 GPS

Investigation of the GPS receivers determined that even though the time recorded during a location fix was accurate at the time of the fix, this was considered a low priority in the coded output. Therefore, the GPS-provided time was unsuitable for our requirement (accuracy within 1 μs is required). Recent products have addressed a time synchronous requirement and could be considered in the future.

2.5.3 Microwave

A pair of Advanced Receiver Research's model TR10GA 10 GHz "Gunnplexer" transceivers were purchased for the microwave link. Applying a timing pulse directly to the tuning varactor of the Gunn oscillator results in the transmission of a single microwave burst. At the receiving end, the microwave burst is detected as an FM noise burst that is integrated and shaped to provide the laser gate pulse (LPGate) for the LPAcq card.

The microwave link proved to be very reliable and portable (assuming AC power availability), although it did require line-of-sight (LOS) between the transmitter and the receiver.

3.0 HARDWARE

3.1 LASER TRIGGER

The laser pulse trigger/gate circuit provides a pair of pulses. The first pulse, sent to the receiving site (via the microwave link), indicates that a laser pulse is pending and gating the data recording system. The other pulse triggers the laser's Q-switch after a programmable 1- to 256-μs (via dip switch) delay.

3.2 LPAcq CARD

The laser pulse data block was defined as follows:

Word 1:	upper half of a sequential 32-bit Pulse IDentification (PID) number.
Word 2:	lower half of the PID
Words 3 – (N–1):	16-bit data words.
Word N:	16-bit checksum.

The data block size N may be varied by the data collection program. Currently, a 1024-word data block is used to store data.

3.2.1 Control

The LPAcq card uses I/O port addresses 240–243 for reset, setting parameters, and data control. Address 240 addresses the first-in-first-out (FIFO) for reading.

3.2.2 FIFO Buffer

A 4-KB FIFO buffer was used to compensate for the difference between the input rate (1.6 μs per word) and the memory data rate (2 μs per word). Although this simplified the data transfer, the buffer can be overrun with too large of a data block or too fast of a data rate.

3.2.3 Data Block

Under software control, the LPAcq card is enabled to take data. On the receipt of a LPGate pulse from the microwave receiver, the PID counter is incremented and loaded into the FIFO buffer (2 words). Next, the serial input from the PMT is "sliced" at a 10 MHz rate (100 ns), converted into 16-bit words, and loaded into the buffer (the number of words is controlled by the programmable frame size, with the default at 63 words to approximate 100 μs). Finally, the checksum is added to the buffer to complete the data block.

With the default settings and a laser pulse rate of 2400 Hz, the 4-KB buffer will fill in 12 ms. This overrun will stop data from being stored in the buffer, but it will not stop the PID counter from incrementing. This is considered an error condition and full reset capability is provided.

3.2.4 Buffer Status

Three buffer status conditions are provided: empty, half-full, and full. Upon receiving a half-full condition, the software reads the data from the buffer until empty. The data are read onto a 32-MB random access memory (RAM) disk. When the RAM disk is full, the LPAcq card is disabled and the stored data are transferred to the hard disk. This method results in the maximum recording rate and transfer rate (to the hard disk) and increases the overall efficiency.

3.2.5 Summary

By changing the basic clock, a different resolution can be achieved (i.e., 50 ns, 1 μs). The base variable would be frame size versus repetition rate.

With this flexibility, a wide range of data rates and windows (frame sizes) can be accommodated.

4.0 ACKNOWLEDGMENTS

The electronics and software described above have been developed by LeRoy Gibeson and Maureen O'Brien of the NCCOSC RDT&E Division.

APPENDIX L

PHASE I PROPOSALS SUMMARY

1.0 SBIR

In pursuit of alternative technologies in the private sector that can be applied to ISRC missions, a solicitation titled "Optical Scatter Communications" was advertised through the Small Business Innovation Research (SBIR) publication (solicitation N91-308).

Twelve companies submitted proposals to this solicitation (table L-1).

Table L-1 SBIR proposals summary.

	Proposal	UV	IR	RF
1.	Aspen Systems, Inc. Marlborough, MA		X	
2.	Biotronics Technologies, Inc. Waukesha, WI	X	X	
3.	Boulder Nonlinear Systems, Inc Boulder, CO		X	
4.	Deacon Research Palo Alto, CA		X	
5.	Jamar Technology Co. San Diego, CA	X		
6.	Jamieson Science & Engineering, Inc. Bethesda, MD		X	
7.	Line Lite Laser Corp. Mountain View, CA	X		
8.	Optron Systems, Inc. Bedford, MA	X		
9.	Physical Optics Corp. Torrance, CA		X	
10.	Sparta, Inc. San Diego, CA	X		
11.	Surface Optics Corp. San Diego, CA		?	
12.	UBC, Inc. Tampa, FL			X

1.1 SOLICITATION TEXT (AS PUBLISHED)

OBJECTIVE: The objective of this topic is to design and develop communications systems which use optical scattering and/or atmospheric absorption to advantage, resulting in short range, low probability of intercept (LPI) tactical communications.

DESCRIPTION: Initial exploratory investigations into the performance characteristics of electromagnetic emissions at near light frequencies indicate that propagation in this frequency

range offers some tactically useful properties. Atmospheric absorption in this frequency range results in very high propagation losses over very short distances, while optical scattering reduces the dependence on optical line of sight between the transmitter and receiver. Several applications are conceivable which would permit omnidirectional, networked communications among voice and data subscribers. Also, by using directional antennas, range can be extended while maintaining other desirable properties. Such a directional system could provide wideband communications point-to-point if a suitable multiplexing scheme could be devised. The current limiting technologies appear to be achieving frequency diversity and high cost of transmitter and receiver components.

Phase I would consist of concept exploration resulting in a preliminary design study which produces a system design drawing supported by theoretical determinations of system performance. These calculations should verify that the specified performance can be achieved.

Phase II would consist of assembly and demonstration of the prototype systems. The demonstration(s) must be designed to verify the theoretical calculations from Phase I.

1.2 EVALUATORS

Five evaluators were involved, three from NCCOSC RDT&E Division and two from MCSC. The NCCOSC evaluators were John Yen and Dan Katz of Code 843, and Victor Moberg of Code 842. The MCSC evaluators were Kevin Smith and Robert Stip of Code AW.

1.3 SELECTION

The sponsor selected Sparta as the best proposal of those submitted to MCSC. Sparta was awarded an SBIR contract (N66001-92-C-7007) on 30 January 1992. In May 1992, Sparta was granted an extension of the contract to 6 November 1992.

1.4 STATUS

This contract was completed as of November 1992.

2.0 BAA

In pursuit of alternative technologies in the private sector that can be applied to the ISRC missions, a Broad Agency Announcement (BAA) solicitation was advertised through the Commerce Business Daily.

Twenty-two companies submitted proposals (table 1-2).

Table L-2. BAA proposals summary.

	Proposal	UV	IR	RF	Other
1.	Battelle Columbus, OH			X	
2.	Comm Concept Chesp Chesapeake, VA			X	
3.	Dataproducts Wallingford, CT				X
4.	DiRad Redondo Beach, CA	X			
5.	Galaxy Micro Austin, TX			X	
6.	GTE Mt View Mt. View, CA	X			
7.	GTE Waltham Waltham, MA			X	
8.	Honeywell Bloomington, MN			X	
9.	HSS Bedford, MA		X		
10.	Hughes Fullerton, CA			X	
11.	Jamar San Diego, CA	X			
12.	Jaycor San Diego, CA		X		
13.	LCR Littleton, CO	X			
14	Line Lite Mt. View, CA	X			
15.	Litton Tempe, AZ	X			
16.	LSA Arlington, VA		X		
17.	Millitech South Deerfield, MA			X	
18.	Mission Res Corp Los Alamos, NM	X			
19.	Petite Res Falls Church, VA			X	
20.	Raytheon Marlborough, MA			X	
21.	Surface Optics San Diego, CA		X		
22.	Titan San Diego, CA		X		

2.1 SOLICITATION TEXT (AS PUBLISHED)

A — INTENTIONALLY SHORT-RANGED COMMUNICATIONS TECHNOLOGY DEVELOPMENT SOL N66001-92-X-6005 POC Cindy Jensen, Contract Specialist, (619) 553–4490. Celia Vaughn, Contracting Officer. Debra M. Gookin, Technical Contact, (619) 553–2538. Broad Agency Announcement.

The Naval Ocean Systems Center (NOSC) is seeking proposals (technical and cost) with innovative approaches for a technology development effort for short-ranged communications. The objective of this program is to design and develop communications systems that use scattering and/or atmospheric absorption properties to advantage, resulting in short-range, low-probability of intercept (LPI) tactical communications. The final communications system must be rugged, mobile in a High Mobility Multipurpose Wheeled Vehicle (HMMV) or similar Marine Corps vehicle, and must work on available power (100 A at 27 V). Any technological approach will be considered. This effort will be coordinated with a Marine Corps SBIR program and related in-house work at NOSC.

Previous approaches which have been tried include optical systems using ultra-violet lamps, ultra-violet lasers, or infra-red laser and millimeter wave systems. This effort should result in a prototype communications systems with the detection range limited to less than 5 kilometers. The communications link should be non-line-of-sight or should result in a detectable signal for a detector at least 5 degrees from transmitter bore sight. The systems developed under all three phases of this program must all meet the detection range and angle requirements.

Phase I is a 6-month design phase. At the end of Phase I, contractors are expected to provide a demonstration of the concept technology and a detailed plan of their approach to the Phase II effort. The plan must contain sufficient detail to allow the Government to assess the probability of success of the approach. Phase I contractor performance will be evaluated and downselections made for Phase II.

Phase II will be a 12-month program. Phase II contractors are expected to complete a field test with at least 2.4 kilobits per second one-way data transmission. They must also provide a detailed plan of their approach to the Phase III effort.

Phase III will be another 12-month program following completion of Phase II. Phase III contractors are expected to demonstrate two-way communications at the 2.4 kilobits per second rate and one-way data transmission at 2 megabits per second. Both of these demonstrations will be done in the field.

Proposed efforts for Phase I will be evaluated according to the following criteria:

1. scientific and technical merit of the proposed effort;
2. potential of proposed effort to meet the final objectives;
3. the qualifications, capabilities and relevant experience of the proposed principal investigator,
4. the offeror's capabilities, related experience and facilities; and
5. realism of the proposed cost.

Proposals submitted must contain sufficient specific information to allow the Government to adequately evaluate the proposal in accordance with these criteria. The Government desires unlimited data rights with regard to data to be delivered under this procurement. Proprietary concepts/information should be clearly identified upfront and marked in the proposal. It is anticipated that the following data deliverables will be required under the resulting contracts: Monthly Progress Report, Quarterly Program Reviews, and Final Technical Report (for each phase).

It is expected that one to three Phase I contracts will be awarded. No Phase I contract will exceed $100K. The availability of funds may dictate the number of proposals accepted by the Government. The technical volume of the proposal is limited to 30 pages, excluding resumes and management/facilities. The cost volume should:

1. be a separated document which clearly costs each proposed task separately; and
2. provide a Standard Form 1411, Contracting Pricing Proposal Cover Sheet, supported by adequate breakout of cost elements and rates for the purpose of cost/price analysis.

Cost proposals shall be valid for a period of 120 days after the date of submission. An original plus three copies of the technical volume, plus three copies of the cost volume should be submitted to NOSC, Attn:C. Jensen, Code 213; San Diego, California 92152-5000. Any other questions may be addressed to Ms. Jensen or C. Vaughn.

Proposals are to be submitted no later than 13 January 1992, and should be unclassified. This notice constitutes a BAA as contemplated in FAR 6.102(d)(2). No additional written information is available, nor will a formal RFP or other solicitation regarding this announcement be issued. Interested parties are invited to respond to this synopsis. All responsible parties responses will be considered.

2.2 EVALUATORS

Five NCCOSC personnel evaluated these proposals: Debra Gookin, Dan Katz, and John Yen of Code 843; Victor Moberg of Code 842; and MAJ Scott Minturn of Code 033 (Marine Corps Liaison Office).

2.3 SELECTION

The evaluations were submitted to MCSC. The sponsor concurred that GTE Waltham, Mission Research Corporation, and Titan had the best proposals. Each of these three was awarded a BAA contract (GTE: N66001-92-C-6010, awarded on 30 April 1992; Mission Research Corporation: N66001-92-C-6007, awarded on 6 April 1992; Titan: N66001-92-C-6005, awarded on 14 May 1992).

2.4 STATUS

All three contracts were completed as of this writing.

REPORT DOCUMENTATION PAGE

Form Approved
OMB No. 0704-0188

1 AGENCY USE ONLY (Leave blank)	2 REPORT DATE	3 REPORT TYPE AND DATES COVERED
	May 1993	Final

4 TITLE AND SUBTITLE
INTENTIONALLY SHORT RANGE COMMUNICATIONS (ISRC)
1992 Report

5 FUNDING NUMBERS
PE: 0602131M
AC: DN303121
PN. C3125

6 AUTHOR(S)
J. Yen, P. Poirier, M. E. O'Brien, and L. Gibeson

7 PERFORMING ORGANIZATION NAME(S) AND ADDRESS(ES)
Naval Command, Control and Ocean Surveillance Center (NCCOSC)
RDT&E Division
San Diego, CA 92152-5001

8 PERFORMING ORGANIZATION REPORT NUMBER
TR 1600

9 SPONSORING/MONITORING AGENCY NAME(S) AND ADDRESS(ES)
U.S. Marine Corps Systems Command
Arlington, VA 22217

10 SPONSORING/MONITORING AGENCY REPORT NUMBER

11 SUPPLEMENTARY NOTES

12a DISTRIBUTION/AVAILABILITY STATEMENT
Approved for public release; distribution is unlimited.

12b DISTRIBUTION CODE

13 ABSTRACT (Maximum 200 words)

This document details the feasibility studies conducted for the Intentionally Short Range Communications (ISRC) project. The short-range limitation arises from the need for low probability of intercept (LPI), low probability of detection (LPD) communication links. The detection of an undecipherable transmission would still provide an enemy with information regarding transmitter location. The technologies being studied are ultraviolet (UV) lamps, UV lasers, infrared (IR) lasers, millimeter waves (MMW), and direct sequence spread spectrum.

14 SUBJECT TERMS
ultraviolet lasers
Company Radio
Local Area Network Backbone
Wideband Data Link

15 NUMBER OF PAGES
117

16 PRICE CODE

17 SECURITY CLASSIFICATION OF REPORT	18 SECURITY CLASSIFICATION OF THIS PAGE	19 SECURITY CLASSIFICATION OF ABSTRACT	20 LIMITATION OF ABSTRACT
UNCLASSIFIED	UNCLASSIFIED	UNCLASSIFIED	SAME AS REPORT

21a NAME OF RESPONSIBLE INDIVIDUAL	21b TELEPHONE *(Include Area Code)*	21c OFFICE SYMBOL
J Yen	(619) 553-6502	Code 843

INITIAL DISTRIBUTION

Code 0012	Patent Counsel	(1)
Code 80	R. J. Kochanski	(1)
Code 84	C. E. Gibbens	(1)
Code 843	D. A. Gookin	(1)
Code 843	J. Yen	(60)
Code 961	Archive/Stock	(6)
Code 964B	Library	(2)

Defense Technical Information Center
Alexandria, VA 22304–6145 (4)

NCCOSC Washington Liaison Office
Washington, DC 20363–5100

Center for Naval Analyses
Alexandria, VA 22302–0268

Navy Acquisition, Research and Development
Information Center (NARDIC)
Washington, DC 20360–5000

GIDEP Operations Center
Corona, CA 91718–8000

NCCOSC Division Detachment
Warminster, PA 18974–5000